NACA

RESEARCH MEMORANDUM

for the

U. S. Air Force

AN INVESTIGATION AT MACH NUMBERS OF 1.41 AND 2.01 OF THE AERODYNAMIC CHARACTERISTICS OF AN 0.025-SCALE MODEL OF THE MX-1712

By Norman F. Smith and Lowell E. Hasel

Langley Aeronautical Laboratory
Langley Field, Va.

NATIONAL ADVISORY COMMITTEE
FOR AERONAUTICS

WASHINGTON
1952

14

NATIONAL ADVISORY COMMITTEE FOR AERONAUTICS

RESEARCH MEMORANDUM

for the

U. S. Air Force

AN INVESTIGATION AT MACH NUMBERS OF 1.41 AND 2.01 OF THE AERODYNAMIC CHARACTERISTICS OF AN 0.025-SCALE MODEL OF THE MX-1712

By Norman F. Smith and Lowell E. Hasel

SUMMARY

An investigation of the aerodynamic characteristics of an 0.025-scale model of the MX-1712 configuration has been conducted in the Langley 4- by 4-foot supersonic pressure tunnel. The tests were performed at Mach numbers of 1.41 and 2.01 at a Reynolds number of approximately 2.6×10^6 based on the wing mean aerodynamic chord.

The MX-1712 is a proposed swept-wing, jet-powered supersonic bomber aircraft. The wing is of aspect ratio 3.5, taper ratio 0.2, and thickness ratio 5.5 percent (streamwise) and has 47° sweep of the quarter-chord line.

The longitudinal and lateral force characteristics of the model and various combinations of its components, including several nacelle installations, were investigated. The effects of a modified wing, two horizontal tail positions, and a shortened fuselage were also studied. The results obtained from these investigations are presented in this report.

The aerodynamic investigation of this model disclosed no unusual stability characteristics or Mach number effects. The choice of nacelle installations appears to be a major decision, one greatly affecting the performance of the airplane. At $M = 1.41$ and $C_L = 0.1$, the buried nacelles increased the drag of the basic model by 9 percent, while the best pod nacelles increased the drag of the basic model by 27 percent.

INTRODUCTION

An investigation of a 0.025-scale model of the MX-1712 configuration has been made in the Langley 4- by 4-foot supersonic pressure tunnel and the 8-foot transonic tunnel. The MX-1712 is a proposed swept-wing, jet-powered supersonic bomber aircraft. These tests were performed at the request of the Wright Air Development Center, Wright Patterson Air Force Base, Ohio, and were conducted in close cooperation with an Air Force contractor. This report presents the results of the investigation in the Langley 4- by 4-foot supersonic pressure tunnel at Mach numbers of 1.41 and 2.01 and a Reynolds number of 2.6×10^6 based on wing mean aerodynamic chord. Longitudinal and lateral force characteristics of the complete aircraft configuration and of various combinations of its components, including several nacelle installations, are shown. The effects of a modified wing, a shortened fuselage, and two horizontal-tail heights were also studied.

Because of the specific nature of this project, no detailed or pointed analysis has been made. Instead, a general discussion of the data is presented, along with some comparisons with simple theories.

COEFFICIENTS AND SYMBOLS

The results of the investigation are presented in terms of standard NACA coefficients and are referenced to the stability axes (fig. 1).

The coefficients and symbols are defined as follows:

C_L lift coefficient, $\frac{\text{Lift}}{qS}$, where Lift = -Z

C_D drag coefficient, $\frac{\text{Drag}}{qS}$, where Drag = -X

C_m pitching-moment coefficient, $M'/qS\bar{c}$

C_Y lateral-force coefficient, Y/qS

C_n yawing-moment coefficient, N'/qSb

C_l rolling-moment coefficient, L'/qSb

X force along X-axis, lb

Y force along Y-axis, lb

Z	force along Z-axis, lb
M'	moment about Y-axis, lb-ft
N'	moment about Z-axis, lb-ft
L'	rolling moment about X-axis, lb-ft
q	free-stream dynamic pressure, lb/sq ft
M	Mach number
S	wing plan-form area, 1.367 sq ft
b	wing span, 2.188 ft
c	wing-section chord, ft
$\bar{c}$	wing mean aerodynamic chord, 0.718 ft
α	angle of attack of fuselage center line, deg
i_t	incidence angle of stabilizer chord line with respect to fuselage center line, deg (positive with trailing edge down)
δ_e	deflection angle of elevator chord line with respect to stabilizer chord line, deg
δ_r	deflection angle of rudder, deg
ψ	angle of yaw, deg
L/D	lift-drag ratio
$C_{L_{trim}}$	lift coefficient at trim ($C_m = 0$)

APPARATUS AND MODELS

Tunnel

The Langley 4 by 4-foot supersonic pressure tunnel is a rectangular, closed-throat, single-return wind tunnel designed for a Mach number range of 1.2 to 2.2. The tunnel is powered by a 45,000-horsepower electric drive and has a stagnation pressure range of from about 1/4 atmosphere to about 2 atmospheres. The test section is 54 inches wide and approximately 53 inches high for M = 1.4, approximately 61 inches high for

M = 2.0. An external air-drying system supplies air of a sufficiently low moisture content to preclude moisture condensation in the test section.

Models

A two-view drawing of the MX-1712 model is shown in figure 2 and photographs are shown in figure 3. The geometric characteristics of the model are presented in table I. The model was sting-mounted from the rear. Forces were measured by means of an internal six-component strain-gage balance. Static pressures were measured at the base of the model and in the nacelle ducts. All strain-gage wiring was carried internally through the sting and support strut to outside the tunnel, while the pressure tubes were run externally along the sting to a manifold in the vicinity of the support-strut leading edge.

The model-support system provided for changes in angle of attack or yaw in the horizontal plane while maintaining the model approximately in the center of the test section. Figure 4(a) shows a configuration installed in the tunnel for yaw tests, while figure 4(b) shows another configuration oriented for pitch tests.

The angle of attack or yaw of the model was set to a nominal value by means of the support system. The actual angles were then measured during the tests by means of an optical system which reflected light from a small mirror imbedded in the surface of the fuselage.

The model was constructed with a number of joints in order that the components might be tested in various combinations. These joints are visible in figure 3. Although the model construction was of very high quality, some filling and fairing of joints was necessary. As will be shown later, the condition of the fuselage and fuselage-wing-juncture joints had no measurable effect on the force data. An attempt was nevertheless made during all the tests to keep these joints in a faired condition with glazing compounds (fig. 4).

The fuselage fineness ratio (with canopy nose) is 14.35. Several tests were also made with the fuselage shortened 4 inches to a fineness ratio of 12.96 (fig. 2). Four fuselage nose shapes were tested for comparative purposes (fig. 5). The majority of the tests were made with the canopy nose (fig. 5(a)). The aft end of the fuselage is of arbitrary shape to accommodate a sting of size adequate for the loads involved.

The wing is of aspect ratio 3.5, taper ratio 0.2, and has 47° sweep of the quarter-chord line. The wing incorporated twist which varied

linearly across the span to $2\frac{1}{2}^{\circ}$ washout at the tip. The airfoil section is 5.5 percent thick (streamwise) and is a rounded-leading-edge section of the contractor's design. Ordinates are given in table II. The wing incidence and dihedral for the majority of the tests were 4° and 0°, respectively. The wing and mounting were so constructed as to permit installation of the wing with angles of incidence of 2° and 4°, and with angles of dihedral of 0° and 5°. The lower inboard section of this wing is removable for installation of buried nacelles which have an air inlet in the leading edge of the wing root (fig. 4(b)).

A modified wing which was designed to alleviate certain low-speed problems was investigated. The original and modified wings are identical over the inboard 50 percent of the wing semispan stations. From the 80- to 100-percent semispan stations, the forward 15 percent of the original wing was modified (fig. 6) by adding the full camber of an NACA 230-series section to the original mean line. (The original mean line and the 230 camber line were assumed to coincide at the 15-percent-chord station.) From the 50- to 80-percent semispan stations, the amount of camber which was added to the original mean line varied in an arbitrary manner. Section ordinates for the original and modified wings are presented in tables II and III.

The center of gravity (and moments) was assumed to be at the 35-percent-chord station of the wing mean aerodynamic chord (fig. 2).

The horizontal stabilizer is geometrically similar to the wing in plan form and has a symmetrical $5\frac{1}{2}$-percent-thick section (table IV). Provisions were made for mounting the stabilizer at various angles of incidences in two positions (fig. 2): on the sides of the fuselage at the center line and on the sides of the vertical tail. In these two positions the horizontal stabilizers have the same exposed areas but different total areas when the areas "blanketed" by the fuselage or vertical tail are considered (table I). An elevator is included as a part of the horizontal tail. Elevator deflections were obtained by installing elevator sections which had been machined to the desired deflection. The elevator area is approximately 15 percent of the complete exposed stabilizer area, and the elevator chord is 21 percent of the stabilizer chord.

The vertical tail is of the same taper ratio and thickness ratio as the horizontal stabilizer, but has an aspect ratio of 1.5 (fig. 2). The rudder angle was changed by a method similar to that for the elevator. The rudder area is approximately 14 percent of the total area. Ordinates for the horizontal and vertical tails are presented in table IV.

The configuration having the original fuselage, original wing, vertical tail, and horizontal tail with incidence angle of -3° will be identified throughout the report as the "basic model."

Three types of nacelles were added to the basic model. The buried-nacelle installation which employs a wing-root inlet is shown in figures 7 and 4(b). The duct behind the single inlet in each wing is divided into two passages, each leading to a circular exit aft of the wing trailing edge. Venturi sections with static-pressure orifices were provided in the two port-nacelle exits for determination of internal-flow conditions.

The cone nacelle is of the pod type, mounted on sweptforward struts (figs. 8 and 3). Each nacelle contains two separate inlets and ducts. The outboard duct of the port nacelle was provided with a venturi and static-pressure orifices for determination of internal-flow conditions. The cone-nacelle was tested on the wing in two spanwise positions: 0.50 semispan and 0.60 semispan.

The wedge nacelle is a twin-duct pod nacelle designed around a common vertical wedge at the inlet (figs. 8 and 4(a)). Internal static-pressure orifices were provided as in the other pod nacelle. The wedge nacelles were tested at $M = 1.41$ only and were located at the 0.50- and 0.60-wing-semispan positions.

The models, support sting, balance, and associated indicating equipment were supplied by an Air Force contractor.

TESTS

Conditions

The nominal tunnel conditions for these tests are given in the following table:

	$M = 1.41$	$M = 2.01$
Stagnation pressure, psia	11.5	14.7
Stagnation temperature, $^{\circ}F$	110	110
Stagnation dewpoint, $^{\circ}F$	<-30	<-30
Dynamic pressure, psf	720	740
Reynolds number (based on wing M.A.C.)	2.6×10^6	2.6×10^6

The nominal test angles for model and model control surfaces are as follows:

Angle of attack	-8° to 10° in 2° increments
Angle of yaw	-4° to 6° in 2° increments
i_t	2°, -3°, -8° (occasionally 7°, -13°)
δ_e	0°, -10°, -20°
δ_r	0°, -5°, -10°

Corrections and Accuracy

The angles of attack and angles of sideslip were measured by an optical system which reflected light from a small mirror imbedded in the surface of the fuselage. The accuracy of this system is estimated to be $\pm 0.1^\circ$ at low angles and $\pm 0.15^\circ$ at high angles.

The strain-gage balance was temperature-compensated. Component interactions were determined in calibration and all data are corrected for interactions.

The estimated errors in the force data are as follows:

C_L	± 0.002
C_m	± 0.002
C_D	± 0.001
C_l	± 0.001
C_Y	± 0.0006
C_n	± 0.0001

The base pressure was measured and the drag data were corrected to correspond to a base pressure equal to free-stream static pressure.

No corrections for interference forces caused by the sting support have been applied to the data.

As an over-all check on the accuracy and repeatability of the data, a number of repeat runs were made on identical configurations at various times during the test program. Data from repeat runs are plotted in figure 9.

Calibration data for the $M = 1.4$ nozzle which were obtained at a stagnation pressure of 4 psia are presented in reference 1. A partial survey of this nozzle (data unpublished) has also been made at a stagnation pressure of 15 psia. From these data an estimate of the Mach number and flow-angle variation at a stagnation pressure of 11.5 psia has been

made. Unpublished results for the M = 2.01 nozzle show that the magnitude of the variations of Mach number, flow angle, and static pressure in the vicinity of the model are small, and no corrections for these variations have been applied to the data. The variations are summarized in the following table:

	M = 1.41	M = 2.01
Mach number	±0.01	±0.01
Flow angle in horizontal plane, deg	±0.2	±0.1
Flow angle in vertical plane, deg	±0.2	±0.1

PROCEDURE

The order in which the wind-tunnel tests were performed is given by the run numbers tabulated in the run log (tables V and VI). This order was set up to best expedite the program in accordance with the peculiarities of the tunnel and model. Also, an attempt was made to group, insofar as possible, runs to be compared or analyzed as a group.

In order to determine the sensitivity of the force results to the surface condition of the fuselage, runs were made with the fuselage and fuselage-wing-juncture joints (fig. 3) faired and unfaired. No differences in the force measurements were obtained in these two tests.

Similarly, tests were made to determine the effect of sealing the small gap which existed at the juncture of the horizontal and vertical tails. No significant effect upon the longitudinal stability was measured. In both of the foregoing cases, the data are presented in the tabulated results but have not been plotted.

Because it was considered possible for the pressure tubes which were required for duct pressure measurement to introduce extraneous forces into the results, several check runs were made with tubes connected and disconnected. These duplicate sets of force data (given in tables VII and VIII) showed that the pressure tubes had no significant effect upon the balance readings. No distinction is therefore made in the figures between force data obtained with and without the pressure tubes connected.

PRESENTATION AND DISCUSSION OF RESULTS

The data which were obtained from this series of tests are tabulated in tables VII to X. Most of these data are presented and discussed in

the following sections of the report except for a few runs made to check research techniques and repeatability of data. The run numbers are presented on the data figures to correlate these data with the tabulated data. The run logs (tables V and VI) identify the model configuration for each run number.

Longitudinal Force and Moment Characteristics

Model breakdown.- The variation with angle of attack of the lift, drag, and pitching-moment characteristics of the various combinations of model components, excluding nacelles, are presented in figure 10. The minimum drags of the basic model are approximately the same at both Mach numbers and have a value of about 0.028. Throughout the report, the configuration having the original wing, original fuselage, vertical tail, and horizontal tail with incidence angle of -3° will be identified as the basic model. Also, unless otherwise stated, wing incidence is 4°, wing dihedral 0°. The increase in drag with angle of attack (fig. 10) is greater at a Mach number of 1.41, as would be expected, since the data show that the increase is primarily due to induced drag of the wing, and the wing has a higher lift-curve slope at a Mach number of 1.41.

The fuselage alone is unstable (fig. 10). Addition of either the wing or the horizontal tail to the fuselage produces a stable configuration. The low-tail configuration is slightly more stable than the high-tail configuration. Several factors can contribute to this condition, namely, the fact that the area (including that blanketed by the fuselage or vertical tail) of the low tail is about 24 percent greater than the area of the high tail, and the probability that the high tail is in a region of greater downwash at both Mach numbers. At both Mach numbers the slopes of the pitching-moment curves of the complete-model configurations decrease at the higher angles of attack.

The values of C_{m_α} and C_{L_α} (measured at the trim angles of attack for the basic models) for the various model configurations are presented in the following table:

Configuration	M = 1.41		M = 2.01	
	C_{m_α}	C_{L_α}	C_{m_α}	C_{L_α}
Fuselage	0.0035	0.0008	0.0036	0.0014
Fuselage, vertical and low horizontal tail	-.012	.0075	-.0068	.0057
Fuselage, vertical and high horizontal tail	-.0097	.0061	-.0045	.0046
Fuselage and wing	-.0092	.060	-.0043	.040
Basic model with low horizontal tail	-.020	.062	-.012	.043
Basic model with high horizontal tail	-.019	.061	-.011	.042

Using linear-theory methods (refs. 2 and 3) the theoretical lift-curve slopes of the isolated wing have been computed to be 0.064 and 0.043 at $M = 1.41$ and $M = 2.01$, respectively. The corresponding experimental slope increments due to the addition of the wing to the fuselage are 0.059 and 0.039 and are about 91 percent of the theoretical value for the isolated wing.

Effectiveness of horizontal stabilizer and elevator.- The longitudinal stability characteristics of the basic model with various incidences of the high and low horizontal stabilizer are shown in figures 11 and 12, respectively. Figure 13 shows corresponding data for the basic model with various elevator deflections on the high stabilizer. From these three figures, figure 14 has been prepared to show the effectiveness of the stabilizers and elevator in changing trim lift coefficient. The high stabilizer is shown to be slightly more effective than the low stabilizer in changing trim lift coefficient at the higher incidence angles because, as has been shown previously, the configuration with high stabilizer is less stable. The two tails have approximately the same effectiveness near zero incidence. Both the low and high stabilizer lose about 30 percent of their effectiveness when the Mach number is increased from 1.41 to 2.01. This loss in effectiveness is proportional to the decrease of stabilizer lift-curve slope with increasing Mach number.

The effectiveness of the elevator is approximately 16 percent of the stabilizer effectiveness, which corresponds closely to the ratio of elevator area to total stabilizer area.

Lift-drag ratios.- The lift-drag ratios of the basic-model configurations are presented in figure 15. At a Mach number of 1.41, the high- and low-tail configurations have maximum lift-drag ratios (trimmed) of about 5.35 and 5.55, respectively. At the higher Mach number, the corresponding values are 4.25 and 4.35. Lift-drag ratios for the untrimmed condition are also presented for comparison.

Wing incidence.- A comparison of the results obtained from tests of configurations having 2° and 4° of wing incidence is made in figure 16. At both Mach numbers, the effects on stability of changing the wing incidence on the basic model are small. Decreasing the wing incidence reduced the stability at trim conditions by about 5 percent at a Mach number of 1.41, but had no effect at a Mach number of 2.01. The lift-curve slopes at both Mach numbers were independent of the incidence angle.

Modified wing.- A comparison of the results obtained from tests of the original and the modified (drooped leading edge) wing are presented in figure 17. At trim the modified wing increased the drag coefficient of the basic model by 10 percent or less at both Mach numbers. The use of the modified wing at a Mach number of 1.41 resulted in a negligible

increase in stability at lift coefficients less than 0.35. At the higher Mach number, no change in stability resulted from using the modified wing. The lift-curve slopes of the basic model with the two wings were the same.

Nacelles.- The effects of adding the buried and pod nacelles to the basic model with the original wing are shown in figures 18 and 19, respectively. The effects of adding the pod nacelles to the basic model with the modified wing are shown in figure 20. For all nacelle data presented in these figures, the drag values include the internal drag of the nacelles. Internal drag measurements were made only on several typical buried and pod nacelle configurations. These data, the corresponding mass-flow data, and the methods of computation are presented in the appendix.

The buried nacelles have a negligible effect on the model stability at both Mach numbers (fig. 18). Near the trim point, the pod nacelles (fig. 19) have either a negligible or small destabilizing effect at a Mach number of 1.41. As the lift coefficient is increased, however, these nacelles cause an appreciable decrease in the slope of the pitching-moment curve. At a Mach number of 2.01, the pod nacelles decrease the stability of the basic model by a small amount. Both types of nacelles produce a slight increase in the lift-curve slope. It should be mentioned that the buried-nacelle configuration has an additional exposed wing area which is about 8 percent of the basic wing area.

The effects of adding the wedge-pod nacelles to the basic model with the modified wing (fig. 20) are similar to the effects of the wedge-pod nacelles on the basic model with the original wing.

External drag increments due to the addition of typical nacelle configurations to the basic model are shown in figure 21. These increments were obtained by subtracting from the data of the model with nacelles on, the drag of the model with nacelles off and the measured internal drag (see appendix). The data presented in figure 21 therefore include mutual interference effects and for the pod nacelles also include the strut drag. It will be noted that although the horizontal tail is in different positions for the various nacelle tests (fig. 21), the drag increments presented are not affected by tail position. At both Mach numbers, the buried nacelles have much lower drag than do the pod nacelles. The maximum increments of external drag for all nacelles occur near zero lift and are about 0.0025 for the buried nacelles as compared to 0.011 and 0.008 for the cone-pod and wedge-pod nacelles, respectively. At lift coefficients above about 0.25 at a Mach number of 2.01, the external drag increment for the buried nacelles becomes negative. Obviously the choice of nacelle installation is important, one greatly affecting the performance of the airplane. At low lift coefficients (C_L = 0.1) at

$M = 1.41$ the external drag increment of the submerged nacelles increases the drag of the basic model by 9 percent, while the best pod nacelles increase the drag of the basic model by about 27 percent.

The lift-drag ratios (based on external drag) of the untrimmed basic model with and without typical nacelle configurations are presented in figure 22. The buried nacelles have either a negligible or a small adverse effect on the lift-drag ratio of the basic model (high horizontal tail) at both Mach numbers. The pod nacelles decrease considerably at both Mach numbers the lift-drag ratios of the basic model (low horizontal tail) at lift coefficients below about 0.4. For example, at $M = 1.41$, the buried nacelles decreased the maximum untrimmed L/D for the basic model (with high horizontal stabilizer) by 2 percent while the best pod nacelles decreased the L/D of the basic model (with low horizontal stabilizer) by 11 percent. Since the general shapes of the lift-drag-ratio curves of the trimmed and untrimmed basic model (fig. 15) are similar, it is thought that the effects of nacelles on the lift-drag ratio of the untrimmed model (fig. 22) are indicative of the effects of nacelles on the lift-drag ratio of the trimmed model.

Short fuselage.- The effect of shortening the fuselage length between the wing and tail by 4 inches, or nearly 10 percent (see fig. 2), is shown in figure 23 ($M = 1.41$ only). The characteristics of this model are essentially the same as those of the long fuselage model. The shortened tail decreased the stability of the complete model by about 5 percent. This is only 25 percent of the stability decrease which would be predicted from the change in length of the two tail moment arms (center of pressure of stabilizer was computed by means of linear theory). It appears that shortening the distance between the wing and tail has resulted in an increase in the effectiveness of the horizontal tail in producing pitching moment, probably as a result of decreased downwash.

Fuselage nose shapes.- The effects of four fuselage nose shapes (fig. 5) are shown in figure 24. The lift and moment characteristics of the four configurations were essentially the same at each Mach number. At both Mach numbers, the model with the cusp-nose had the highest minimum drag of 0.029; the ogive-nose configurations had the lowest minimum drags of 0.027.

Lateral Force and Moment Characteristics

Model breakdown.- The lateral stability characteristics of various combinations of fuselage, wing, and tail are shown in figure 25.

The configurations which do not include the vertical tail are directionally unstable. The vertical tail produces a high degree of

directional stability. Addition of the wing to the fuselage has a small effect, changing the slope of the curve in a stable direction. When added to the fuselage with tails, however, the wing introduces unfavorable sidewash and changes the slope of the curve slightly in the direction of decreased stability.

The following table compares the measured values of C_{n_ψ} due to adding the vertical tail to the fuselage and to the fuselage plus wing with the values of C_{n_ψ} calculated for the vertical tail by means of linear theory (refs. 2 and 3):

Configuration	ΔC_{n_ψ} due to vertical tail	
	M = 1.41	M = 2.01
Wing on	-0.0041	-0.0027
Wing off	-.0043	-.0031
Linear theory	-.0037	-.0026

The calculation assumed a lifting surface whose semispan plan form was identical with that of the vertical tail. This assumption effectively introduces a reflection plane at the root of the vertical tail, a condition not exactly fulfilled by the fuselage. The table shows that the magnitude of this incremental stability derivative can be approximately calculated by the linear theory in this case. The magnitude is slightly underestimated, as is the change with Mach number.

The rolling-moment characteristics (fig. 25) show that the configurations without the vertical tail have approximately zero effective dihedral. The positive effective dihedral measured for the basic configuration is produced largely by the vertical tail. The position of the horizontal tail is shown to have (at M = 1.41) an important effect upon the rolling moment produced by the vertical tail. The slope of the rolling-moment curve for the basic model is decreased by about one-half when the horizontal tail is moved from the high to the low position. Examination of the yawing-moment and side-force curves shows that only a small increase in vertical-tail load occurred; hence, the change in rolling moment is due principally to a vertical shift in lateral center of pressure of the tail group. Insufficient configurations were tested to explain the nature of this interference effect.

The wing displaces the rolling-moment curves appreciably but has a negligible effect upon the slopes at M = 1.41. At M = 2.01, the wing contributes a significant amount of positive effective dihedral. This result is in accord with the results of some theoretical investigations,

such as reference 4 which indicates that C_{l_ψ} for swept wings with supersonic leading edges can change in this manner as the Mach number is increased.

The fact that many of the yawing-moment and lateral-force curves do not pass through the zero point of the axes is due to a slight asymmetry of the model. The displacement of the rolling-moment curves is, however, too large to be explained by asymmetry. Because balance zeros taken before and after each test were in agreement and because acceptable repeat-points were regularly obtained (see tabulated data) the slopes of the curves obtained are believed to be reliable. The reason for the displacement of the curves is unknown, but appears to be due to some unknown characteristic of the balance.

Rudder effectiveness.- Figure 26 shows the lateral stability characteristics of the model with three rudder deflections. The rolling moment at trim conditions is essentially constant for the three rudder deflections. Thus the rudder deflection essentially cancels the effective dihedral of the airplane which, as has been pointed out previously, is due almost entirely to the vertical tail. The rudder has relatively low effectiveness in producing yaw. The derivative $d\psi/d\delta_r$ is approximately -0.1 at both Mach numbers.

Wing dihedral.- A comparison of the lateral stability characteristics with 0° and 5° of wing dihedral is shown in figure 27. The contribution of the 0° dihedral wing to C_{l_ψ} is small at both Mach numbers (fig. 25). The increment due to the 5° dihedral wing is large at both Mach numbers.

The following table compares the incremental values of C_{l_ψ} computed for an increase in wing dihedral of 5° by the method of reference 5 with the measured difference in rolling moments between the 0° and 5° dihedral wings:

Configuration	M	ΔC_{l_ψ}	
		Measured	Computed, ref 5
Basic model	1.41	0.0008	0.0009
Basic model	2.01	.0005	.0008
Tail off	1.41	.0009	.0009
Tail off	2.01	.0007	.0008

In general, the agreement between the measured and calculated values is good.

As would be expected, increasing the dihedral to 5° decreased slightly the directional stability of the basic model but had virtually no effect upon the lateral-force coefficients.

Wing incidence.- From figure 28 it can be seen that the effects on the lateral stability characteristics of changing wing incidence from 4° to 2° are small, the principal effect being a decrease in the effective dihedral at $M = 2.01$.

Nacelles.- Figure 29 shows that the largest effect of the nacelles on the lateral stability is on the rolling-moment coefficient.

The high positive effective dihedral of the model without nacelles is increased slightly by the addition of the buried nacelles. The effect of all pod nacelles is to decrease the effective dihedral of the basic configuration because the lateral center of area of the nacelle-strut combination is well below the center line of the fuselage (fig. 8). The effective dihedral for the model (fig. 29) with the pod nacelles at 0.60 semispan is less than that for the model with pod nacelles at 0.50 semispan and is actually slightly negative for small yaw angles at $M = 1.41$ (horizontal tail in low position). Examination of the lift variation with angle of yaw (not presented) shows no difference in lift between these two configurations; hence, the interference which causes the difference in rolling moment between the pod nacelles at 0.50 and 0.60 semispan is not defined by the data obtained.

The yawing-moment variation is little affected by the nacelle installation. The slope of the lateral-force-coefficient curve (fig. 29) is higher for the model with pod nacelles installed as a consequence of the lateral area presented by the nacelle-strut combination.

Comparison of original and shortened fuselage.- Two tests were made at $M = 1.41$ with the fuselage shortened 4 inches from its original length of 41.32 inches. Figure 30 shows a comparison of the lateral characteristics of the model with the shortened and long (original) fuselage.

The changes in lateral force are small because the change in lateral area is small.

The directional stability is lowered for the short fuselage in the case of the tail-on configuration because of the decreased moment arm of the vertical tail. The ratio of the values of C_{n_ψ} for the short and long fuselage at trim (tail on) is almost exactly equal to the ratio of tail lengths, that is, the distances from center of moments to the calculated centers of pressure of the vertical tail.

The rolling moment is unaffected by change in tail length for configurations without the vertical tail. The effective dihedral of the basic configurations with original and shortened fuselage is essentially the same at high positive and negative yaw angles. The shift in the rolling-moment curve which occurs at low angles is believed due to increased sidewash effects which occur when the tail is moved closer to the wing.

CONCLUDING REMARKS

An investigation of the aerodynamic characteristics of the MX-1712 configuration was performed in the Langley 4- by 4-foot supersonic pressure tunnel at Mach numbers of 1.41 and 2.01 at a Reynolds number of 2.6×10^6. The model incorporated a tapered wing having a thickness ratio of 5.5 percent, 47° sweep of the quarter-chord line, an aspect ratio of 3.5, and a taper ratio of 0.2.

The investigation disclosed no unusual stability characteristics or Mach number effects. The various nacelle installations were found to differ greatly in their effect upon the airplane L/D; hence, the choice of engine-nacelle installation is of major importance. At $M = 1.41$ and $C_L = 0.1$, the buried nacelles increased the drag of the basic model by 9 percent, while the best pod nacelles increased the drag of the basic model by 27 percent.

The effectiveness of the horizontal tail in changing trim lift coefficient was about the same for the high and low positions, and the relative effectiveness of the elevator was proportional to the ratio of elevator area to stabilizer area.

The wing modification was found to have negligible effects on lift and stability and increased the drag (at trim) of the basic model by 10 percent or less at both Mach numbers.

The positive effective dihedral of the basic model was due entirely to the increment produced by the vertical tail. This increment was found to be approximately equal to that produced by changing wing dihedral from 0° to 5°. The rudder was of relatively low effectiveness in producing sideslip.

The shortened fuselage affected the lateral stability in proportion to the change in moment arm of the vertical tail. The longitudinal stability, however, was less affected due evidently to an accompanying increase in horizontal-tail effectiveness as a result of decreased downwash in the field closer to the wing.

Langley Aeronautical Laboratory,
National Advisory Committee for Aeronautics,
Langley Field, Va.

Norman F. Smith
Aeronautical Research Scientist

Lowell E. Hasel
Aeronautical Research Scientist

Approved:

John V. Becker
Chief of Compressibility Research Division

vr

APPENDIX

Several assumptions must be made before the two static orifices which were installed in the nacelle ducts can be used to compute the internal drag and mass-flow coefficients of the nacelles. The stagnation pressure and temperature must be assumed to be the same at the two stations, and the flow across the duct must be assumed to be uniform. The latter assumption appears to be the more questionable, particularly at angles of attack. It should be remembered, however, that the errors which may be introduced by the above assumptions will have only a minor influence on the external drag of the basic model with nacelles because the absolute magnitude of the internal drag is small.

The internal drag, D_I, is defined as

$$D_I = A_e(p - p_e) + m_e(V - V_e) \tag{1}$$

where

A duct area

p static pressure

V velocity

$m = \rho AV$

ρ density

Symbols with subscript e refer to duct exit conditions and symbols without subscripts refer to free-stream conditions.

Using the assumptions discussed above, the following equation for the internal drag coefficient of each nacelle duct can be derived:

$$C_{D_I} = \frac{2}{\gamma M^2}\frac{A_e}{S}\left\{1 - \frac{p_e}{p} + \frac{p_e}{p}\gamma M_e^2\left[\frac{M}{M_e}\left(\frac{1 + \frac{\gamma - 1}{2}M_e^2}{1 + \frac{\gamma - 1}{2}M^2}\right)^{1/2} - 1\right]\right\} \tag{2}$$

where γ is the ratio of specific heats, for air, 1.40.

The value of M_e is a function of the static-pressure ratio and the area ratio at the two orifice stations. It should be noted that the values obtained from equations (1) and (2) are axial forces. The absolute magnitude of these forces is small enough, however, so that the $\cos \alpha$ correction which must be applied to obtain true drag forces is negligible and has therefore been neglected.

The mass-flow ratio m_e/m is defined by the ratio

$$\frac{m_e}{m} = \frac{\rho_e A_e V_e}{\rho A_e V} \tag{3}$$

The internal drag (based on wing area) and mass-flow characteristics of the nacelles are presented in figures 31 and 32, respectively. The mass-flow ratios are based on the duct exit area since this area was the same for all nacelle installations and therefore provides a common basis for comparison. No data are presented for the inboard duct of the buried nacelles at $M = 1.41$ because unsatisfactory measurements of the internal static pressure were made.

The internal drag of the individual ducts (fig. 31) varied little with Mach number or angle of attack. At a Mach number of 2.01, the outboard and inboard ducts of the buried nacelles have the same value of internal drag. The value is slightly higher than that of the cone-pod nacelle. At a Mach number of 1.41, the wedge-pod has the lowest internal drag. Assuming an average internal drag value of 0.0006 per duct, the total internal drag of a four-duct installation is about 9 percent of the drag of the basic model. It should be mentioned that these values are not necessarily optimum values for a well-designed installation, since no effort was made to control the shock position in the diffuser.

At both Mach numbers, the variation of the mass flow with angle of attack (fig. 32) of the pod nacelles is less than that of the buried nacelles. Over the entire angle range, the mass flow of the wedge-pod nacelle varies less than 0.02 at a Mach number of 1.41.

The cone-pod nacelle was designed so that there would be no spillage at a Mach number of 2.01. Therefore, since the entrance area is equal to the exit area upon which the coefficients are based, the mass-flow ratio should be 1.0 at 0° angle of attack, and figure 32 shows this to be true. According to reference 6, the design mass-flow ratio of the conical inlet should be about 0.77 at a Mach number of 1.41. The lower value of 0.69 obtained experimentally may be caused by too much internal contraction. At a Mach number of 1.41, the mass flow through the buried nacelles is greater than through the cone-pod nacelle and, at a Mach number of 2.01, the mass flow through the cone-pod nacelle is greater. It is thought (on the basis of the inlet geometry) that the mass-flow ratio through the wedge-pod nacelle would also have been 1.0 if it had been tested at a Mach number of 2.01.

REFERENCES

1. Hasel, Lowell E., and Sinclair, Archibald R.: A Pressure-Distribution Investigation of a Supersonic-Aircraft Fuselage and Calibration of the Mach Number 1.40 Nozzle of the Langley 4- by 4-Foot Supersonic Tunnel. NACA RM L50B14a, 1950.

2. Harmon, Sidney M., and Jeffreys, Isabella: Theoretical Lift and Damping in Roll of Thin Wings With Arbitrary Sweep and Taper at Supersonic Speeds. Supersonic Leading and Trailing Edges. NACA TN 2114, 1950.

3. Malvestuto, Frank S., Jr., Margolis, Kenneth, and Ribner, Herbert S.: Theoretical Lift and Damping In Roll at Supersonic Speeds of Thin Sweptback Tapered Wings With Streamwise Tips, Subsonic Leading Edges, and Supersonic Trailing Edges. NACA Rep. 970, 1950. (Supersedes NACA TN 1860.)

4. Jones, Arthur L., Spreiter, John R., and Alksne, Alberta: The Rolling Moment Due to Sideslip of Triangular, Trapezoidal, and Related Plan Forms in Supersonic Flow. NACA TN 1700, 1948.

5. Purser, Paul E.: An Approximation to the Effect of Geometric Dihedral on the Rolling Moment Due to Sideslip for Wings at Transonic and Supersonic Speeds. NACA RM L52B01, 1952.

6. Sibulkin, Merwin: Theoretical and Experimental Investigation of Additive Drag. NACA RM E51B13, 1951.

TABLE I.- GEOMETRIC CHARACTERISTICS OF MODEL

Wing:	
Area, sq ft (includes area blanketed by fuselage)	1.367
Span, ft	2.188
Aspect ratio	3.5
Sweepback of quarter-chord line, deg	47
Taper ratio	0.2
Mean aerodynamic chord, ft	0.718
Airfoil section thickness in streamwise direction, percent (see tables II and III for ordinates)	5.5
Twist, deg (linear variation from root to tip)	0 to 2.5 washout at tip
High horizontal tail:	
Area, sq ft (includes area blanketed by vertical tail)	0.154
Span, ft	0.733
Aspect ratio	3.5
Sweepback of quarter-chord line, deg	47
Taper ratio	0.2
Airfoil section thickness in streamwise direction, percent (see table IV for ordinates)	5.5
Total elevator area, sq ft	0.0226
Low horizontal tail:	
Area, sq ft (includes area blanketed by fuselage)	0.191
Span, ft	0.768
Aspect ratio	3.65
Sweepback of quarter-chord line, deg	47
Taper ratio	0.2
Airfoil section thickness in streamwise direction, percent (see table IV for ordinates)	5.5
Total elevator area, sq ft	0.0226
Vertical tail:	
Area (exposed), sq ft	0.121
Span (exposed), ft	0.425
Aspect ratio (based on exposed span and area)	1.5
Sweepback of quarter-chord line, deg	47
Taper ratio (based on exposed span and area)	1.5
Airfoil section thickness in streamwise direction, percent (see table IV for ordinates)	5.5
Rudder area, sq ft	0.0166

TABLE I.- GEOMETRIC CHARACTERISTICS OF MODEL - Concluded

Fuselage:	
Fineness ratio (original fuselage, canopy nose)	14.35
Fineness ratio (shortened fuselage, canopy nose)	12.96
Frontal area, sq ft	0.0452
Miscellaneous:	
Tail length from 0.35 wing M.A.C. to 0.35 tail M.A.C. (original fuselage), ft	1.636
Tail length from 0.35 wing M.A.C. to 0.35 tail M.A.C. (shortened fuselage), ft	1.302

TABLE II.- ORDINATES OF ORIGINAL WING

[Values are in inches]

Semispan station 1.440			Semispan station 4.437			Semispan station 13.054		
Chord station	Upper ordinate	Lower ordinate	Chord station	Upper ordinate	Lower ordinate	Chord station	Upper ordinate	Lower ordinate
0	0.0057	0	0	0.0046	0	0	0.0013	0
.057	.0608	.0384	.046	.0486	.0307	.0128	.0136	.0086
.086	.0753	.0456	.068	.0602	.0365	.0192	.0169	.0102
.143	.0981	.0539	.114	.0784	.0431	.0319	.0220	.0121
.285	.1385	.0618	.228	.1108	.0495	.0639	.0310	.0138
.570	.201	.074	.456	.1608	.0593	.128	.0460	.0166
.855	.249	.086	.684	.199	.069	.192	.056	.019
1.140	.285	.098	.912	.228	.078	.255	.064	.022
1.710	.339	.122	1.368	.271	.098	.383	.076	.027
2.281	.372	.146	1.824	.297	.117	.511	.083	.033
2.851	.395	.168	2.280	.316	.134	.639	.088	.038
3.421	.413	.183	2.736	.330	.146	.766	.093	.041
3.991	.422	.196	3.192	.337	.156	.894	.094	.044
4.561	.425	.201	3.648	.340	.161	1.022	.095	.045
5.131	.421	.203	4.104	.336	.162	1.149	.094	.046
5.701	.408	.198	4.560	.326	.159	1.277	.091	.044
6.272	.387	.186	5.015	.310	.149	1.405	.087	.042
6.842	.358	.168	5.471	.286	.135	1.532	.080	.038
7.412	.322	.148	5.927	.258	.118	1.660	.072	.033
7.982	.281	.127	6.383	.225	.102	1.788	.063	.028
9.122	.192	.085	7.295	.153	.068	2.043	.043	.019
10.263	.096	.042	8.207	.077	.034	2.299	.022	.010
11.403	.011	.011	9.119	.009	.009	2.554	.0025	.0025
Leading-edge radius, 0.023 *d = 0.0123			Leading-edge radius, 0.018 d = 0.0379			Leading-edge radius, 0.005 d = 0.1114		

*d is the vertical distance between the leading-edge point of a section chord line and the root-chord plane.

TABLE III.- ORDINATES OF MODIFIED WING

[Values are in inches]

Semispan station 1.440			Semispan station 2.625			Semispan station 10.500			Semispan station 13.054		
Chord station	Upper ordinate	Lower ordinate	Chord station	Upper ordinate	Lower ordinate	Chord station	Upper ordinate	Lower ordinate	Chord station	Upper ordinate	Lower ordinate
0	0.006	0	0	0.005	0	0	-0.093	0.099	0	-0.053	0.056
.057	.061	.038	.052	.056	.035	.022	-.063	.106	.013	-.036	.060
.086	.075	.046	.079	.069	.042	.034	-.054	.106	.019	-.030	.060
.143	.098	.054	.131	.090	.050	.056	-.038	.103	.032	-.022	.058
.285	.138	.062	.262	.128	.057	.112	-.007	.092	.064	-.004	.052
.570	.201	.074	.525	.185	.068	.225	.041	.072	.128	.023	.041
.855	.249	.086	.788	.229	.079	.338	.076	.059	.192	.043	.033
1.140	.285	.098	1.050	.262	.090	.450	.101	.052	.255	.057	.029
1.710	.339	.122	1.575	.312	.112	.675	.133	.050	.383	.075	.028
2.281	.372	.146	2.100	.342	.134	.900	.147	.058	.511	.083	.033
3.421	.413	.183	3.150	.380	.168	1.350	.163	.072	.766	.092	.041
4.561	.425	.201	4.200	.391	.185	1.800	.168	.079	1.022	.095	.045
5.701	.408	.198	5.250	.376	.183	2.250	.161	.078	1.278	.091	.044
6.842	.358	.168	6.300	.329	.155	2.700	.141	.066	1.532	.080	.038
7.982	.281	.127	7.350	.259	.117	3.150	.111	.055	1.788	.063	.028
9.122	.192	.085	8.400	.176	↕	3.600	.076	↕	2.043	.043	↕
10.263	.096	.042	9.450	.088	↕	4.050	↕	↕	-----	↕	↕
11.403	.011	.011	10.500	.010	.010	4.500	.0045	.0045	2.554	.0025	.0025
Leading-edge radius, 0.023 *d = 0.0123			Leading-edge radius, 0.021 d = 0.0224			Leading-edge radius, 0.009 d = 0.0896			Leading-edge radius, 0.005 d = 0.1114		

*d is the vertical distance between the leading-edge point of a section chord line and the root-chord plane.

TABLE IV.- SECTION ORDINATES FOR HORIZONTAL AND VERTICAL TAILS

[Values are in percent of total chord length]

Chord	Symmetrical ordinate
0	0
.50	.436
.75	.526
1.25	.675
2.50	.876
5.00	1.201
7.50	1.456
10.00	1.672
15.00	2.014
20.00	2.275
25.00	2.472
30.00	2.614
40.00	2.748
50.00	2.658
60.00	2.308
70.00	1.774
100.00	0

Leading-edge radii:

Horizontal tail, root, in.	0.011
Horizontal tail, tip, in.	0.002
Vertical tail, root, in.	0.008
Vertical tail, tip, in.	0.002

TABLE V.- TABULATION OF CONFIGURATIONS FOR PITCH TESTS

(a) M = 1.41

Run	Fuselage length	Fuselage nose shape	Wing configuration	Wing incidence, deg	Wing dihedral, deg	Horizontal tail position	Horizontal tail incidence, deg	Elevator angle, deg	Vertical tail	Rudder angle, deg	Nacelle configuration	Nacelle semispan location, percent	Remarks
48	Standard	Canopy	Original	4	0	High	-8	0	On	0	Off	---	
49							-3					---	
50							2					---	
51							-3	-10				---	
52								-20				---	
53						Off	---	---				---	
54						Low	2	0				---	
55							-8					---	
56							-3					---	
57			Off	---	---							---	
58				---	---	High						---	
59			Modified	4		Low					Wedge-pod	60	
60											Off	---	
61			Original								Wedge-pod	60	
62						Off	---	---					
63						Low	-3	0			Wedge-pod	50	Nacelle internal drag measured
64											Cone-pod		Nacelle internal drag measured
65												60	
66													
71											Off	---	Check of run 56
72						High					Buried		Nacelle internal drag measured
73													
74						Off	---	---					
81			Off	---	---		-3	0	Off	---	Off	---	
86			Original	2						---		---	
87						Low			On	0		---	
88				4		Off	---	---			Cone-pod	60	
89			Modified				-3	0			Off	---	
90	Shortened		Original						Off	---		---	
93						Low			On	0		---	
94		Blunt ogive cusp										---	
95												---	
96		Sharp ogive										---	

TABLE V.- TABULATION OF CONFIGURATIONS FOR PITCH TESTS - Concluded

(b) M = 2.01

Run	Fuselage length	Fuselage nose shape	Wing configuration	Wing incidence, deg	Wing dihedral deg	Horizontal tail position	Horizontal tail incidence, deg	Elevator angle, deg	Vertical tail	Rudder angle, deg	Nacelle configuration	Nacelle semispan location, percent	Remarks
1	Standard	Canopy	Original	4	0	Low	2	0	On	0	Off	---	Model joints not faired
2							↓					---	
3							-3					---	
4						↓	-8	↓				---	
5						Off	---	---				---	
6						High	-3	0				---	
7							-8					---	
8							-13					---	
9							2					---	
10		↓					7					---	
11		Cusp					-3					---	
12		Blunt ogive										---	
13		Sharp ogive										---	
14		Canopy						↓				---	Check of run 6
15								-5				---	
16								-10				---	
17								10				---	
18							↓	-20			↓	---	
20						Off	---	---			Cone-pod	50	Nacelle internal drag measured
21							---	---			↓	↓	
22							---	---			Off	---	
23						↓	---	---			Cone-pod	60	
24						Low	-3	0			↓	↓	
34				↓		Off	---	---			Off	---	
35				2		Low	-3	0				---	
36			Off	↓	↓	↓						---	
37			↓	---	---	High	↓	↓	↓	↓	↓	---	
39			↓	---	---	Off	---	---	Off	---	↓	---	
40			Original	4	0	High	-3	0	On	0	Buried		
41						↓	↓	↓					
42						Off	---	---					
44						High	-3	0			↓		Nacelle internal drag measured
45											Off	---	Check of run 6
46												---	Gap between horizontal and vertical tail filled
47	↓	↓	Modified	↓	↓	↓	↓	↓	↓	↓	↓	---	Gap between horizontal and vertical tail filled

TABLE VI.- TABULATION OF CONFIGURATIONS FOR YAW TESTS

Run	Fuselage length	Fuselage nose shape	Wing Configuration	Wing incidence, deg	Wing dihedral, deg	Horizontal tail position	Horizontal tail incidence, deg	Elevator angle, deg	Vertical tail	Rudder angle, deg	Nacelle configuration	Nacelle semispan location, percent
M = 1.41												
67	Standard	Canopy	Original	4	0	Low	-3	0	On	0	Cone-pod	60
68											Off	---
69											Wedge-pod	60
70											Cone-pod	50
75						High					Buried	
76			Off	---	---						Off	---
77			Original	4	0					0		---
78										-5		---
79										-10		---
80					5					0		---
82			Off	---	---	Off	---	---	Off	---		---
83			Original	4	0		---	---		---		---
84					5		---	---		---		---
85				2	0		---	---		---		---
91	Shortened			4			---	---		---		---
92						Low	-3	0	On	0		---
M = 2.01												
19	Standard		Original	4	0	High	-3	0	On	0	Off	---
25											Cone-pod	60
26												50
27										-5	Off	---
28										-10		---
29						Off	---	---	Off	---		---
30					5	High	-3	0	On	0		---
31						Off	---	---	Off	---		---
32			Off	---	---		---	---		---		---
33			Original	2	0		---	---		---		---
38			Off	---		High	-3	0	On	0		---
43			Original	4							Buried	

TABLE VII.- TABULATED DATA FOR PITCH TESTS, M = 1.41

Run	α	C_L	C_D	C_m
48	-1.8	0.028	0.034	0.101
	.4	.163	.039	.062
	2.6	.292	.055	.021
	4.6	.417	.077	-.017
	6.7	.535	.110	-.050
	8.8	.645	.149	-.077
	10.9	.743	.195	-.097
	-1.8	.027	.034	.102
49	-8.5	-0.361	0.062	0.164
	-6.3	-.231	.042	.125
	-4.1	-.086	.030	.079
	-1.9	.054	.029	.038
	.3	.182	.035	-.002
	2.5	.318	.053	-.047
	4.5	.441	.077	-.085
	6.7	.559	.109	-.117
	8.8	.667	.150	-.142
	10.9	.767	.198	-.162
	4.5	.440	.076	-.084
	.3	.184	.035	-.003
	-.8	.117	.030	.019
	-2.9	-.015	.028	.058
50	-4.1	-0.061	0.025	0.013
	-8.4	-.341	.055	.103
	-6.3	-.209	.036	.061
	-1.9	.077	.026	-.027
	.2	.208	.034	-.066
	2.4	.341	.052	-.110
	4.5	.467	.078	-.148
	5.6	.524	.094	-.166
	-3.0	.010	.025	-.008
	-4.1	-.062	.025	.013
51	-4.0	-0.093	0.032	0.101
	-6.2	-.239	.043	.148
	-1.8	.043	.031	.061
	.3	.177	.038	.019
	2.5	.311	.054	-.026
	4.5	.436	.078	-.066
	6.7	.554	.111	-.099
	8.8	.662	.150	-.125
	10.9	.762	.198	-.143
	-1.8	.043	.031	.060
52	-6.1	-0.243	0.047	0.165
	-4.0	-.100	.035	.120
	-1.8	.039	.034	.079
	.4	.171	.040	.037
	2.5	.307	.057	-.009
	4.5	.431	.081	-.048
	6.7	.550	.113	-.082
	8.8	.657	.153	-.109
	10.9	.756	.200	-.127
	-4.0	-.099	.035	.119
53	-8.5	-0.312	0.051	0.021
	-6.3	-.188	.034	.002
	-4.1	-.049	.024	-.021
	-1.9	.082	.025	-.040
	.3	.209	.033	-.059
	2.4	.332	.051	-.080
	4.5	.448	.075	-.099
	6.7	.560	.109	-.114
	8.8	.663	.148	-.125
	10.9	.757	.196	-.133
	-4.1	-.050	.024	-.021
54	-4.1	-0.058	0.025	0.005
	-8.4	-.339	.055	.099
	-6.3	-.206	.035	.055
	-1.9	.081	.026	-.039
	.2	.218	.035	-.082
	2.4	.348	.053	-.127
	4.5	.472	.078	-.165
	5.0	.502	.087	-.174
	-4.1	-.059	.025	.005
	5.0	.502	.087	-.174
55	-4.0	-0.106	0.036	0.131
	-6.1	-.248	.069	.179
	-1.8	.034	.034	.091
	.4	.167	.040	.050
	2.5	.295	.056	.007
	4.5	.419	.079	-.032
	6.7	.538	.110	-.066
	8.8	.648	.149	-.095
	10.9	.748	.196	-.121
	-4.0	-.107	.037	.132
56	-4.0	-0.080	0.030	0.070
	-8.3	-.362	.061	.163
	-6.2	-.228	.040	.121
	-1.9	.062	.029	.026
	.3	.191	.035	-.015
	2.5	.324	.052	-.060
	4.5	.448	.077	-.098
	6.6	.566	.110	-.131
	8.8	.675	.151	-.160
	10.9	.776	.198	-.186
	-4.0	-.085	.029	.072
57	-5.9	-0.063	.019	0.110
	-3.9	-.047	.015	.088
	-1.9	-.033	.012	.064
	0	-.017	.011	.040
	2.0	-.002	.010	.017
	4.0	.011	.011	-.004
	6.0	.027	.012	-.026
	8.0	.042	.015	-.048
	10.0	.058	.018	-.068
	-5.9	-.062	.019	.110
58	-5.9	-0.063	.019	0.109
	-3.9	-.048	.016	.089
	-1.9	-.036	.013	.070
	.1	-.022	.012	.050
	2.0	-.010	.011	.031
	4.0	.002	.011	.016
	6.0	.014	.012	-.001
	8.0	.027	.013	-.015
	10.0	.038	.016	-.025
	-5.9	-.062	.019	.109
59	-4.1	-0.122	0.045	0.085
	-8.4	-.397	.084	.157
	-6.2	-.263	.059	.122
	-1.9	.035	.040	.040
	.3	.189	.047	-.008
	2.5	.329	.064	-.052
	4.5	.462	.089	-.088
	6.7	.589	.123	-.116
	8.8	.708	.164	-.140
	11.0	.814	.213	-.157
	-4.1	-.115	.044	.084

TABLE VII.- TABULATED DATA FOR PITCH TESTS, M = 1.41 - Continued

Run	α	C_L	C_D	C_m
60	-6.2	-0.234	0.046	0.120
	-4.0	-.092	.032	.073
	-1.9	.051	.031	.027
	.3	.193	.038	-.020
	2.4	.319	.054	-.062
	4.5	.441	.078	-.097
	6.6	.557	.110	-.127
	8.8	.666	.149	-.153
	10.9	.768	.195	-.178
	-6.2	-.235	.046	.122
61	-6.2	-0.246	0.054	0.120
	-4.0	-.102	.040	.079
	-1.9	.047	.038	.034
	.3	.195	.046	-.011
	2.4	.330	.062	-.052
	4.6	.465	.088	-.089
	6.7	.591	.123	-.119
	8.8	.710	.166	-.145
	11.0	.816	.214	-.163
	-6.2	-.245	.054	.120
62	-4.2	-0.068	0.036	-0.021
	-6.4	-.206	.047	-.005
	-2.0	.069	.034	-.039
	.3	.210	.043	-.058
	2.4	.341	.060	-.075
	4.5	.465	.086	-.092
	6.7	.589	.121	-.105
	8.9	.702	.164	-.114
	11.0	.802	.212	-.115
	12.1	.844	.237	-.113
	-4.2	-.071	.035	-.021
63	-6.2	-0.249	0.054	0.109
	-4.1	-.100	.040	.065
	-1.9	.049	.037	.020
	.3	.197	.044	-.023
	2.4	.329	.061	-.059
	4.5	.459	.087	-.089
	6.7	.584	.120	-.117
	8.8	.701	.163	-.138
	11.0	.801	.210	-.152
	-6.2	-.251	.053	.109
64	-6.2	-0.238	0.055	0.129
	-4.0	-.093	.043	.068
	-1.9	.054	.039	.023
	.3	.201	.048	-.020
	2.5	.332	.066	-.056
	4.5	.461	.090	-.086
	6.7	.586	.125	-.114
	8.8	.701	.167	-.136
	11.0	.800	.215	-.152
	-6.2	-.239	.056	.112
65	-4.0	-0.097	0.043	0.072
	.3	.202	.048	-.018
	4.6	.462	.091	-.085
	8.8	.702	.168	-.136
	-4.0	-.096	.043	.072
66	-4.0	-0.096	0.044	0.084
	-8.4	-.378	.080	.164
	-6.2	-.246	.057	.128
	-1.9	.049	.041	.039
	.3	.198	.049	-.007
	2.5	.337	.066	-.050
	4.6	.469	.091	-.087
	6.7	.599	.127	-.118
	8.8	.715	.171	-.144
	11.0	.821	.220	-.164
	-4.0	-.102	.043	.086
71	-4.0	-0.084	0.030	0.071
	.3	.191	.036	-.016
	4.5	.442	.077	-.097
	8.8	.670	.150	-.159
	-1.9	.053	.029	.011
	-4.0	-.084	.030	.071
72	-6.2	-0.234	0.045	0.126
	-4.0	-.083	.035	.077
	-1.8	.066	.034	.033
	.4	.208	.042	-.009
	2.4	.341	.061	-.051
	4.6	.470	.087	-.089
	6.7	.592	.124	-.120
	8.8	.703	.167	-.144
	11.0	.805	.217	-.160
	-6.2	-.235	.045	.127
73	-6.2	-0.235	0.046	0.127
	-1.8	.064	.033	.034
	2.4	.340	.060	-.050
	6.7	.592	.123	-.120
	-6.2	-.241	.045	.129
74	-4.1	-0.054	0.029	-0.019
	-6.4	-.203	.039	.007
	-1.9	.090	.029	-.044
	.3	.227	.039	-.067
	2.4	.355	.059	-.091
	4.5	.471	.085	-.113
	6.7	.597	.122	-.133
	8.8	.706	.165	-.150
	11.0	.809	.217	-.162
	.3	.223	.039	-.065
	-6.3	-.202	.038	.011
	-4.1	-.055	.028	-.018
81	-6.1	-0.007	0.009	-0.020
	-4.0	-.004	.008	-.015
	-2.0	-.002	.008	-.008
	0	-.001	.008	-.001
	2.0	.001	.008	.006
	4.0	.003	.008	.013
	6.0	.005	.008	.019
	8.0	.010	.009	.025
	10.1	.015	.010	.031
	-6.1	-.007	.009	-.020
86	-2.1	-0.028	0.023	-0.017
	-6.5	-.291	.047	.022
	-4.3	-.167	.030	.004
	.1	.100	.024	-.034
	2.3	.221	.033	-.051
	4.4	.342	.051	-.070
	6.5	.457	.077	-.086
	8.7	.567	.111	-.101
	10.8	.667	.152	-.111
	.1	.096	.024	-.033
	-2.1	-.031	.023	-.016
87	-6.4	-0.330	0.055	0.139
	-4.2	-.194	.036	.096
	-2.1	.048	.027	.048
	.2	.086	.028	.008
	2.3	.216	.037	-.032
	4.4	.341	.054	-.072
	6.5	.464	.080	-.108
	8.6	.581	.113	-.142
	10.7	.691	.154	-.174
	-6.4	-.330	.055	.139

TABLE VII.- TABULATED DATA FOR PITCH TESTS, M = 1.41 - Concluded

Run	α	C_L	C_D	C_m
88	-6.5	-0.200	0.050	-0.001
	-4.2	-.062	.038	-.018
	-2.0	.080	.037	-.038
	.3	.221	.045	-.059
	2.4	.348	.064	-.076
	4.6	.473	.091	-.092
	6.7	.596	.125	-.105
	8.8	.708	.168	-.114
	11.0	.810	.218	-.117
	-6.4	-.196	.049	-.001
89	-4.1	-0.155	0.034	-0.020
	-6.4	-.196	.039	.003
	-1.9	.074	.027	-.041
	.3	.210	.036	-.063
	2.5	.331	.052	-.083
	4.6	.447	.077	-.100
	6.7	.555	.109	-.113
	8.8	.657	.146	-.122
	10.9	.752	.193	-.129
	13.0	.839	.243	-.133
	-4.1	-.063	.026	-.019
90	-6.4	-0.174	0.030	-0.001
	-4.3	-.043	.021	-.024
	-2.0	.085	.022	-.042
	.2	.209	.030	-.061
	2.3	.324	.046	-.081
	4.3	.437	.071	-.098
	6.4	.546	.101	-.114
	8.5	.648	.139	-.125
	10.6	.740	.185	-.133
	-6.3	-.176	.029	0
93	-6.2	-0.226	0.040	0.098
	-4.0	-.082	.029	.054
	-1.8	.055	.028	.015
	.4	.190	.035	-.027
	2.4	.316	.051	-.067
	4.4	.436	.074	-.101
	6.4	.552	.105	-.132
	8.5	.661	.143	-.159
	-6.1	-.223	.038	.098
94	-6.2	-0.227	0.039	0.100
	-4.0	-.081	.028	.055
	-1.9	.056	.027	.016
	.4	.191	.033	-.026
	2.4	.318	.050	-.066
	4.4	.437	.073	-.101
	6.4	.554	.105	-.132
	8.5	.662	.142	-.159
	-6.2	-.228	.039	.100
95	-6.2	-0.226	0.042	0.098
	-4.0	-.081	.030	.054
	-1.8	.056	.030	.015
	.4	.191	.037	-.026
	2.4	.316	.053	-.065
	4.4	.437	.076	-.100
	6.4	.553	.107	-.131
	8.5	.663	.146	-.158
	-6.2	-.226	.042	.098
96	-6.1	-0.222	0.038	0.098
	-4.0	-.082	.028	.055
	-1.8	.056	.027	.015
	.4	.191	.034	-.026
	2.4	.317	.050	-.065
	4.4	.436	.073	-.101
	6.4	.554	.104	-.132
	8.5	.663	.142	-.159
	-6.1	-.223	.038	.098

TABLE VIII.- TABULATED DATA FOR PITCH TESTS, M = 2.01

Run	α	C_L	C_D	C_m
1	-6.4	-0.152	0.034	0.037
	-4.2	-.058	.026	.008
	-2.0	.036	.025	-.021
	.1	.128	.032	-.048
	.1	.128	.032	-.048
	2.2	.219	.043	-.077
	4.3	.306	.061	-.100
	6.3	.387	.083	-.122
	8.2	.463	.113	-.141
	-6.4	-.155	.034	.038
	4.3	.305	.061	-.099
	-4.2	-.060	.025	.010
2	-8.4	-0.239	0.047	0.064
	-4.1	-.059	.026	.010
	.1	.132	.031	-.047
	4.3	.309	.062	-.098
	8.3	.468	.112	-.140
	-4.2	-.061	.026	.011
3	-8.3	-0.254	0.053	0.103
	-6.3	-.167	.037	.079
	-4.0	-.074	.029	.051
	-1.9	.020	.027	.023
	.2	.111	.032	-.001
	2.4	.204	.044	-.030
	4.4	.290	.060	-.054
	6.5	.373	.082	-.077
	8.4	.450	.109	-.097
	10.4	.526	.102	-.121
	.2	.110	.032	-.002
4	-8.1	-.267	0.059	0.143
	-6.2	-.181	.044	.119
	-4.0	-.089	.034	.092
	-1.9	.004	.032	.065
	.3	.094	.036	.042
	2.3	.182	.046	.018
	4.5	.269	.062	-.007
	6.6	.353	.083	-.029
	8.5	.432	.108	-.051
	10.5	.508	.140	-.074
	-4.0	-.092	.034	.093
	11.8	.561	.163	-.092
5	-6.5	-0.139	0.032	-0.006
	-4.3	-.050	.024	-.015
	-2.1	.037	.024	-.026
	0	.124	.029	-.035
	2.2	.206	.041	-.044
	4.3	.289	.059	-.053
	6.4	.363	.080	-.060
	8.5	.437	.107	-.066
	10.5	.506	.138	-.072
6	-8.4	-0.251	0.052	0.100
	-6.3	-.166	.038	.080
	-4.1	-.076	.030	.056
	-2.0	.017	.028	.032
	.2	.109	.033	.009
	2.3	.198	.044	-.015
	4.4	.283	.060	-.037
	6.4	.363	.082	-.057
	8.4	.440	.109	-.073
	10.4	.512	.140	-.087
	-1.9	.016	.028	.033
7	-4.1	-0.092	0.036	0.095
	-6.2	-.178	.044	.116
	-8.3	-.262	.060	.137
	-1.8	.003	.032	.071
	.4	.093	.038	.049
	2.5	.182	.047	.026
	4.6	.269	.064	.003
	6.6	.346	.084	-.015
	8.6	.423	.110	-.031
	10.7	.494	.142	-.044
	12.7	.562	.177	-.059
	14.7	.628	.216	-.082
	13.7	.593	.195	-.070
	11.7	.527	.158	-.050
8	-6.1	-0.186	0.052	0.152
	-3.9	-.102	.043	.131
	-1.8	-.011	.040	.108
	.3	.079	.043	.088
	2.5	.167	.053	.065
	4.6	.251	.069	.045
	6.6	.330	.088	.026
	8.6	.407	.113	.010
	10.7	.479	.143	-.003
	12.7	.546	.177	-.015
	13.7	.578	.195	-.025
	-3.9	-.104	.043	.132
9	-8.4	-0.236	0.047	0.063
	-6.4	-.153	.034	.043
	-4.2	-.061	.027	.019
	-2.1	.030	.026	-.006
	0	.123	.031	-.030
	2.1	.211	.043	-.054
	4.2	.300	.061	-.079
	6.3	.381	.084	-.099
	8.4	.457	.111	-.116
	-4.2	-.064	.027	.020
10	-10.4	-0.307	0.064	0.048
	-8.4	-.229	.046	.029
	-6.4	-.141	.033	.007
	-4.3	-.051	.027	-.017
	-2.1	.044	.027	-.044
	0	.137	.033	-.070
	2.1	.225	.046	-.096
	3.2	.272	.055	-.109
	-4.2	-.050	.027	-.017
11	-4.0	-0.075	0.029	0.058
	-6.1	-.166	.037	.081
	-2.0	.016	.027	.034
	.3	.108	.032	.011
	2.4	.201	.044	-.014
	4.5	.282	.060	-.036
	6.5	.364	.082	-.056
	8.5	.441	.109	-.072
	-4.0	-.079	.029	.060
12	-4.1	-0.081	0.031	0.058
	-6.1	-.169	.039	.080
	-2.0	.015	.029	.034
	.3	.107	.034	.011
	2.4	.198	.046	-.012
	4.5	.282	.063	-.034
	6.5	.363	.085	-.053
	8.5	.441	.111	-.068
	-4.0	-.080	.031	.058
	2.4	.198	.046	-.012
13	-4.1	-0.080	0.028	0.059
	-6.1	-.166	.037	.080
	-2.0	.016	.027	.034
	.3	.107	.031	.011
	2.4	.198	.044	-.013
	4.5	.283	.060	-.036
	6.5	.363	.082	-.056
	8.5	.439	.108	-.072
	-4.1	-.080	.029	.059
14	-4.1	-0.078	0.030	0.057
	.3	.105	.033	.010
	2.4	.193	.044	-.014
	4.4	.281	.060	-.037
15	-8.3	-0.255	0.053	0.105
	-4.1	-.080	.030	.062
	-1.9	.013	.029	.037
	.2	.104	.033	.014
	4.4	.279	.061	-.032
	6.2	.361	.081	-.052
	8.5	.437	.109	-.068
	10.5	.513	.140	-.081
	-8.2	-.254	.053	.106

TABLE VIII.- TABULATED DATA FOR PITCH TESTS, M = 2.01 - Continued

Run	α	C_L	C_D	C_m
16	-4.1	-0.082	0.031	0.068
	-6.2	-.169	.039	.091
	-2.0	.013	.029	.043
	.3	.104	.034	.020
	2.4	.193	.044	-.004
	4.3	.279	.061	-.026
	6.5	.359	.083	-.046
	8.5	.435	.109	-.062
	-4.1	-.083	.031	.069
17	-4.2	-0.077	0.030	0.050
	-6.2	-.163	.038	.072
	-2.0	.020	.028	.025
	.3	.110	.034	.002
	2.4	.200	.045	-.023
	4.4	.284	.061	-.046
	6.5	.365	.083	-.066
	8.4	.443	.109	-.082
	-4.2	-.078	.030	.051
18	-4.1	-0.087	0.034	0.078
	-6.2	-.171	.041	.101
	-1.9	.009	.031	.052
	.3	.099	.035	.029
	2.4	.190	.046	.005
	4.5	.274	.063	-.017
	6.6	.355	.085	-.037
	8.6	.432	.111	-.053
	-4.1	-.086	.033	.079
20	-7.3	-0.183	0.049	-0.005
	-4.2	-.062	.037	-.012
	-2.0	.028	.036	-.017
	.2	.119	.042	-.023
	2.4	.208	.054	-.030
	4.5	.296	.072	-.037
	6.6	.381	.098	-.040
	8.7	.461	.127	-.042
	-4.1	-.061	.037	-.011
	10.7	.539	.162	-.043
21	-6.3	-0.148	0.045	-0.007
	-1.9	.029	.036	-.017
	2.4	.208	.054	-.030
	6.6	.382	.098	-.040
	10.7	.540	.162	-.043
	-1.9	.028	.036	-.016
22	-4.1	-0.049	0.024	-0.015
	-2.0	.037	.025	-.025
	.2	.123	.030	-.034
	2.4	.206	.042	-.043
	4.5	.287	.060	-.052
	6.5	.363	.081	-.060
	8.6	.435	.108	-.066
	-4.1	-.054	.025	-.014
23	-4.2	-0.063	0.037	-0.011
	-6.4	-.147	.046	-.005
	-2.0	.029	.036	-.017
	.2	.120	.042	-.025
	2.4	.211	.054	-.033
	4.5	.297	.072	-.041
	6.5	.380	.097	-.047
	8.7	.460	.127	-.051
	2.4	.208	.054	-.033
	-4.2	.069	.028	-.010
24	-8.2	-0.264	0.067	0.103
	-6.3	-.180	.052	.085
	-4.1	-.086	.043	.061
	-1.9	.012	.039	.037
	.2	.109	.045	.013
	2.4	.208	.056	-.015
	4.5	.301	.075	-.039
	6.5	.392	.099	-.061
	8.6	.479	.129	-.080
	10.6	.564	.165	-.100
	-8.3	-.270	.068	.105
34	-2.8	-0.060	0.023	-0.009
	.1	.053	.022	-.021
	2.3	.140	.029	-.030
	4.3	.220	.042	-.038
	6.5	.297	.060	-.046
	8.5	.375	.083	-.052
	10.6	.446	.110	-.058
	-2.7	-.060	.023	-.009
35	-2.0	-0.054	0.027	0.042
	-8.4	-.319	.067	.118
	-6.4	-.236	.047	.095
	-4.2	-.147	.034	.069
	-2.0	-.054	.027	.042
	.2	.042	.026	.012
	2.3	.133	.032	-.015
	4.4	.223	.045	-.039
	6.5	.307	.063	-.062
	8.5	.389	.086	-.087
	10.4	.468	.113	-.110
36	-1.9	-0.027	0.012	0.046
	-7.9	-.060	.021	.080
	-6.0	-.049	.017	.070
	-3.9	-.037	.015	.059
	-1.9	-.026	.012	.046
	.1	-.015	.010	.033
	2.2	-.004	.009	.019
	4.1	.006	.010	.006
	6.2	.019	.012	-.006
	8.0	.032	.014	-.018
	10.0	.046	.017	-.027
37	0.1	-0.020	0.011	0.043
	-8.0	-.059	.021	.077
	-6.0	-.049	.018	.070
	-4.0	-.037	.015	.060
	-1.9	-.029	.012	.052
	.1	-.020	.010	.043
	2.1	-.011	.010	.033
	4.1	-.003	.009	.025
	6.1	.008	.010	.017
	8.1	.019	.012	.011
	10.1	.029	.014	.010
39	-8.2	-0.014	0.010	-0.028
	-6.2	-.009	.009	-.022
	-4.2	-.006	.008	-.016
	-2.0	-.003	.008	-.009
	0	-.001	.008	-.002
	2.1	.002	.007	-.006
	4.1	.004	.007	.013
	6.1	.008	.008	.018
	8.0	.013	.009	.025
	10.0	.021	.011	.032
	-8.2	-.015	.011	-.028

TABLE VIII.- TABULATED DATA FOR PITCH TESTS, M = 2.01 - Concluded

Run	α	C_L	C_D	C_m
40	-8.4	-0.265	0.058	0.109
	-6.4	-.145	.040	.085
	-4.2	-.079	.034	.059
	-2.0	.020	.032	.032
	.2	.119	.038	.006
	2.3	.213	.050	-.021
	4.4	.306	.069	-.046
	6.5	.394	.092	-.069
	8.4	.474	.120	-.085
	10.4	.549	.153	-.097
	-4.2	-.082	.034	.059
41	-8.4	-0.266	0.058	0.109
	-6.4	-.177	.043	.085
	-4.1	-.080	.033	.059
	-1.9	.019	.032	.032
	.2	.116	.037	.005
	2.3	.215	.049	-.022
	4.4	.304	.067	-.047
	6.5	.389	.091	-.069
	8.4	.471	.120	-.086
	10.4	.545	.152	-.098
	-4.1	-.081	.033	.059
42	-4.3	-0.052	0.029	-0.013
	-8.7	-.231	.050	.011
	-6.6	-.145	.036	0
	-4.3	-.052	.029	-.013
	-2.1	.043	.029	-.027
	.1	.134	.035	-.040
	2.3	.227	.048	-.053
	4.4	.313	.066	-.066
	6.5	.395	.090	-.078
	8.5	.472	.119	-.089
	10.5	.547	.153	-.098
44	-4.3	-0.052	0.030	-0.011
	-8.8	-.236	.053	.021
	-4.3	-.052	.030	-.011
	0	.136	.035	-.040
	4.3	.313	.066	-.067
	8.5	.473	.118	-.090
	-8.8	-.235	.053	.021
45	-4.1	-0.081	0.029	0.060
	-8.4	-.256	.053	.104
	-6.2	-.168	.038	.082
	-4.1	-.079	.029	.059
	-2.0	.016	.028	.034
	.3	.108	.033	.010
	2.4	.199	.044	-.015
	4.4	.284	.061	-.037
	6.4	.366	.082	-.057
	8.5	.441	.109	-.073
	10.5	.513	.140	-.087
	.2	.110	.033	.009
	-2.0	.015	.027	.033
	-4.2	-.080	.029	.059
	-6.4	-.172	.038	.082
	-8.4	-.257	.053	.104
46	-8.5	-0.257	0.054	0.105
	-4.2	-.081	.029	.061
	.1	.108	.032	.011
	4.4	.286	.061	-.038
	8.4	.444	.110	-.075
	10.5	.517	.141	-.089
	-6.4	-.171	.040	.084
	-8.5	-.256	.054	.105
47	-8.3	-0.264	0.058	0.105
	-6.2	-.180	.042	.084
	-4.0	-.091	.033	.061
	-1.8	.006	.031	.035
	.4	.098	.035	.011
	2.4	.187	.045	-.014
	4.5	.277	.062	-.037
	6.5	.359	.082	-.058
	8.6	.437	.109	-.074
	10.6	.509	.139	-.087
	-8.3	-.264	.058	.105

TABLE IX.- TABULATED DATA FOR YAW TESTS, M = 1.41

Run	ψ	C_L	C_D	C_m	C_l	C_n	C_y
67	-0.1	0.198	0.048	-0.008	-0.001	-0.0008	0.0055
	-4.1	.192	.047	-.006	-.001	.0148	-.0454
	-2.1	.195	.048	-.007	-.001	.0069	-.0201
	2.1	.196	.047	-.007	-.001	-.0084	.0307
	4.2	.196	.048	-.004	-.001	-.0170	.0578
	6.5	.194	.048	.001	-.001	-.0241	.0840
	-.1	.196	.048	-.008	-.001	-.0007	.0056
	4.2	.195	.050	-.003	-.001	-.0169	.0583
68	-0.1	0.189	0.037	-0.017	-0.001	-0.0008	0.0054
	-4.1	.183	.036	-.012	-.004	.0133	-.0281
	-2.1	.186	.036	-.015	-.002	.0061	-.0115
	2.1	.188	.037	-.015	0	-.0077	.0220
	4.2	.189	.037	-.010	.002	-.0154	.0403
	6.5	.184	.037	-.002	.003	-.0224	.0582
	-.1	.189	.037	-.017	-.001	-.0006	.0049
69	-4.1	0.185	0.044	-0.008	-0.001	0.0149	-0.0460
	-2.1	.188	.044	-.009	-.001	.0068	-.0199
	-.1	.189	.044	-.009	-.001	-.0006	.0050
	2.1	.189	.044	-.008	-.001	-.0083	.0308
	4.2	.189	.044	-.005	-.001	-.0167	.0582
	5.9	.187	.044	-.002	-.001	-.0224	.0782
	-4.1	.186	.044	-.007	-.001	.0152	-.0465
70	-6.2	0.186	0.048	-0.008	-0.004	0.0220	-0.0732
	-4.1	.192	.049	-.013	-.003	.0141	-.0462
	-2.1	.196	.048	-.018	-.002	.0063	-.0209
	-.1	.197	.048	-.019	-.001	-.0006	.0038
	2.1	.197	.048	-.016	0	-.0077	.0287
	4.2	.194	.048	-.011	.001	-.0157	.0552
	6.5	.189	.048	-.005	.002	-.0229	.0821
	-2.1	.196	.048	-.018	-.002	.0065	-.0209
	-6.0	.186	.048	-.008	-.005	.0218	-.0737
75	-0.1	0.205	0.040	-0.008	0	-0.0008	0.0055
	-4.1	.201	.040	-.009	-.005	.0148	-.0316
	-2.1	.204	.040	-.009	-.003	.0069	-.0135
	2.1	.205	.041	-.008	.002	-.0084	.0233
	4.2	.205	.041	-.008	.004	-.0161	.0416
	6.5	.207	.041	-.008	.007	-.0222	.0591
	-.1	.204	.040	-.009	0	-.0005	.0046
76	-4.0	-0.020	0.012	0.046	-0.005	0.0137	-0.0283
	-2.0	-.021	.011	.048	-.003	.0061	-.0117
	0	-.021	.011	.049	0	-.0012	.0049
	2.0	-.021	.011	.049	.002	-.0086	.0205
	4.0	-.021	.011	.048	.004	-.0163	.0375
	6.0	-.020	.011	.046	.006	-.0230	.0530
	-4.0	-.020	.010	.046	-.005	.0138	-.0279
77	0.1	0.190	0.036	-0.002	-0.001	-0.0010	0.0061
	-3.9	.189	.035	-.002	-.005	.0133	-.0278
	-1.9	.190	.035	-.002	-.003	.0060	-.0106
	2.0	.192	.035	-.002	.001	-.0082	.0240
	4.0	.192	.036	-.001	.003	-.0157	.0416
	6.1	.193	.037	0	.005	-.0229	.0595
	.1	.191	.036	-.002	-.001	-.0009	.0067
78	0.1	0.188	0.035	-0.002	-0.001	0.0015	0.0032
	-3.9	.183	.034	-.001	-.006	.0159	-.0306
	-1.9	.185	.034	-.002	-.003	.0084	-.0137
	2.0	.188	.035	-.002	.001	-.0058	.0204
	4.0	.188	.037	-.002	.003	-.0133	.0385
	6.1	.188	.035	0	.005	-.0207	.0562
	-.1	.183	.037	-.001	-.001	.0016	.0027

TABLE IX.- TABULATED DATA FOR YAW TESTS, M = 1.41 - Concluded

Run	ψ	C_L	C_D	C_m	C_l	C_n	C_y
79	0.1	0.185	0.035	0.001	-0.002	0.0033	0.0018
	-3.9	.183	.036	.002	-.006	.0178	-.0327
	-1.9	.185	.035	.001	-.004	.0102	-.0152
	2.1	.186	.035	0	0	-.0041	.0189
	4.1	.187	.036	0	.002	-.0116	.0365
	6.1	.187	.035	.001	.004	-.0191	.0547
	0	.185	.034	0	-.003	.0069	.0082
	-2.9	.184	.035	.001	-.005	.0141	-.0242
	-3.9	.183	.035	.002	-.006	.0177	-.0327
	.1	.186	.035	0	-.002	.0033	.0014
80	-0.1	0.183	0.035	-0.001	-0.001	-0.0007	0.0053
	-4.3	.181	.035	0	-.008	.0124	-.0284
	-2.1	.182	.035	0	-.004	.0054	-.0113
	2.0	.182	.035	0	.003	-.0071	.0223
	4.0	.184	.036	.002	.007	-.0142	.0409
	6.0	.183	.036	.007	.011	-.0200	.0582
	4.0	.183	.036	.002	.007	-.0140	.0406
82	-4.1	0	0.008	-0.001	0	-0.0021	-0.0084
	-2.0	0	.008	-.001	0	-.0010	-.0037
	0	0	.008	-.001	0	.0001	-.0006
	2.1	0	.008	-.001	0	.0013	.0041
	4.1	0	.008	-.001	0	.0024	.0087
	6.2	0	.009	-.001	0	.0035	.0135
	-4.1	.001	.008	-.001	0	-.0021	-.0079
83	-4.0	0.200	0.031	-0.053	-0.001	-0.0013	-0.0095
	-2.0	.204	.030	-.055	-.001	-.0004	-.0041
	0	.205	.030	-.056	0	.0004	.0018
	2.1	.207	.031	-.056	0	.0012	.0076
	4.1	.208	.031	-.055	0	.0022	.0139
	6.1	.207	.032	-.053	.001	.0030	.0205
	-4.0	.200	.031	-.053	-.001	-.0013	-.0096
84	0	0.204	0.030	-0.056	0	0.0003	0.0023
	-4.1	.199	.031	-.052	-.005	-.0016	-.0112
	-2.1	.202	.031	-.055	-.002	-.0006	-.0046
	2.1	.206	.031	-.056	.002	.0012	.0093
	4.1	.207	.032	-.053	.004	.0023	.0159
	6.2	.209	.033	-.051	.006	.0033	.0235
	0	.203	.030	-.056	0	.0004	.0023
85	0	0.099	0.024	-0.032	0.001	0.0003	0.0012
	-4.0	.096	.023	-.030	0	-.0014	-.0098
	-2.0	.097	.024	-.032	0	-.0006	-.0044
	2.1	.100	.024	-.032	.001	.0012	.0066
	4.1	.102	.024	-.031	.001	.0020	.0117
	6.2	.103	.024	-.029	.002	.0028	.0182
	0	.010	.024	-.032	.001	.0003	.0006
91	0.1	0.207	0.030	-0.061	0	0.0009	-0.0012
	-4.1	.207	.031	-.058	0	-.0012	-.0117
	-2.1	.207	.030	-.060	0	-.0001	-.0066
	2.0	.207	.031	-.060	0	.0018	.0050
	4.0	.207	.031	-.060	.001	.0029	.0108
	6.0	.205	.031	-.057	.001	.0039	.0174
	.1	.207	.030	-.061	0	.0008	-.0014
92	-0.1	0.191	0.034	-0.029	0	-0.0007	0.0057
	-4.1	.187	.034	-.025	-.002	.0101	-.0297
	-2.1	.189	.034	-.027	-.001	.0045	-.0120
	2.0	.190	.034	-.027	.001	-.0062	.0231
	3.9	.189	.034	-.023	.002	-.0121	.0417
	6.0	.185	.034	-.017	.003	-.0178	.0613
	-.1	.190	.034	-.028	0	-.0005	.0046

TABLE X.- TABULATED DATA FOR YAW TESTS, M = 2.01

Run	ψ	C_L	C_D	C_m	C_l	C_n	C_y
19	4.1	0.112	0.033	0.009	0.004	-0.0091	0.0323
	2.2	.112	.033	.007	.002	-.0048	.0180
	.0	.112	.033	.006	0	-.0004	.0032
	-2.0	.112	.033	.006	-.002	.0038	-.0099
	-4.0	.112	.033	.007	-.004	.0082	-.0248
	6.2	.112	.034	.010	.006	-.0137	.0475
	4.1	.112	.033	.009	.004	-.0091	.0322
25	-4.1	0.108	0.044	0.018	-0.003	0.0082	-0.0381
	-2.1	.109	.044	.018	-.002	.0040	-.0162
	0	.108	.044	.018	-.001	-.0008	.0060
	2.1	.108	.045	.019	.001	-.0055	.0270
	4.2	.108	.045	.020	.002	-.0094	.0479
	6.3	.108	.045	.021	.003	-.0134	.0706
	-4.1	.108	.045	.018	-.003	.0082	-.0380
	1.1	.108	.045	.018	0	-.0032	.0162
	3.1	.108	.044	.019	.001	-.0075	.0377
26	-4.1	0.109	0.044	0.017	-0.004	0.0095	-0.0396
	-2.1	.107	.044	.019	-.002	.0042	-.0164
	0	.106	.044	.021	-.001	-.0008	.0046
	2.1	.106	.044	.020	.001	-.0058	.0277
	3.1	.106	.045	.020	.002	-.0082	.0380
	4.2	.107	.044	.020	.003	-.0108	.0493
	6.3	.109	.045	.020	.004	-.0153	.0728
	2.1	.107	.044	.020	.001	-.0056	.0276
	6.3	.109	.045	.020	.004	-.0153	.0730
	2.1	.107	.044	.020	.001	-.0056	.0271
	-4.1	.109	.044	.017	-.004	.0096	-.0410
27	0	0.113	0.033	0.007	-0.001	0.0007	0.0025
	4.2	.111	.033	.010	.003	-.0082	.0314
	2.1	.113	.033	.008	.001	-.0038	.0172
	-2.0	.113	.033	.007	-.003	.0050	-.0107
	-4.1	.113	.033	.007	-.005	.0094	-.0255
	-6.1	.113	.034	.008	-.007	.0139	-.0407
	0	.113	.033	.007	-.001	.0006	.0029
28	0	0.113	0.033	0.008	-0.001	0.0018	0.0017
	-4.0	.113	.034	.008	-.005	.0106	-.0260
	-2.1	.113	.033	.007	-.003	.0061	-.0118
	6.3	.113	.033	.011	.005	-.0116	.0456
	4.1	.112	.034	.010	.003	-.0071	.0306
	2.0	.113	.033	.008	.001	-.0027	.0158
	0	.113	.033	.007	-.001	.0018	.0018
	-2.0	.113	.033	.008	.001	-.0027	.0159
29	4.2	.128	.029	-.034	.002	.0027	.0140
	6.2	.127	.029	-.033	.002	.0038	.0213
	2.1	.128	.029	-.036	.002	.0015	.0072
	0	.128	.028	-.037	.001	.0004	.0009
	-2.0	.127	.029	-.036	.001	-.0007	-.0049
	-4.1	.126	.029	-.046	0	-.0019	-.0108
	4.2	.127	.029	-.034	.002	.0027	.0139

TABLE X.- TABULATED DATA FOR YAW TESTS, M = 2.01 - Concluded

Run	ψ	C_L	C_D	C_m	C_l	C_n	C_y
30	0	0.115	0.032	0.007	0	-0.0004	0.0037
	-4.1	.114	.033	.009	-.007	.0073	-.0254
	-2.0	.114	.032	.008	-.003	.0034	-.0108
	0	.115	.032	.007	0	-.0004	.0034
	2.1	.114	.033	.008	.003	-.0042	.0186
	4.1	.114	.034	.011	.006	-.0081	.0327
	6.1	.114	.034	.014	.009	-.0121	.0493
	-4.1	.113	.033	.009	-.007	.0075	-.0255
31	0	0.131	0.028	-0.037	0.001	0.0003	0.0018
	-4.1	.129	.029	-.033	-.003	-.0022	-.0118
	-2.0	.131	.029	-.036	-.001	-.0009	-.0049
	0	.131	.028	-.036	.001	.0003	.0015
	2.1	.131	.029	-.036	.003	.0016	.0087
	4.2	.131	.029	-.033	.005	.0028	.0161
	6.2	.131	.030	-.031	.007	.0041	.0248
32	-4.0	0	0.007	-0.001	0	-0.0026	-0.0077
	-2.0	0	.007	-.001	0	-.0013	-.0032
	-.2	0	.008	-.001	0	.0001	.0000
	2.0	0	.007	-.001	0	.0014	.0041
	4.1	0	.008	-.001	0	.0023	.0089
	6.1	0	.008	-.001	0	.0039	.0152
	-4.2	0	.007	-.001	0	-.0026	-.0072
	4.1	0	.007	-.001	0	.0027	.0091
33	-4.1	0.053	0.023	-0.019	0.001	-0.0020	-0.0117
	-2.2	.054	.023	-.020	.001	-.0009	-.0055
	0	.055	.022	-.021	.001	.0002	.0003
	2.1	.055	.023	-.020	.001	.0013	.0057
	4.1	.054	.023	-.018	.001	.0023	.0126
	6.2	.054	.023	-.017	.001	.0034	.0201
	-4.1	.053	.023	-.019	.001	-.0019	-.0114
38	-4.1	-0.017	0.010	0.038	-0.004	0.0086	-0.0220
	-2.1	-.018	.013	.041	-.003	.0039	-.0105
	0	-.018	.011	.041	-.002	-.0009	.0035
	2.0	-.019	.011	.041	0	-.0057	.0168
	4.0	-.019	.006	.041	.001	-.0104	.0297
	6.3	-.019	.012	.040	.003	-.0148	.0433
	-4.0	-.017	.010	.038	-.004	.0087	-.0223
	6.1	-.019	.012	.041	.003	-.0147	.0429
43	0	0.123	0.037	0.003	0	-0.0005	0.0035
	-4.0	.124	.038	.001	-.005	.0097	-.0270
	-2.0	.124	.037	.002	-.002	.0046	-.0110
	0	.124	.037	.003	0	-.0005	.0037
	2.2	.123	.037	.003	.002	-.0056	.0195
	4.1	.124	.037	.003	.004	-.0105	.0348
	6.2	.124	.037	.003	.006	-.0156	.0522

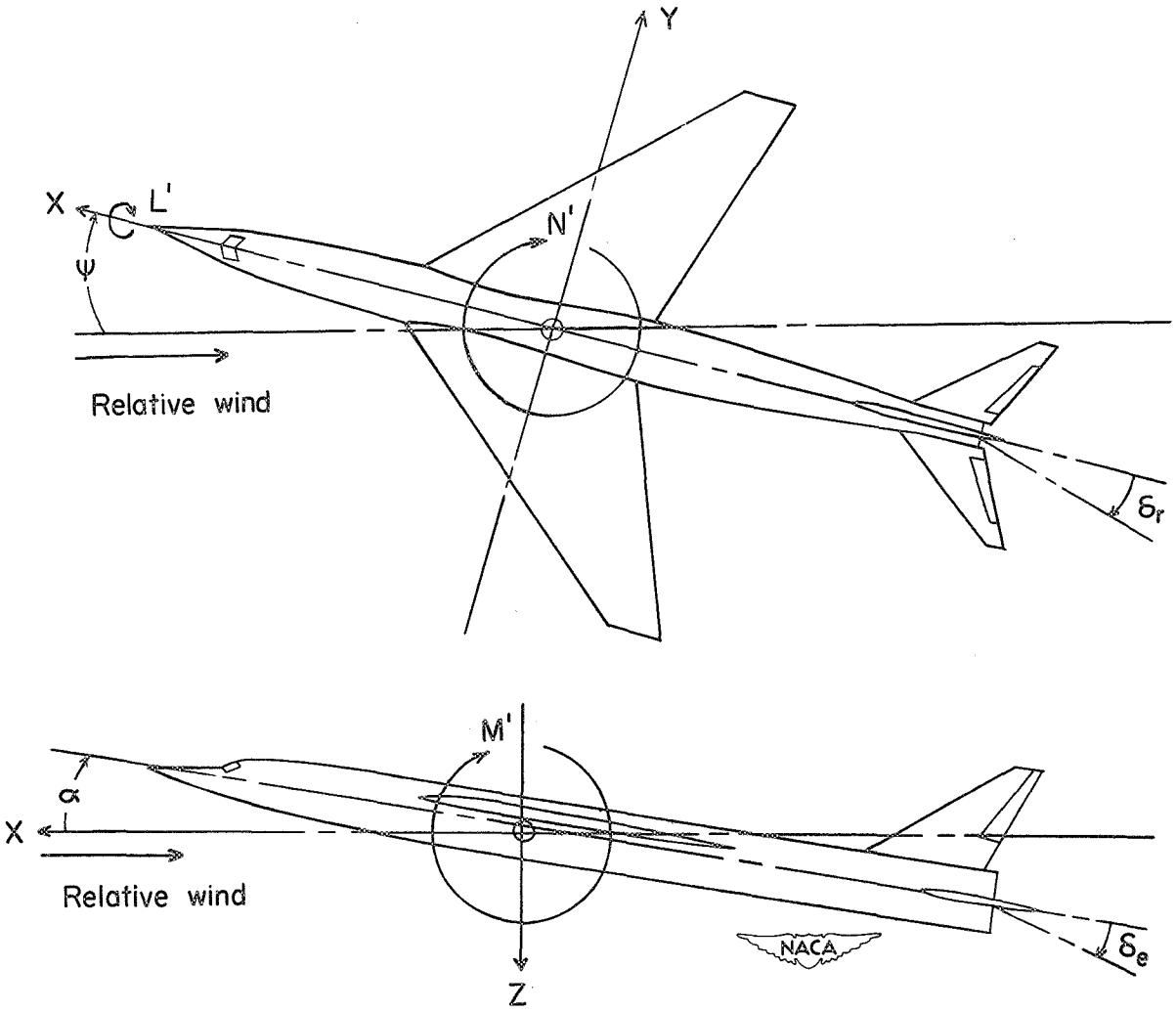

Figure 1.- System of axes and control-surface deflections. Positive values of forces, moments, and angles are indicated by arrows.

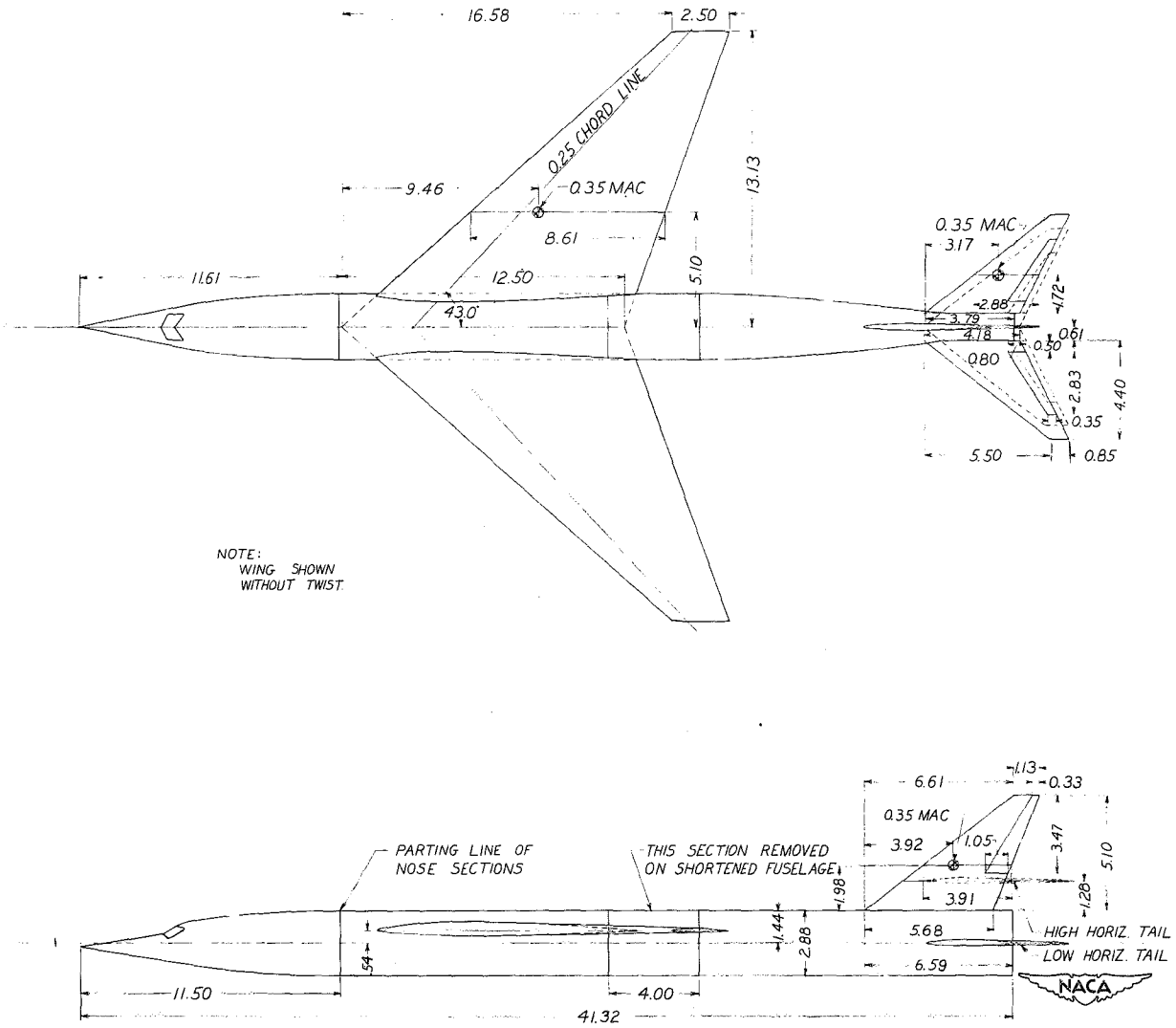

Figure 2.- Two-view drawing of the basic MX-1712 model.

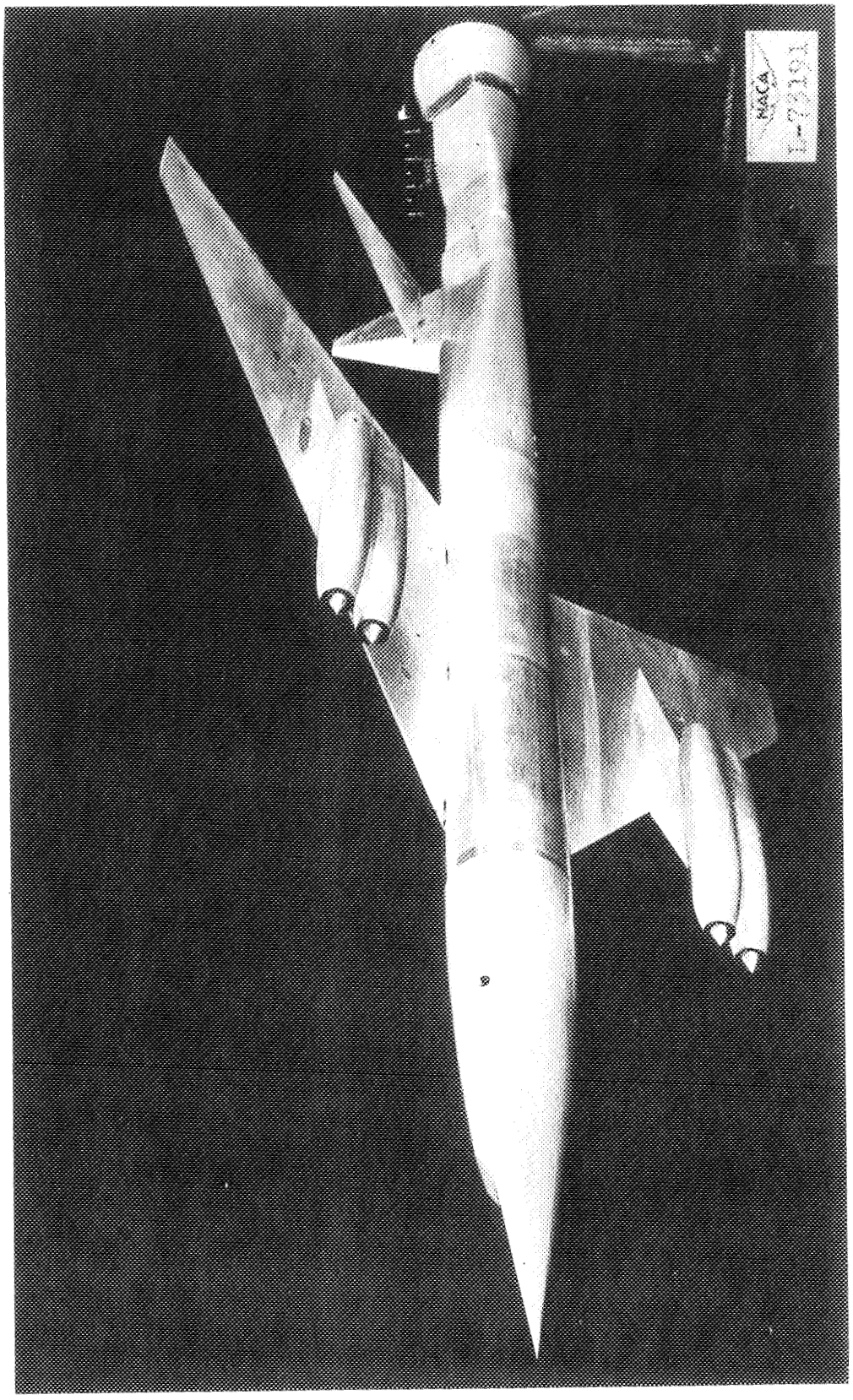

(a) Three-quarter view.

Figure 3.- Photographs of MX-1712 model.

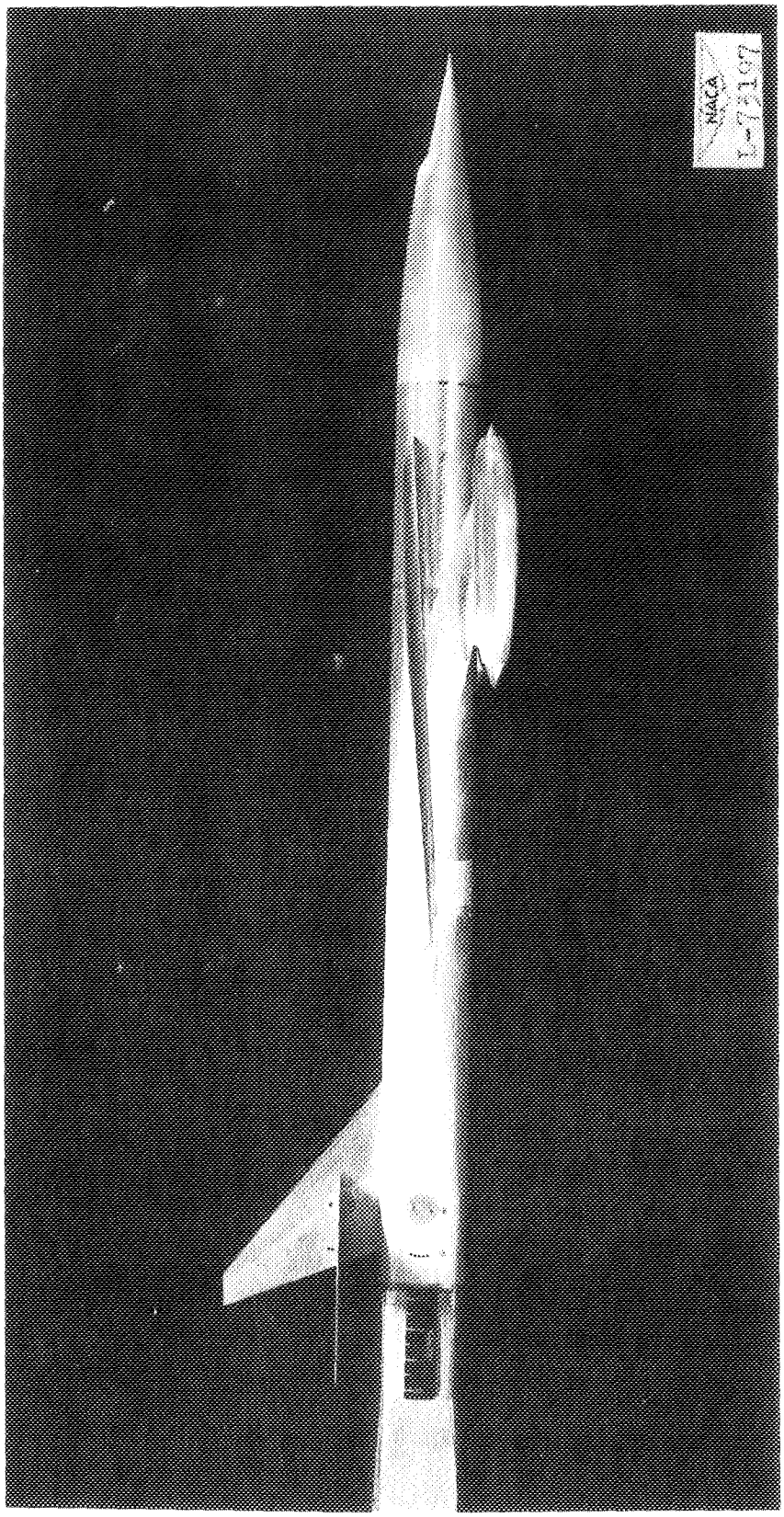

(b) Side view.

Figure 3.- Continued.

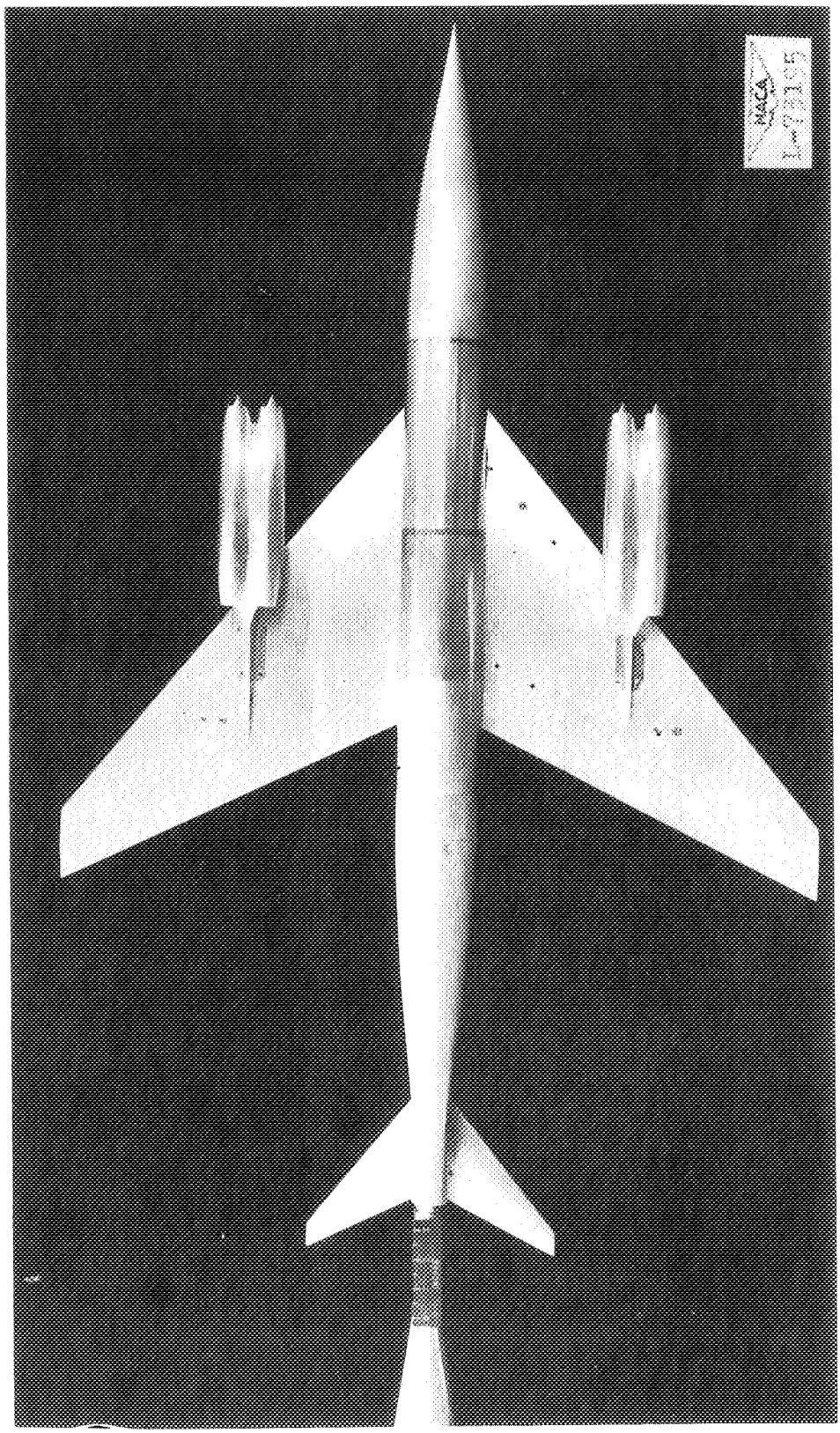

(c) Bottom view.

Figure 3.- Concluded.

(a) With wedge-pod nacelles; mounted for yaw tests.

Figure 4.- MX-1712 model mounted in the Langley 4- by 4-foot supersonic pressure tunnel.

(b) With buried nacelles; mounted for pitch tests.

Figure 4.- Concluded.

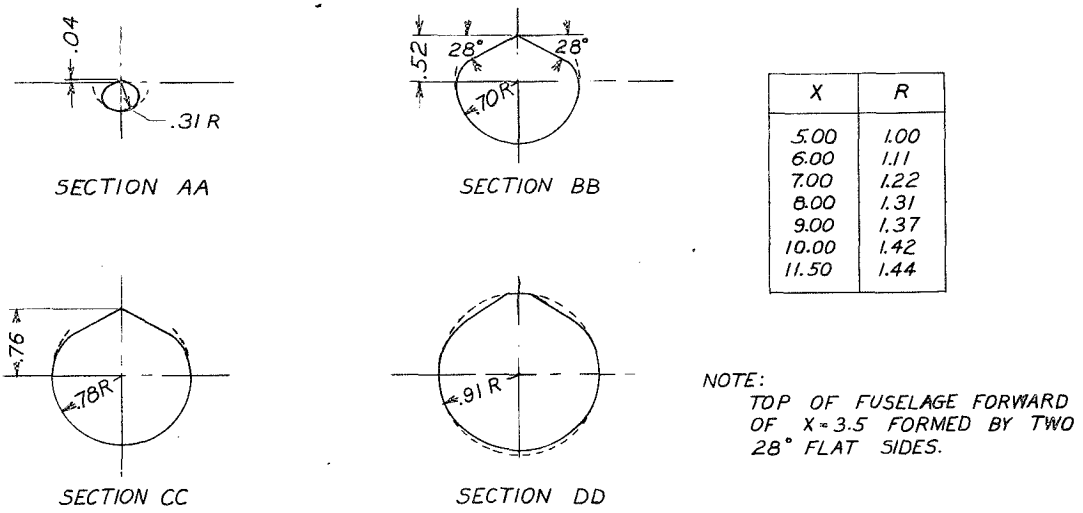

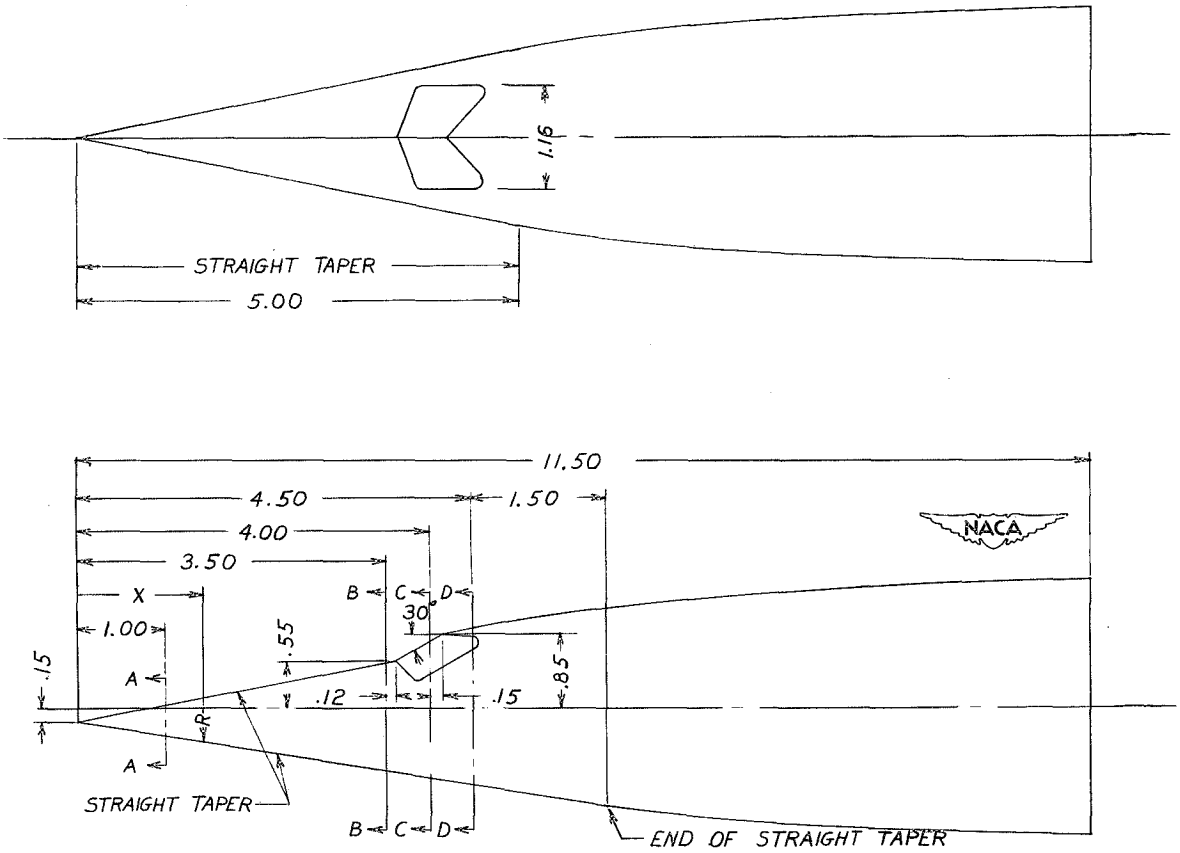

(a) Canopy.

Figure 5.- Details of fuselage nose shapes.

X	Y
0	0
.50	.12
1.00	.22
1.50	.35
2.00	.48
2.50	.62
3.00	.76
3.50	.91
4.00	1.04
4.50	1.15
5.00	1.24
6.00	1.36
7.00	1.42
8.00	1.44
10.48	1.44

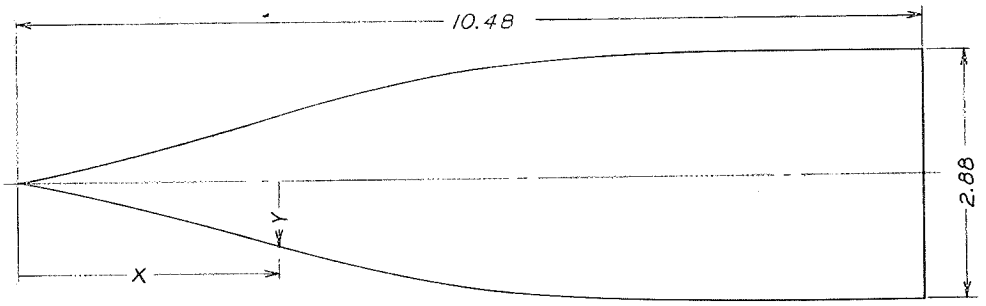

(b) Cusp.

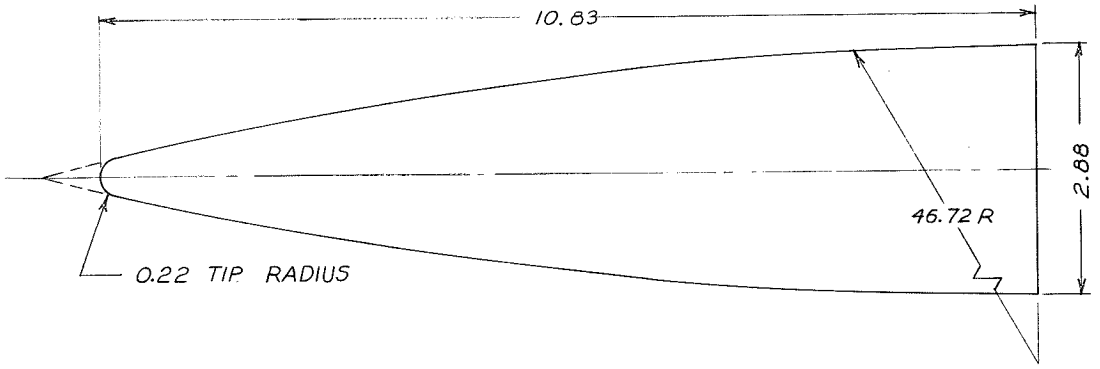

(c) Blunt ogive.

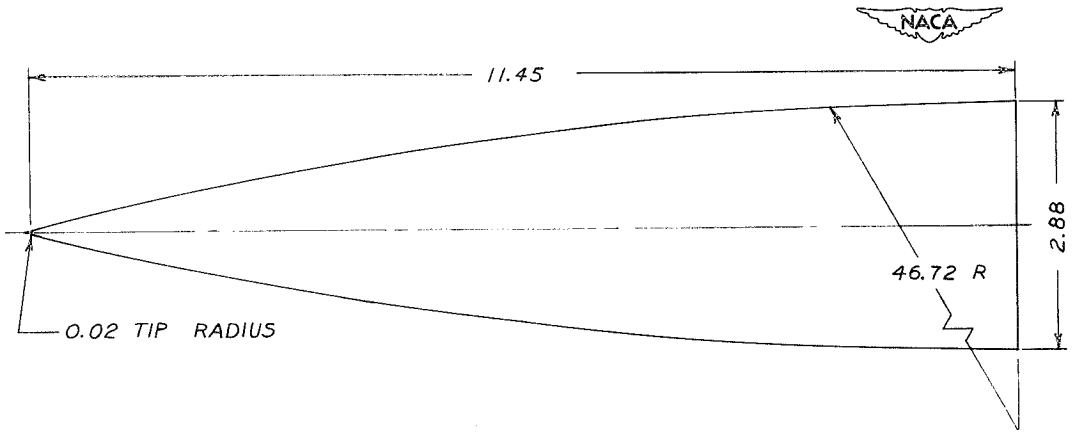

(d) Sharp ogive.

Figure 5.- Concluded.

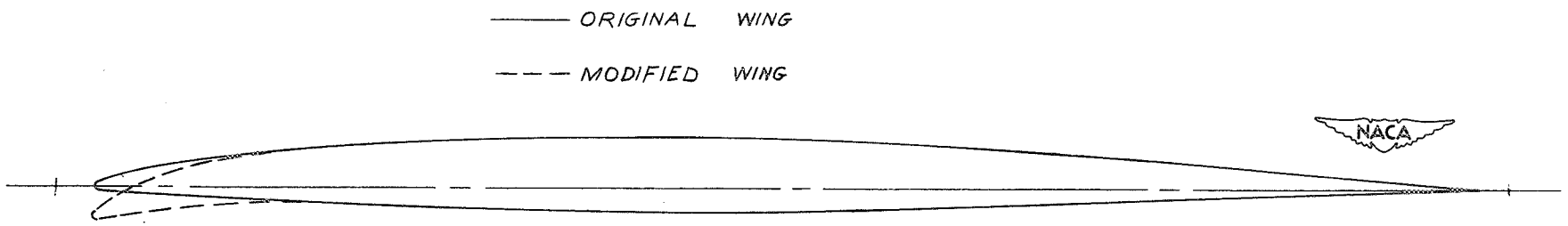

Figure 6.- Comparison of the original and modified wing sections outboard of the 80-percent-semispan station.

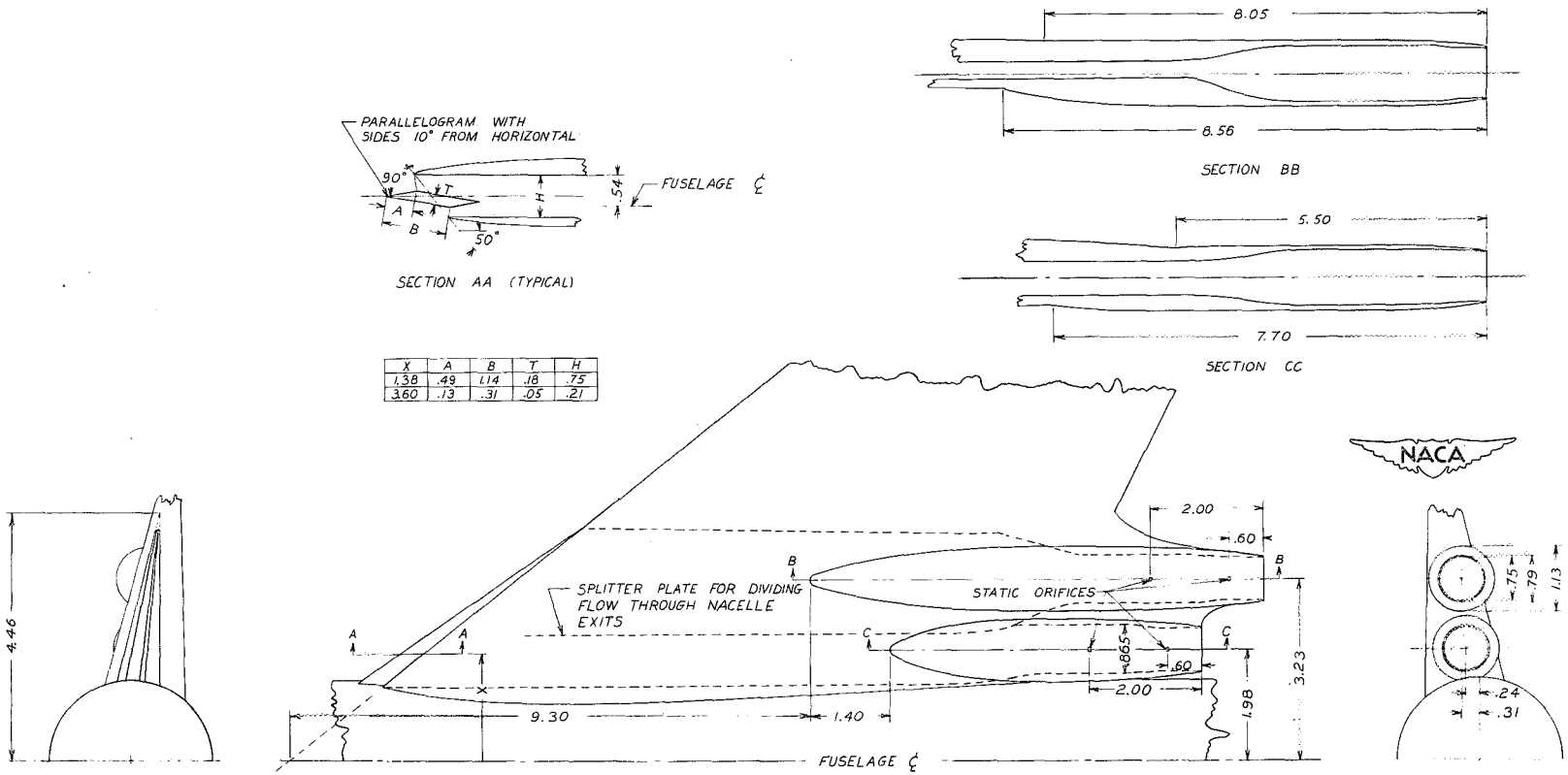

Figure 7.- Details of buried nacelles.

NACELLE COORDINATES			
X	1.60	3.00	4.75
R_1	.19	.38	.44
Z	Y	Y	Y
-.40	.48	.52	.46
-.20	.65	.66	.62
0	.70	.75	.67
.20	.66	.70	.63
.40	.52	.57	~
.58	.42	.52	.49

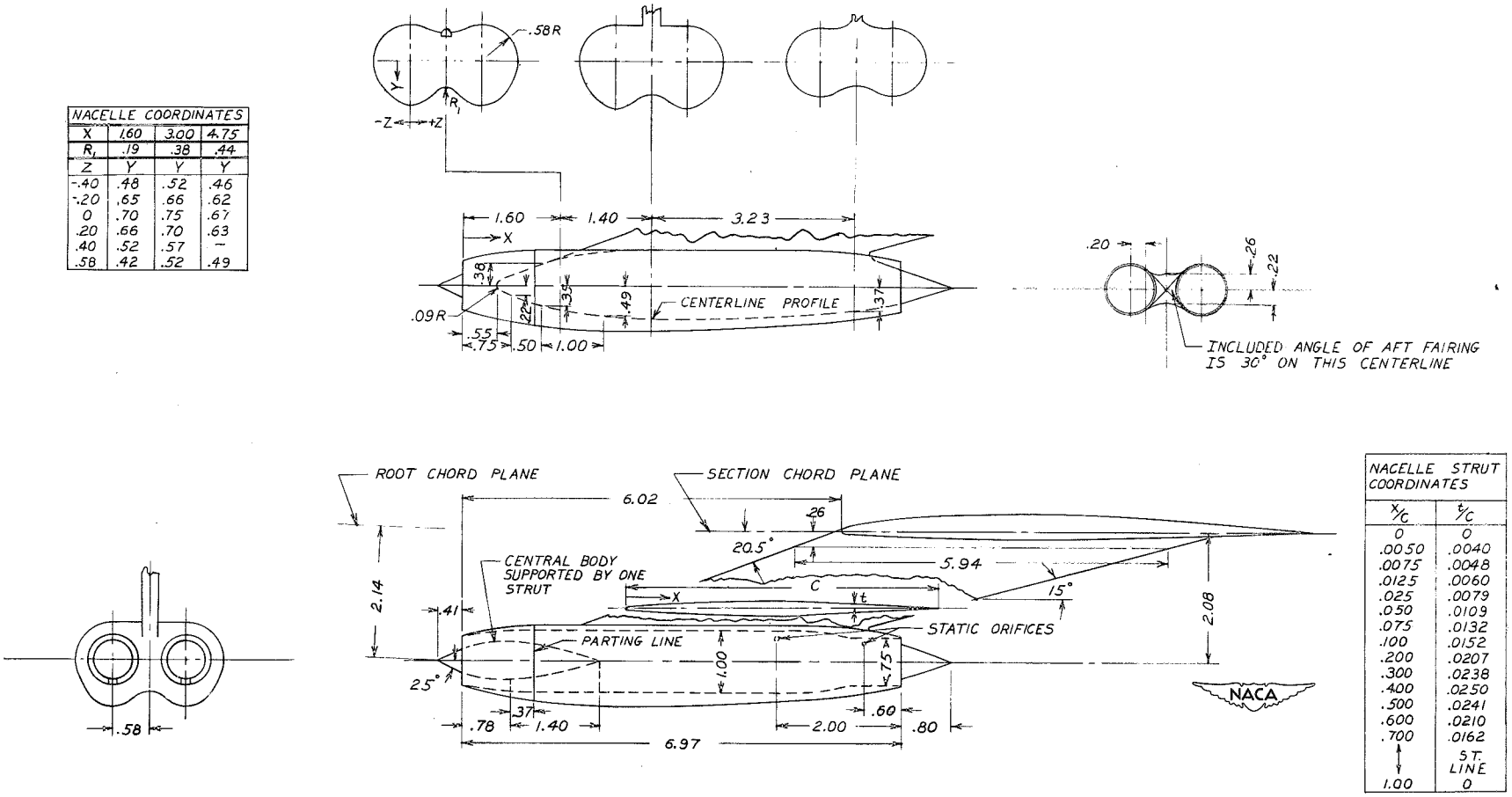

NACELLE STRUT COORDINATES	
x/c	t/c
0	0
.0050	.0040
.0075	.0048
.0125	.0060
.025	.0079
.050	.0109
.075	.0132
.100	.0152
.200	.0207
.300	.0238
.400	.0250
.500	.0241
.600	.0210
.700	.0162
↕	ST. LINE
1.00	0

(a) Cone-pod nacelles.

Figure 8.- Details of pod nacelles.

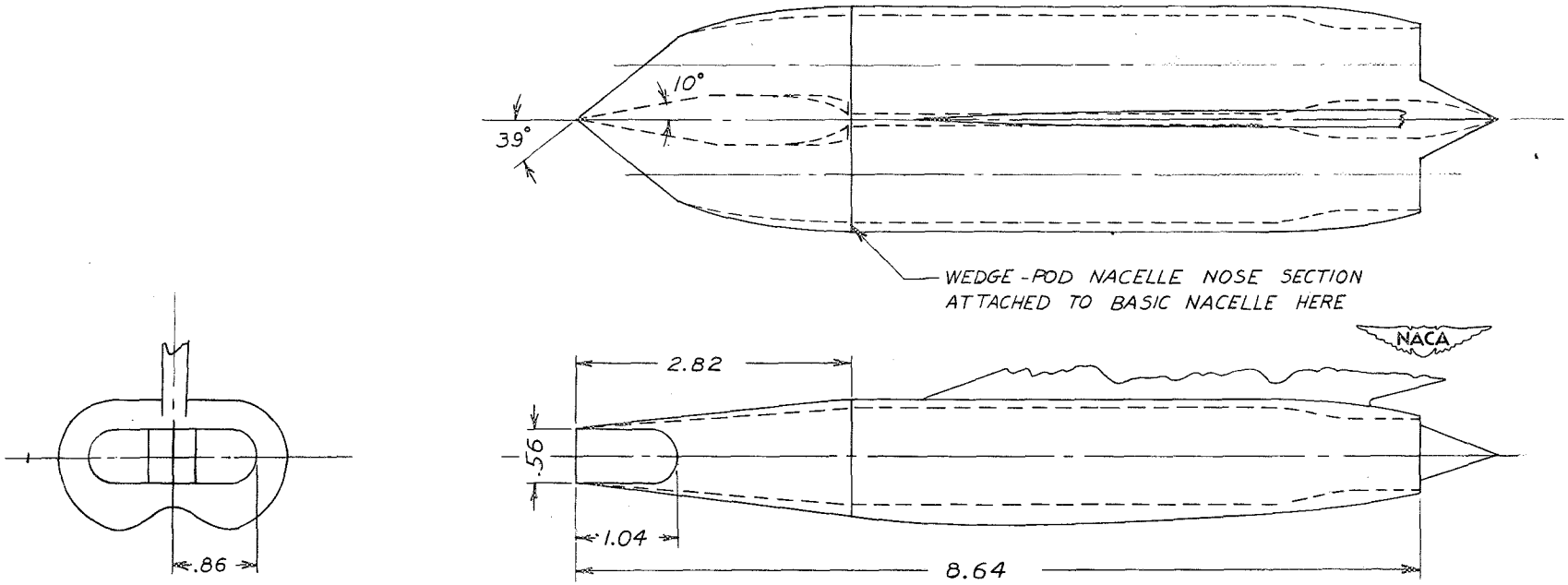

(b) Wedge-pod nacelles.

Figure 8.- Concluded.

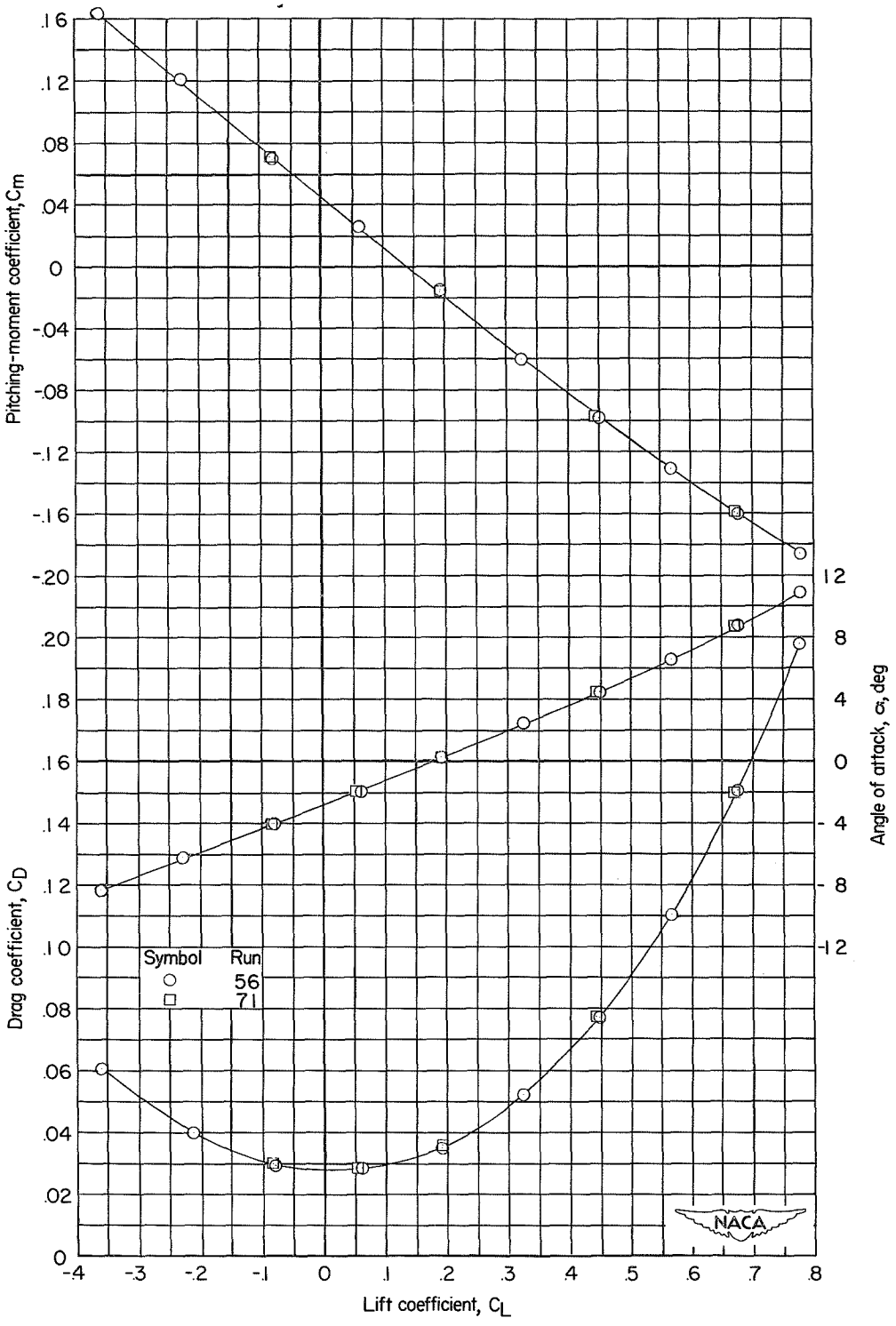

(a) M = 1.41; low horizontal tail.

Figure 9.- Comparison of data obtained from repeat runs of basic model.

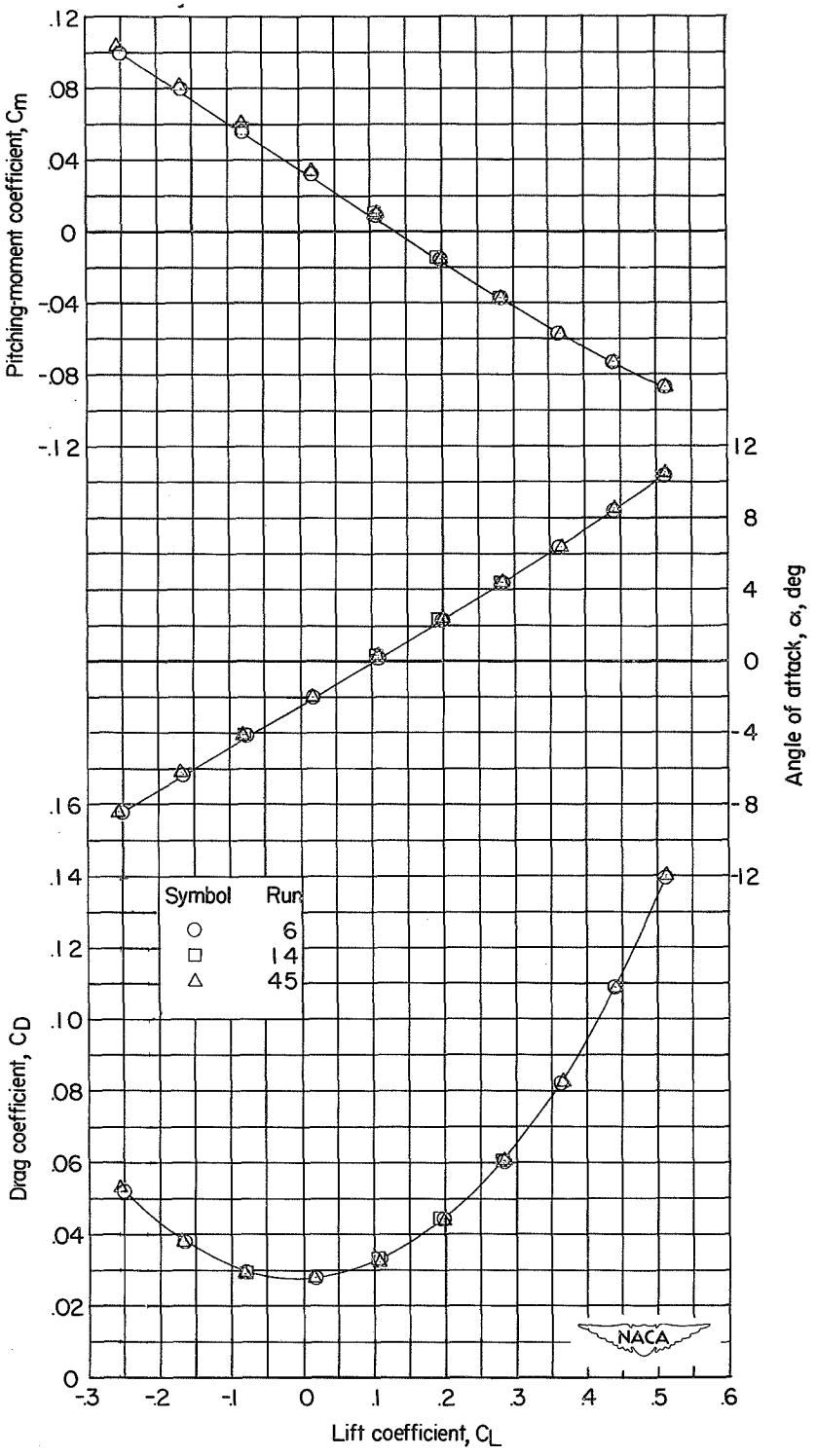

(b) M = 2.01; high horizontal tail.

Figure 9.- Concluded.

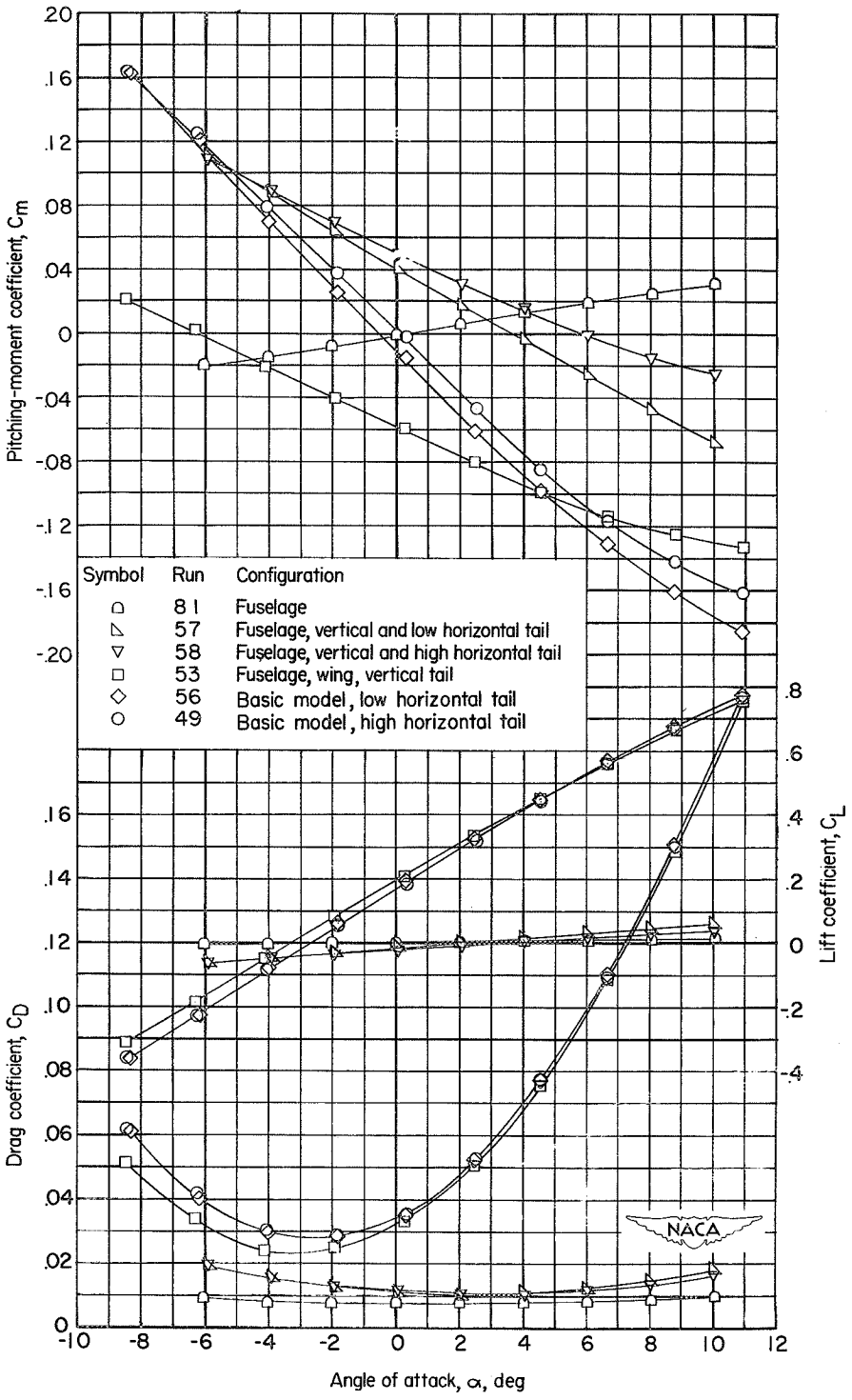

(a) M = 1.41.

Figure 10.- Longitudinal stability characteristics of various combinations of fuselage, wing, and tail.

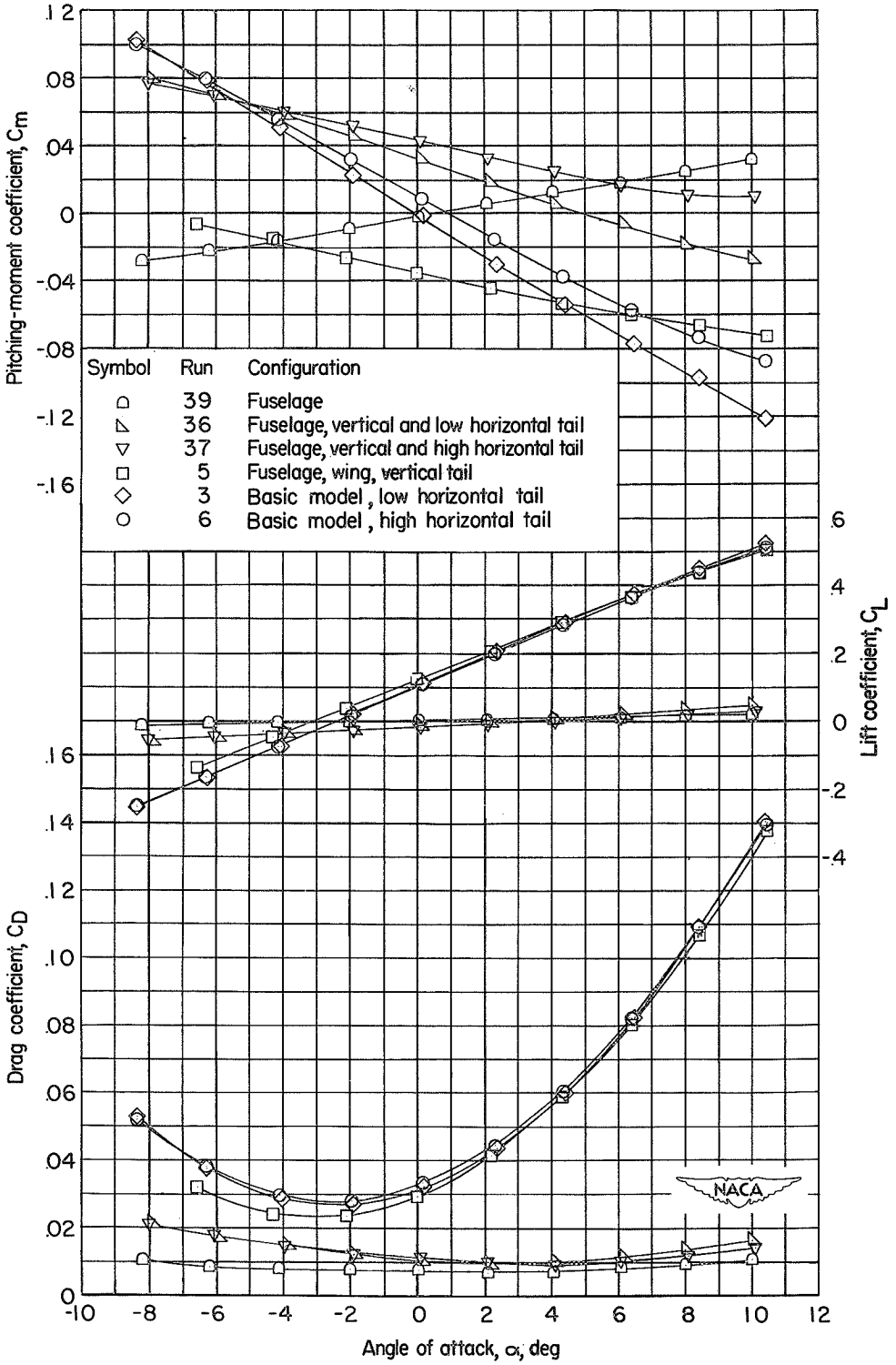

(b) M = 2.01.

Figure 10.- Concluded.

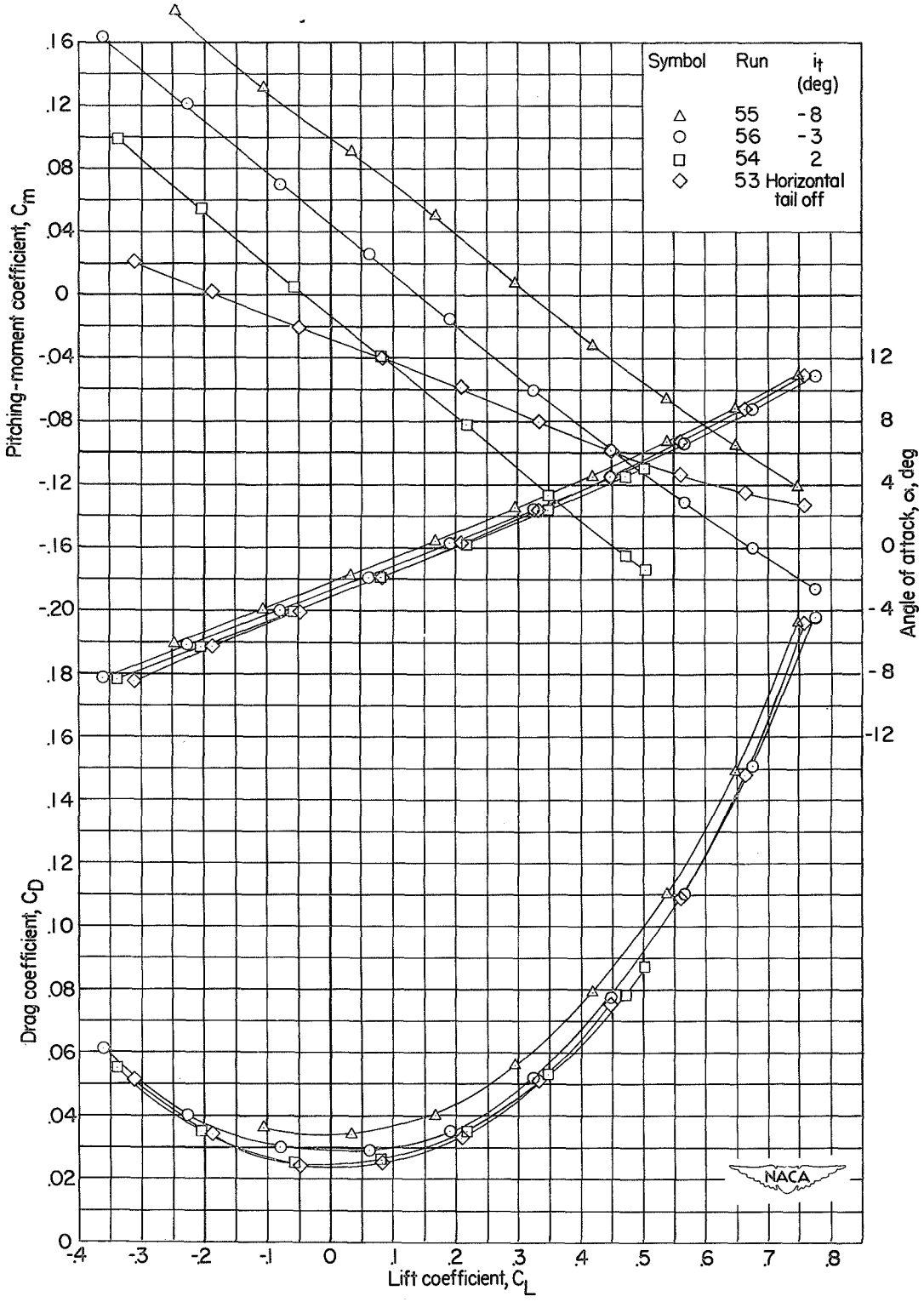

(a) M = 1.41.

Figure 11.- Longitudinal stability characteristics of the basic model with various incidences of the low horizontal stabilizer.

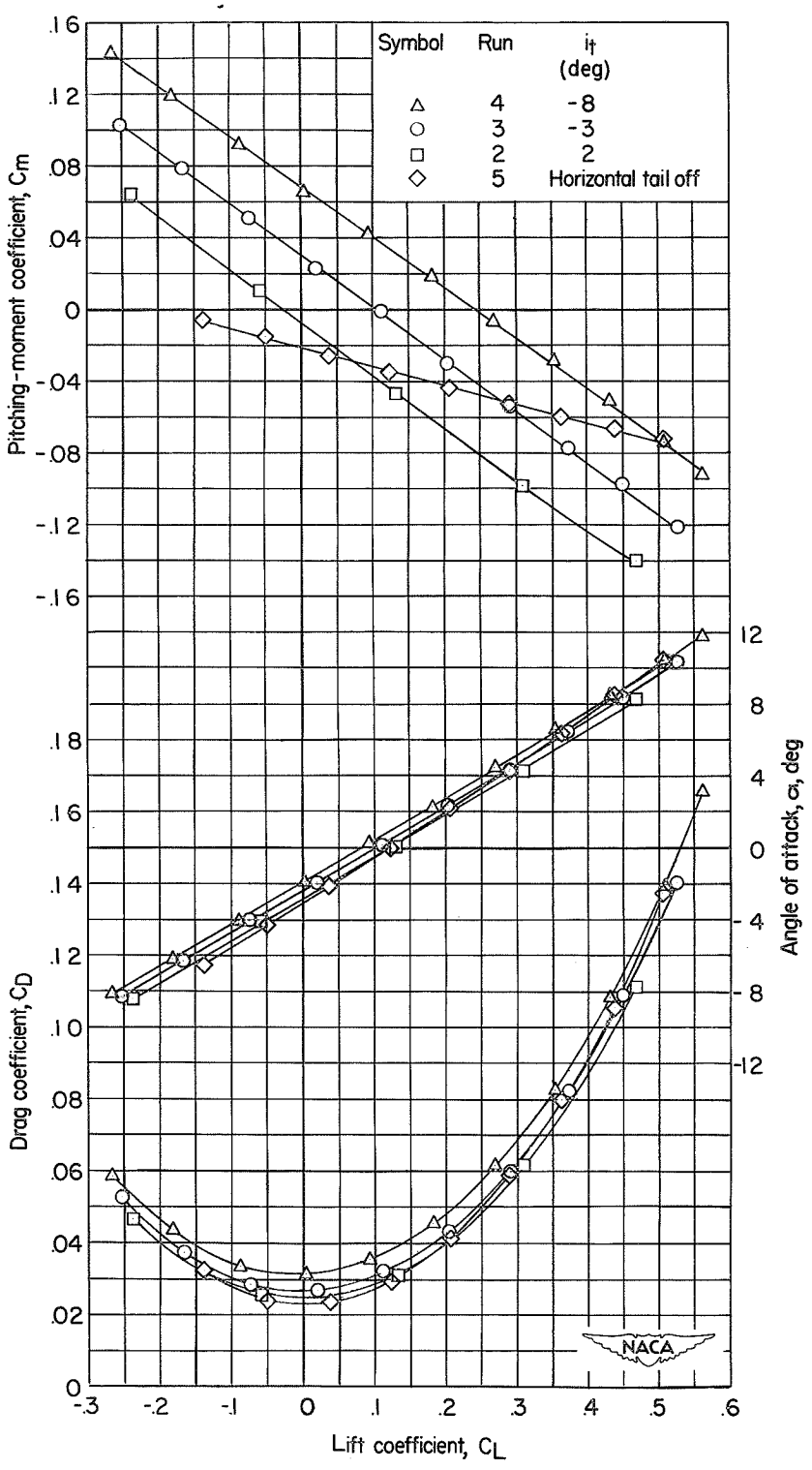

(b) M = 2.01.

Figure 11.- Concluded.

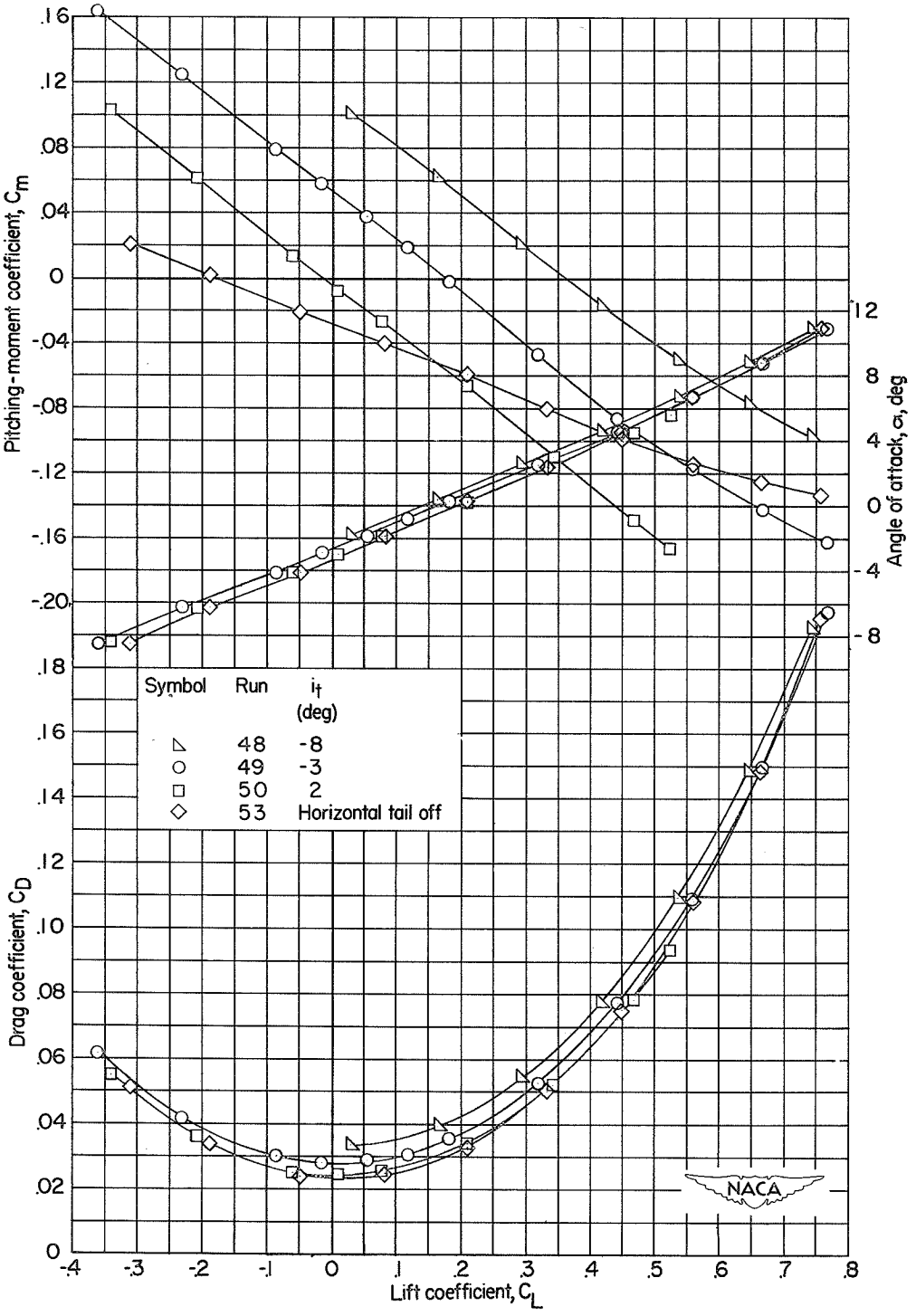

(a) M = 1.41.

Figure 12.- Longitudinal stability characteristics of the basic model with various incidences of the high horizontal stabilizer.

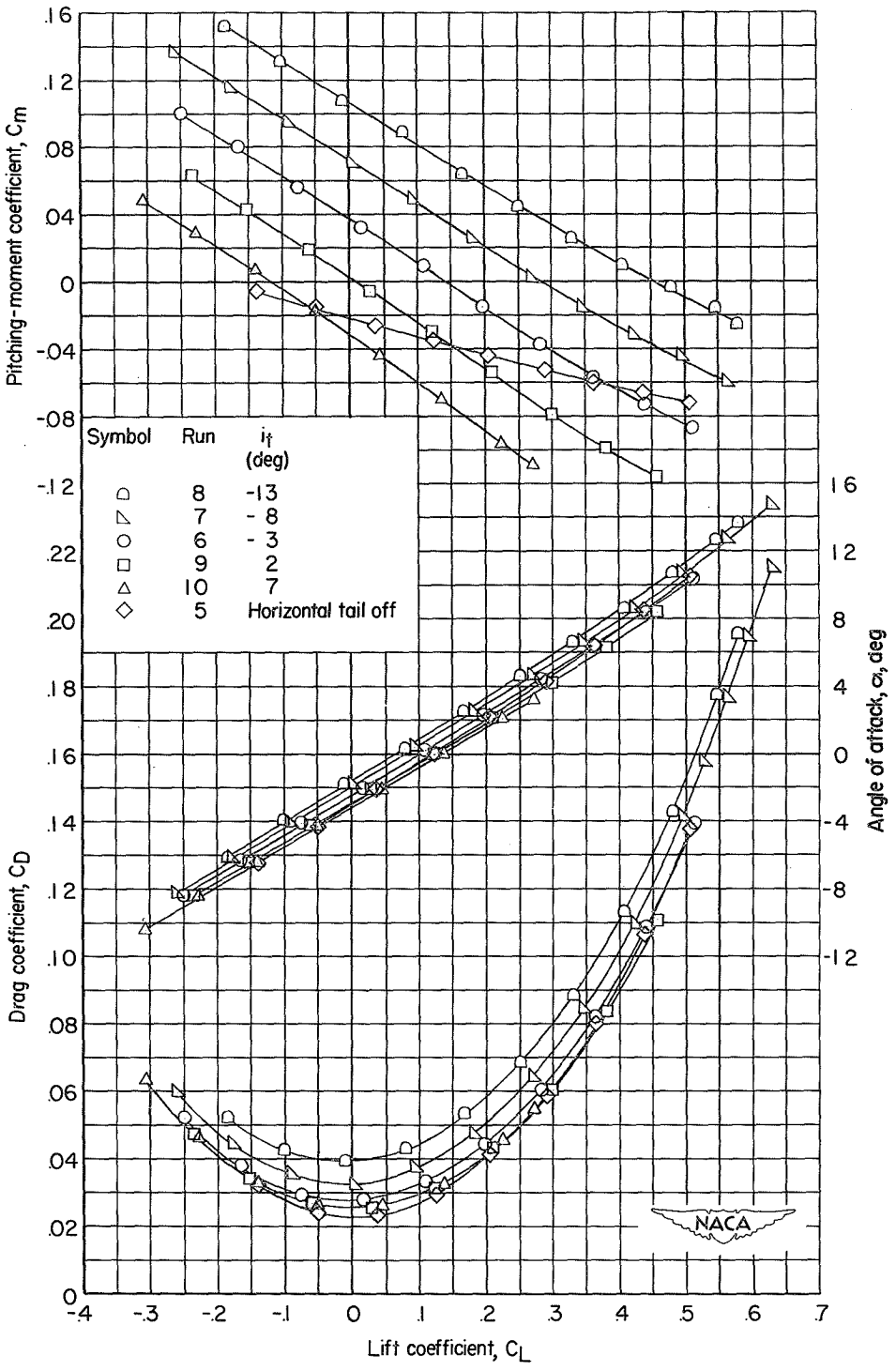

(b) M = 2.01.

Figure 12.- Concluded.

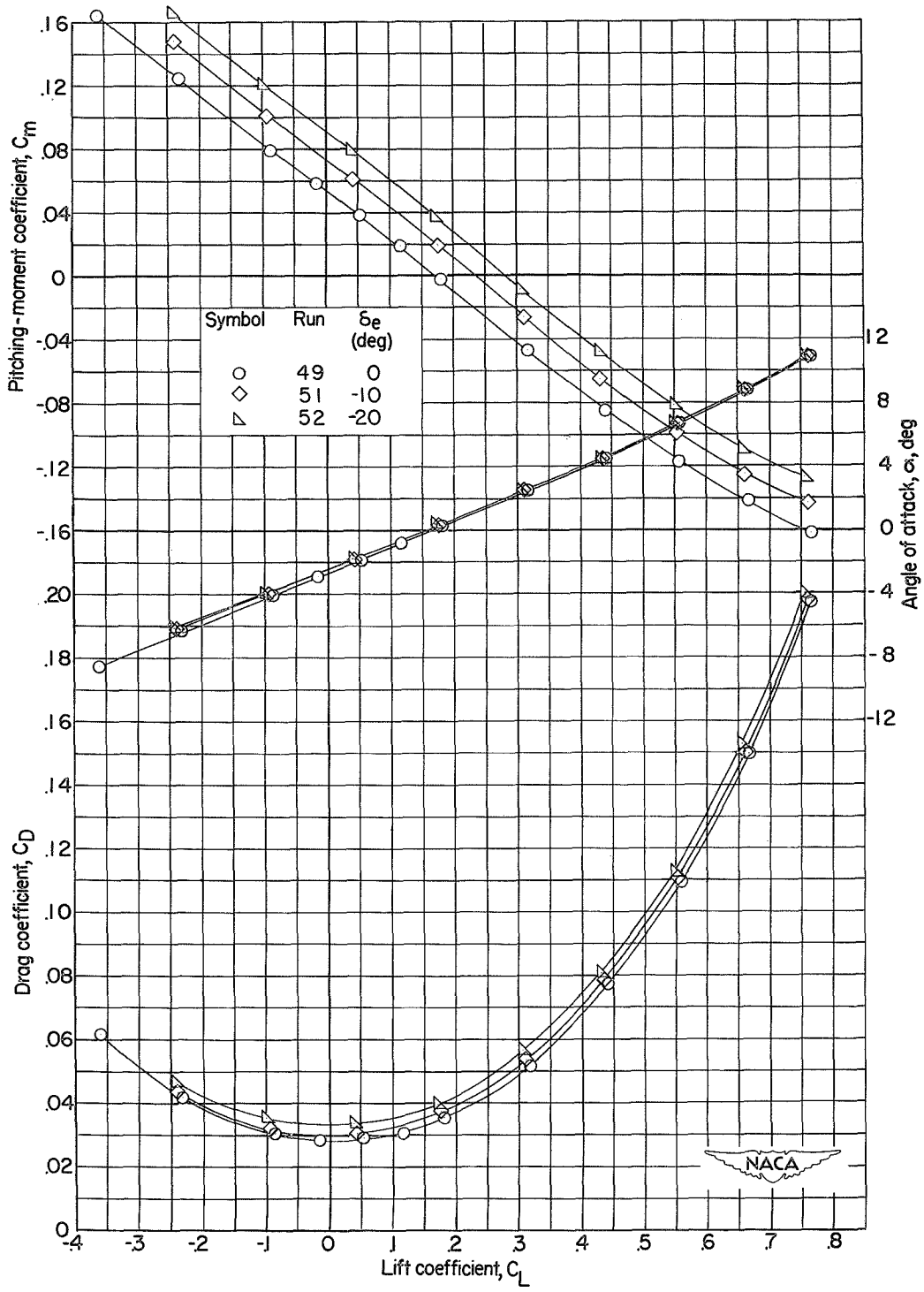

(a) M = 1.41.

Figure 13.- Longitudinal stability characteristics of the basic model with various elevator deflections on the high horizontal tail.

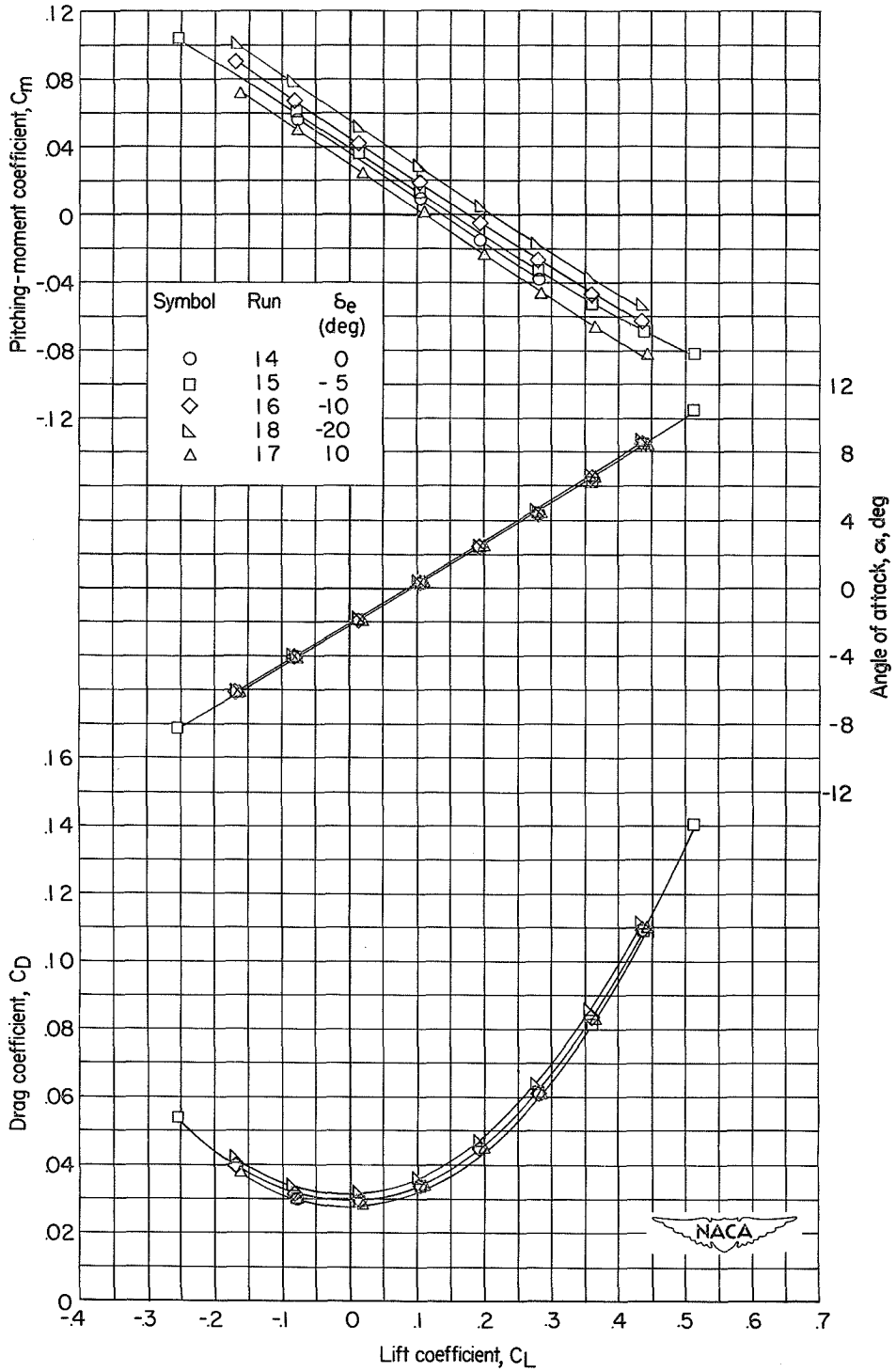

(b) M = 2.01.

Figure 13.- Concluded.

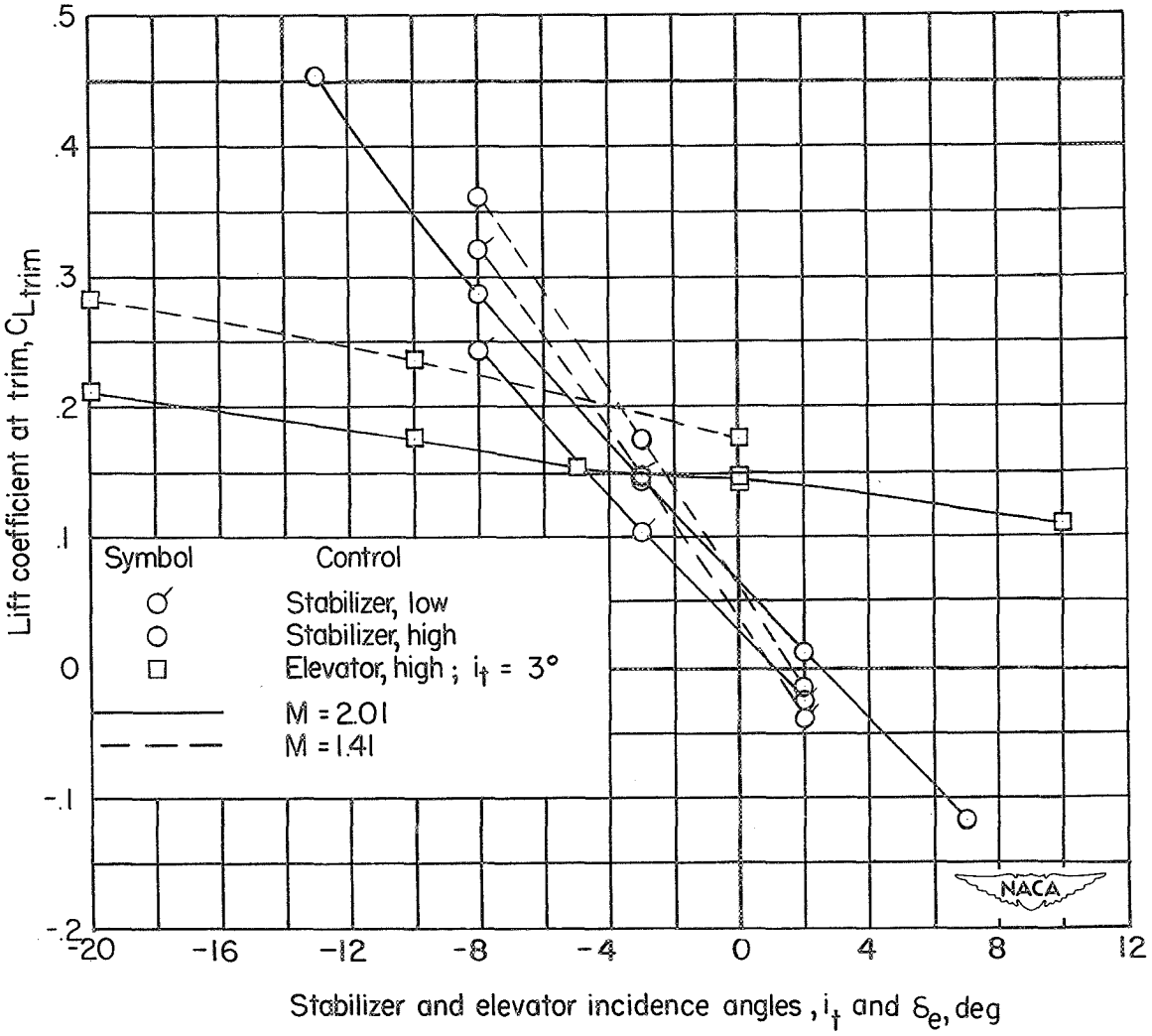

Figure 14.- Effectiveness of elevator and high and low stabilizer in changing trim lift coefficient of the complete model.

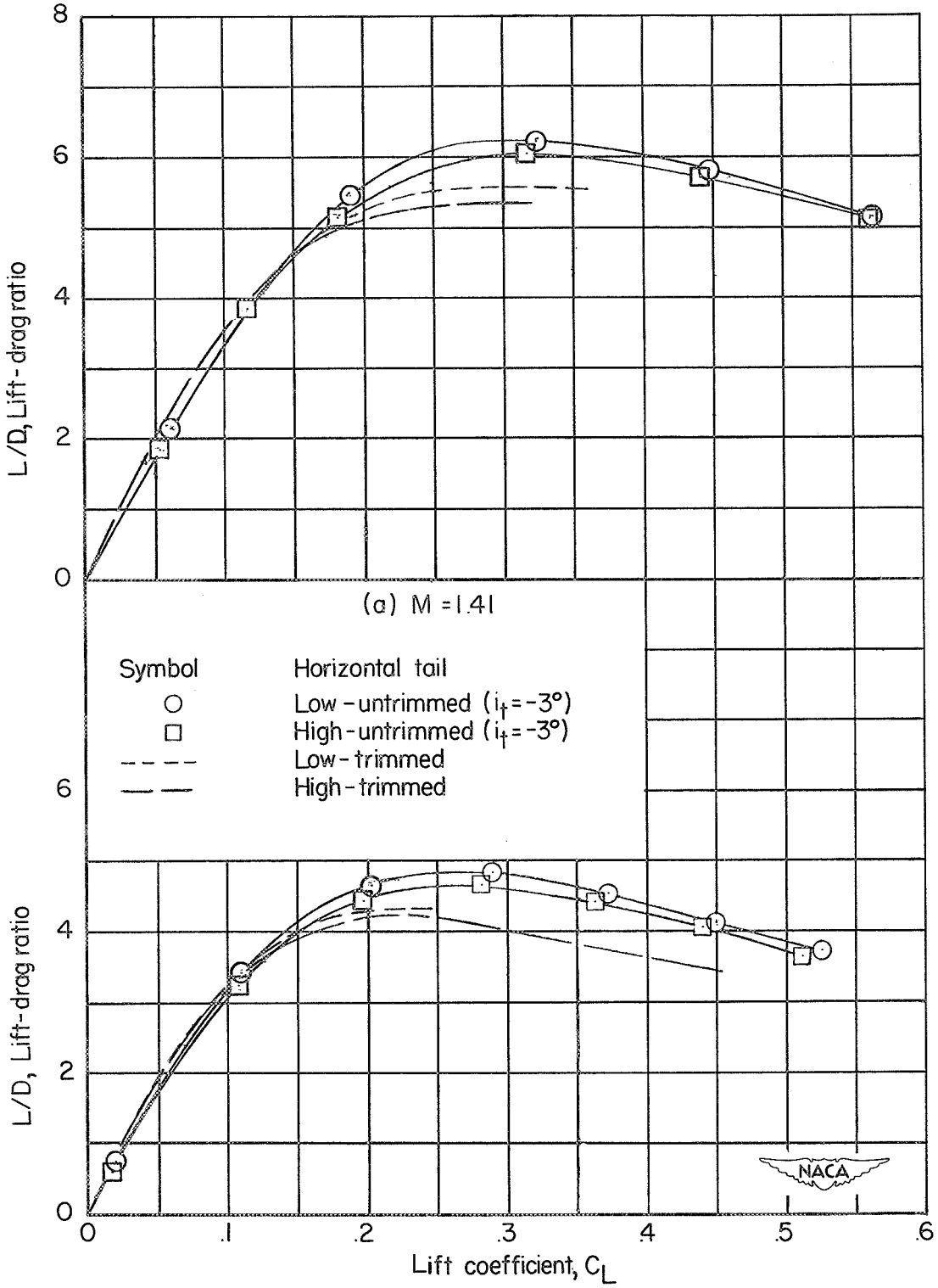

Figure 15.- Lift-drag ratios of the basic model, trimmed and untrimmed.

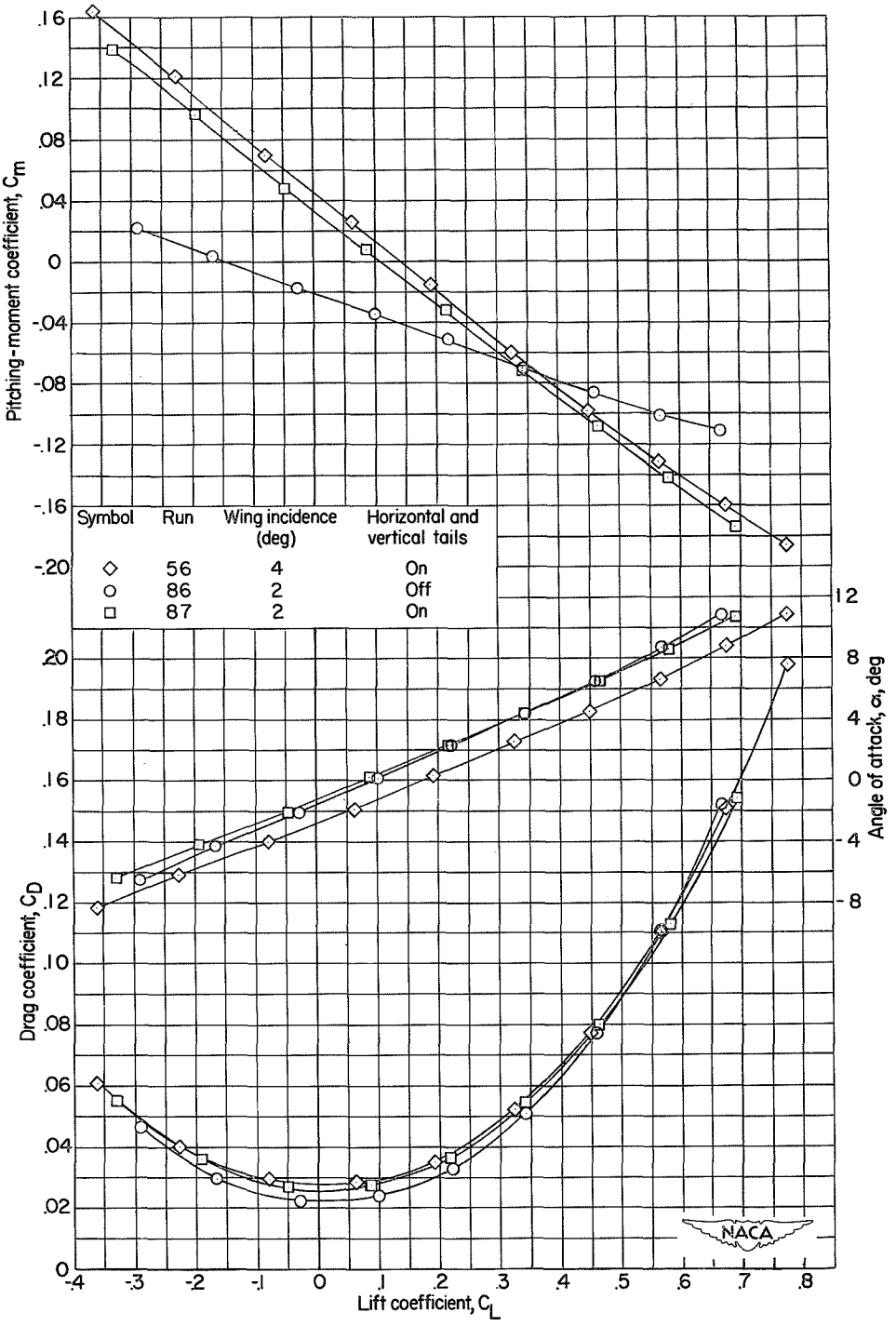

(a) M = 1.41.

Figure 16.- Effect of wing incidence on the longitudinal stability characteristics of the wing plus fuselage and basic model with low horizontal tail.

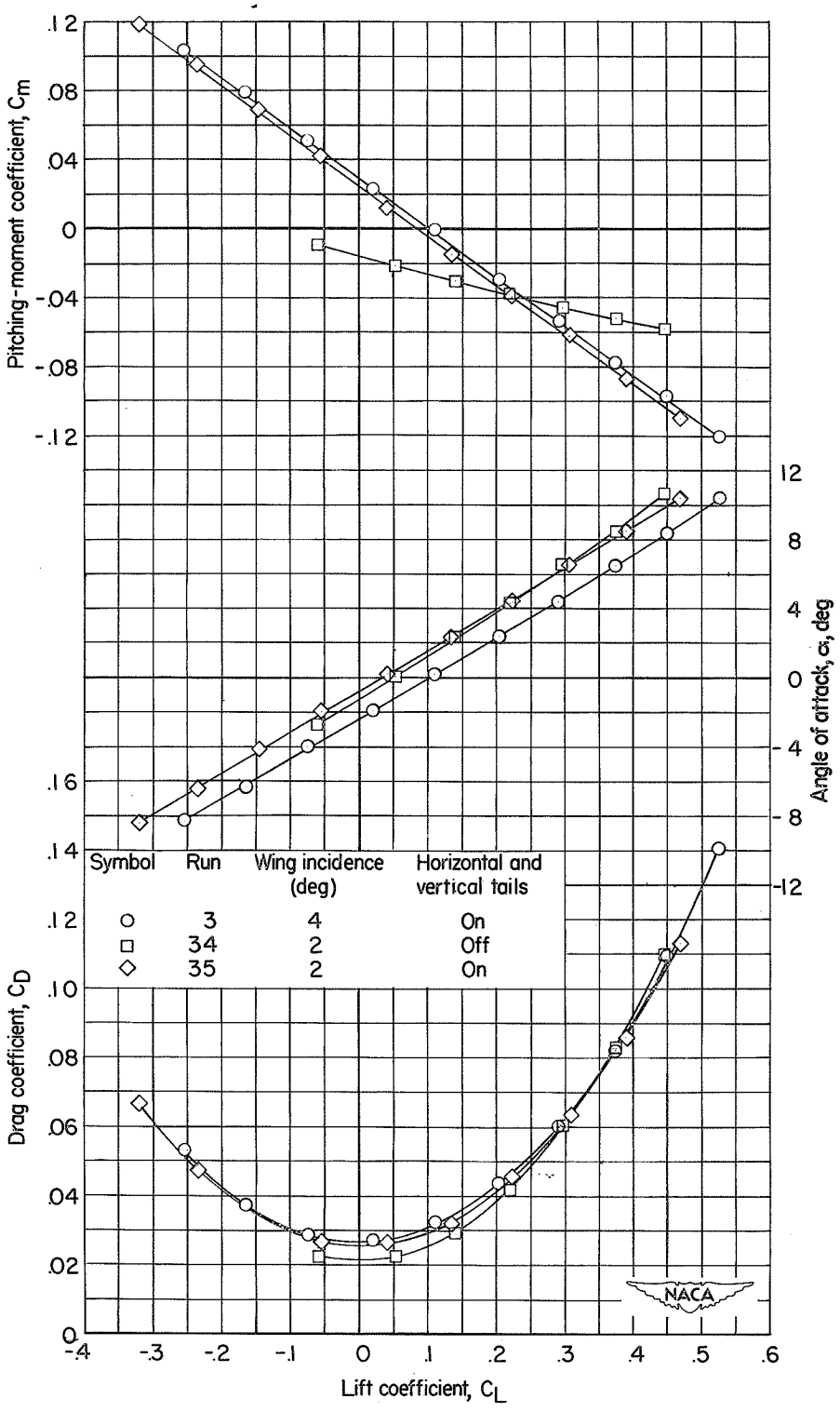

(b) M = 2.01.

Figure 16.- Concluded.

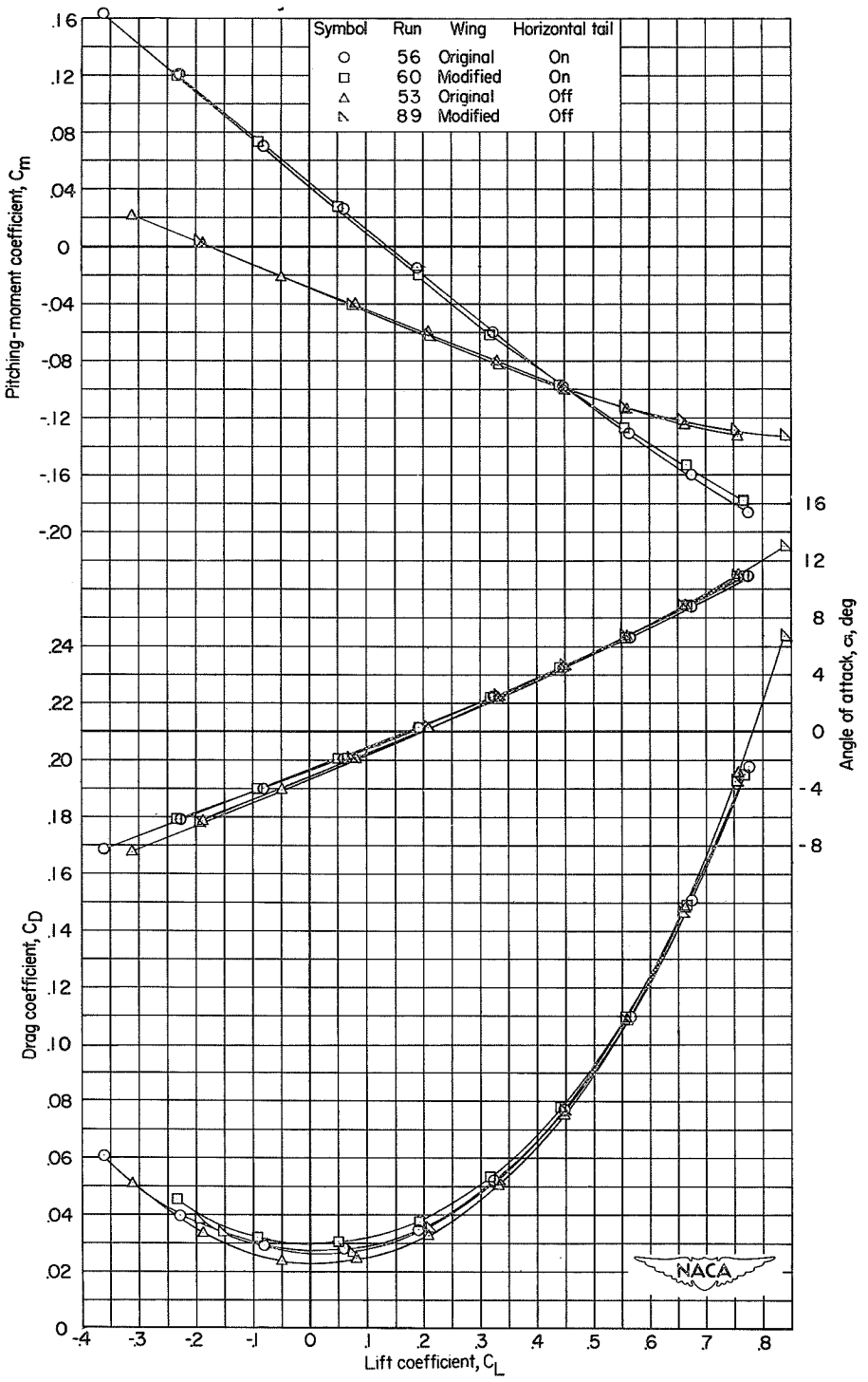

(a) M = 1.41; low horizontal tail, $i_t = -3^o$.

Figure 17.- Comparison of the longitudinal stability characteristics of two configurations with the original and modified wings.

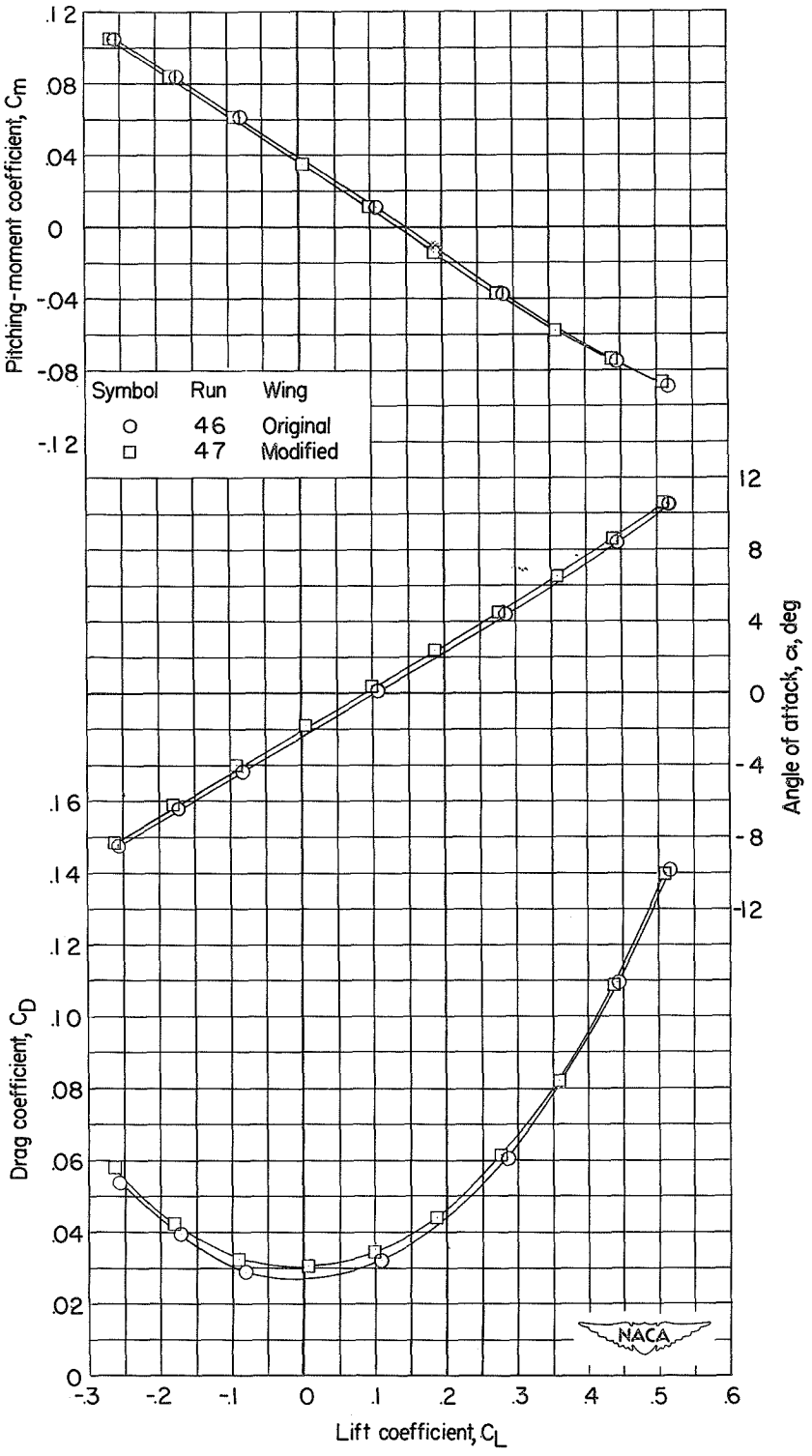

(b) M = 2.01; high horizontal tail, $i_t = -3^\circ$.

Figure 17.- Concluded.

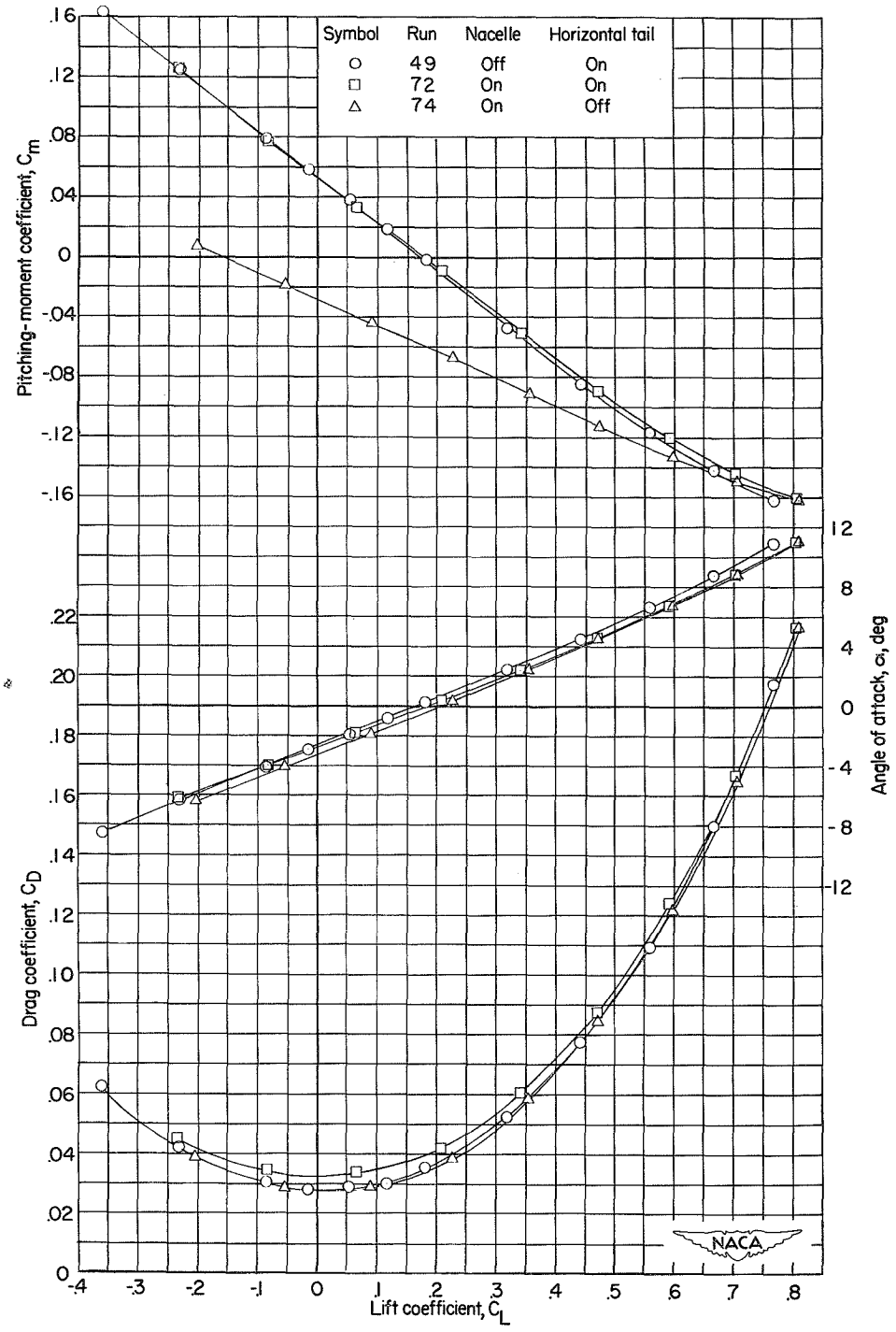

(a) M = 1.41.

Figure 18.- Effect of buried nacelles on the longitudinal stability characteristics of the basic model with and without the high horizontal tail.

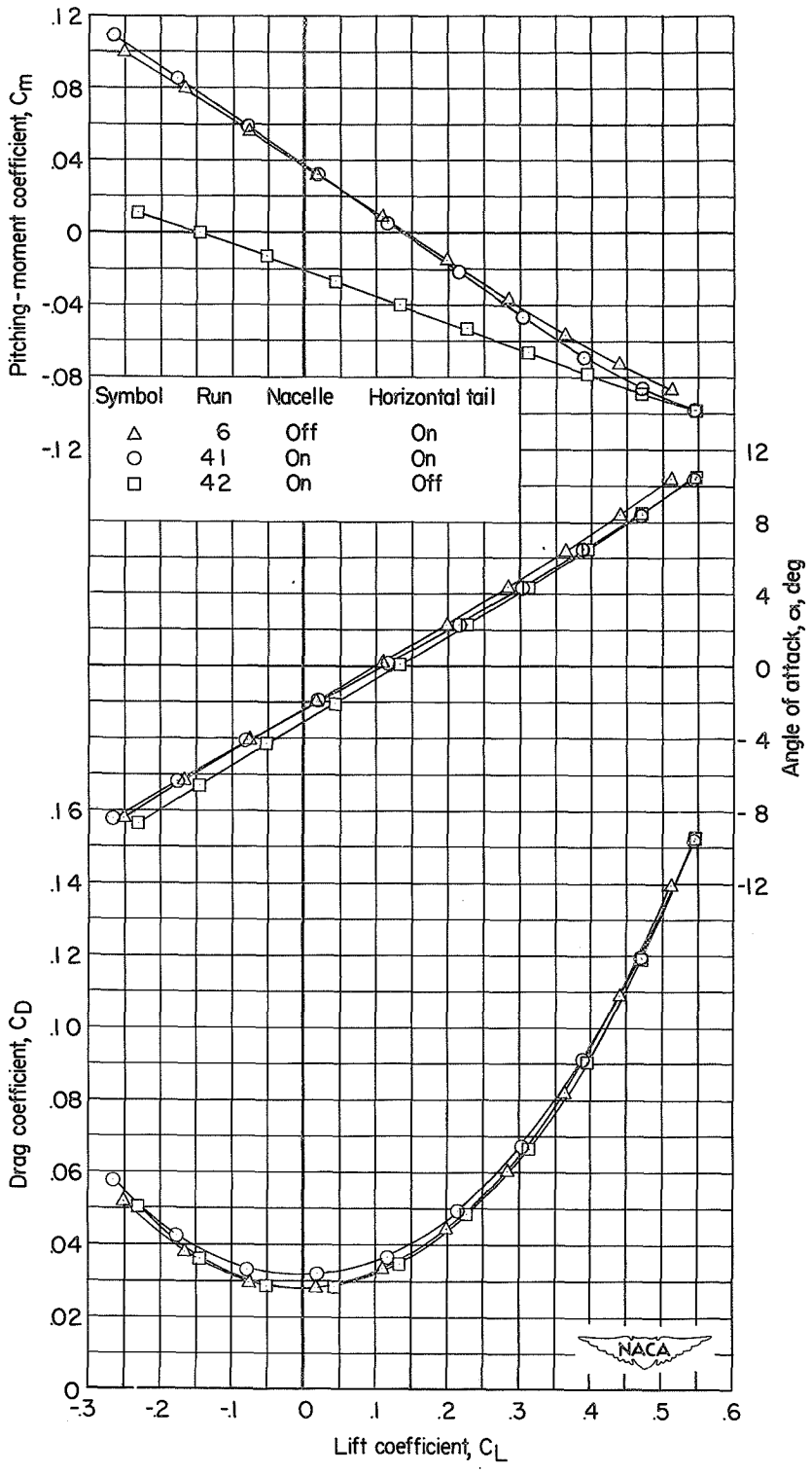

(b) M = 2.01.

Figure 18.- Concluded.

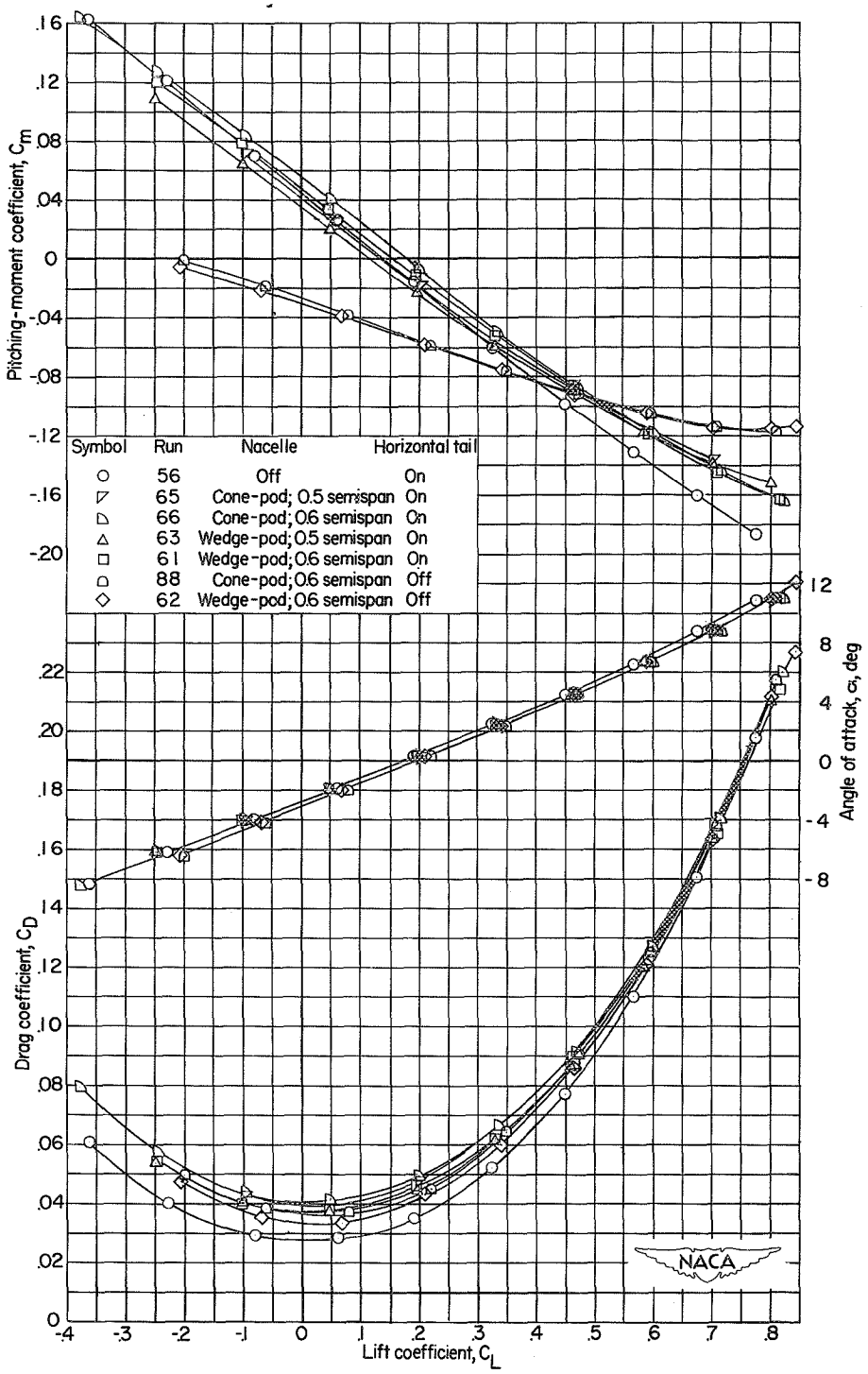

(a) M = 1.41.

Figure 19.- Effect of pod nacelles on the longitudinal stability characteristics of the basic model with and without the low horizontal tail.

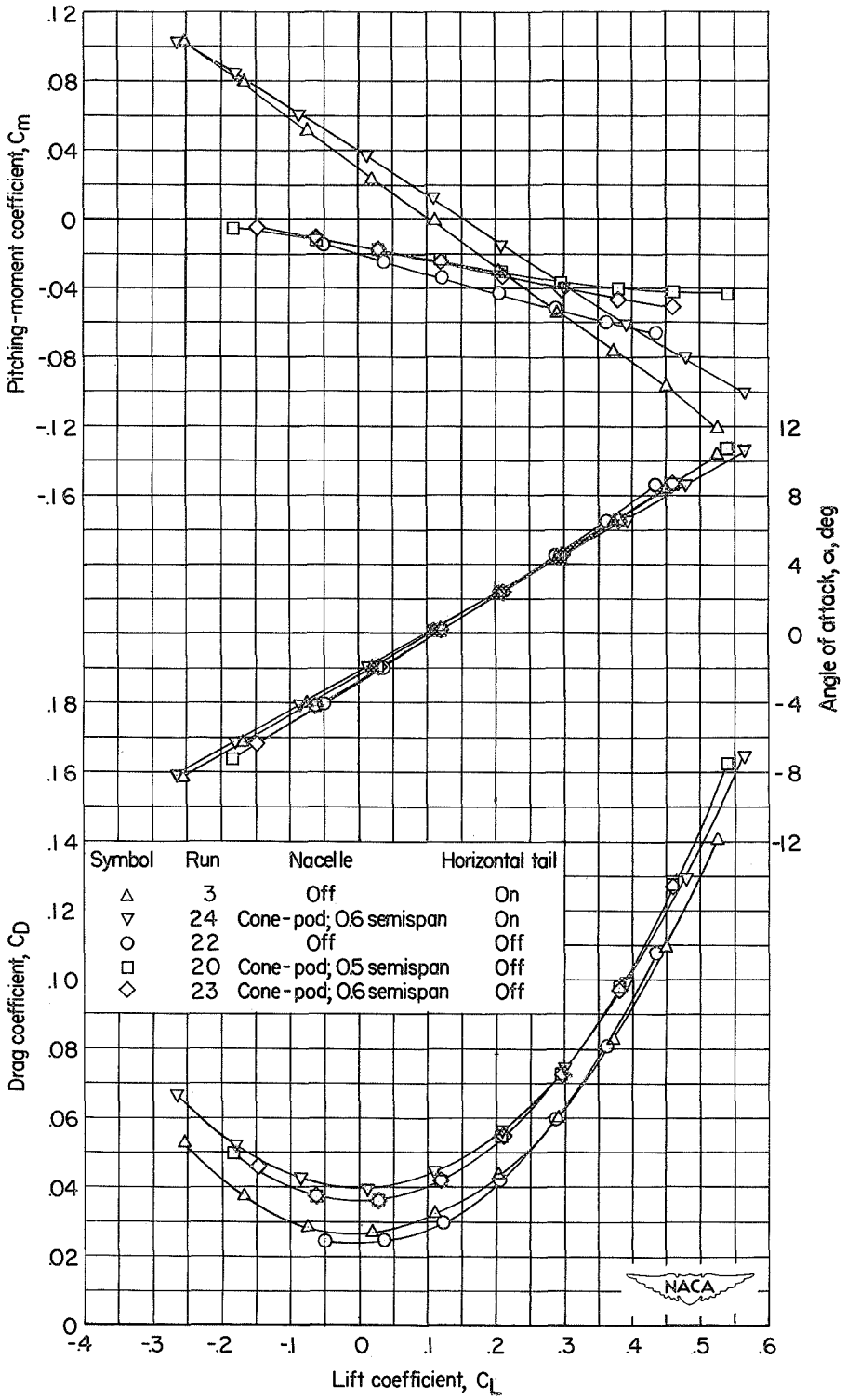

(b) M = 2.01.

Figure 19.- Concluded.

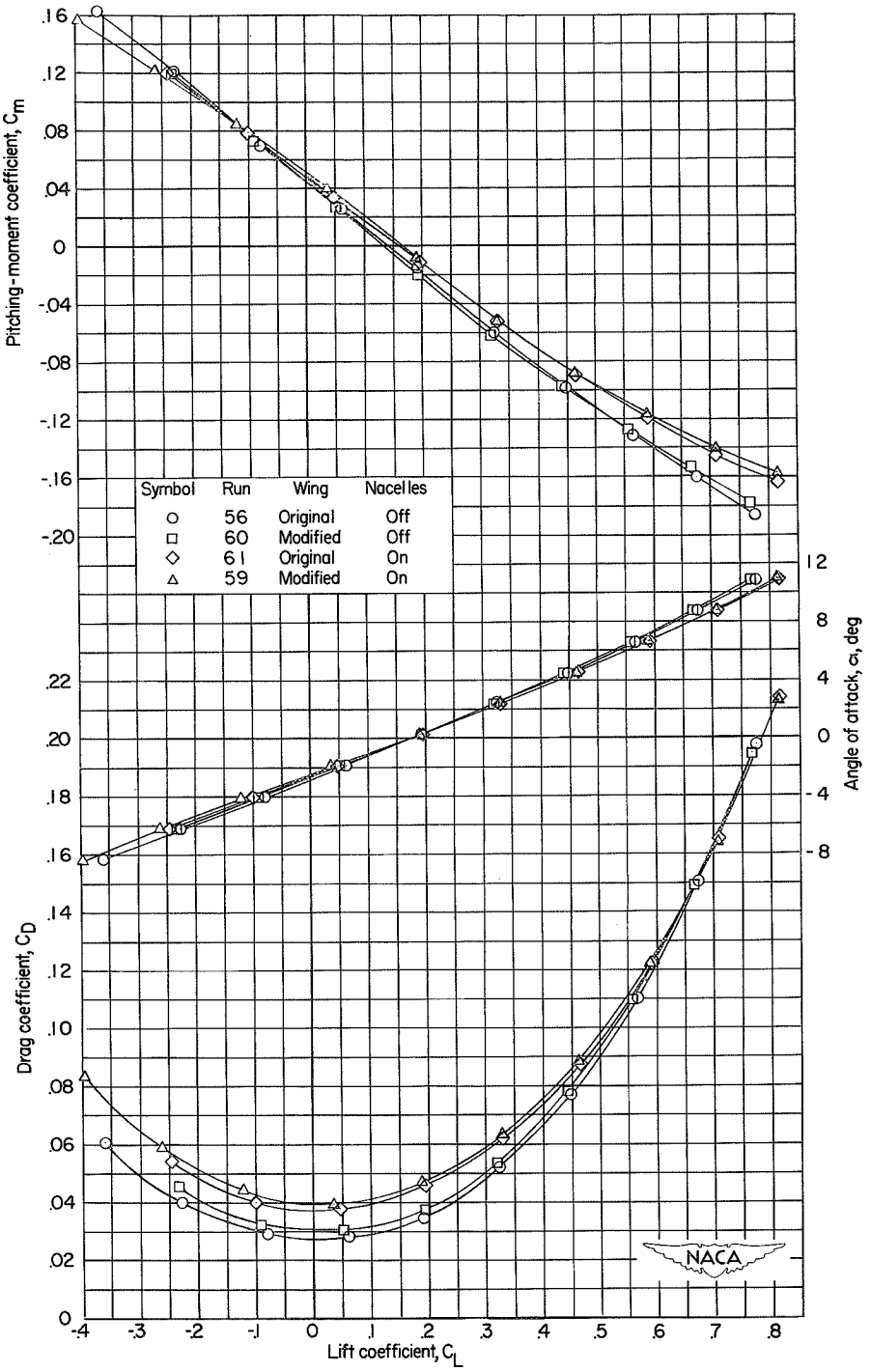

Figure 20.- Effect of wedge-pod nacelles on the longitudinal stability characteristics of the basic model with the original and modified wings. Nacelles located at the 60-percent-semispan station. Horizontal tail in the low position. M = 1.41.

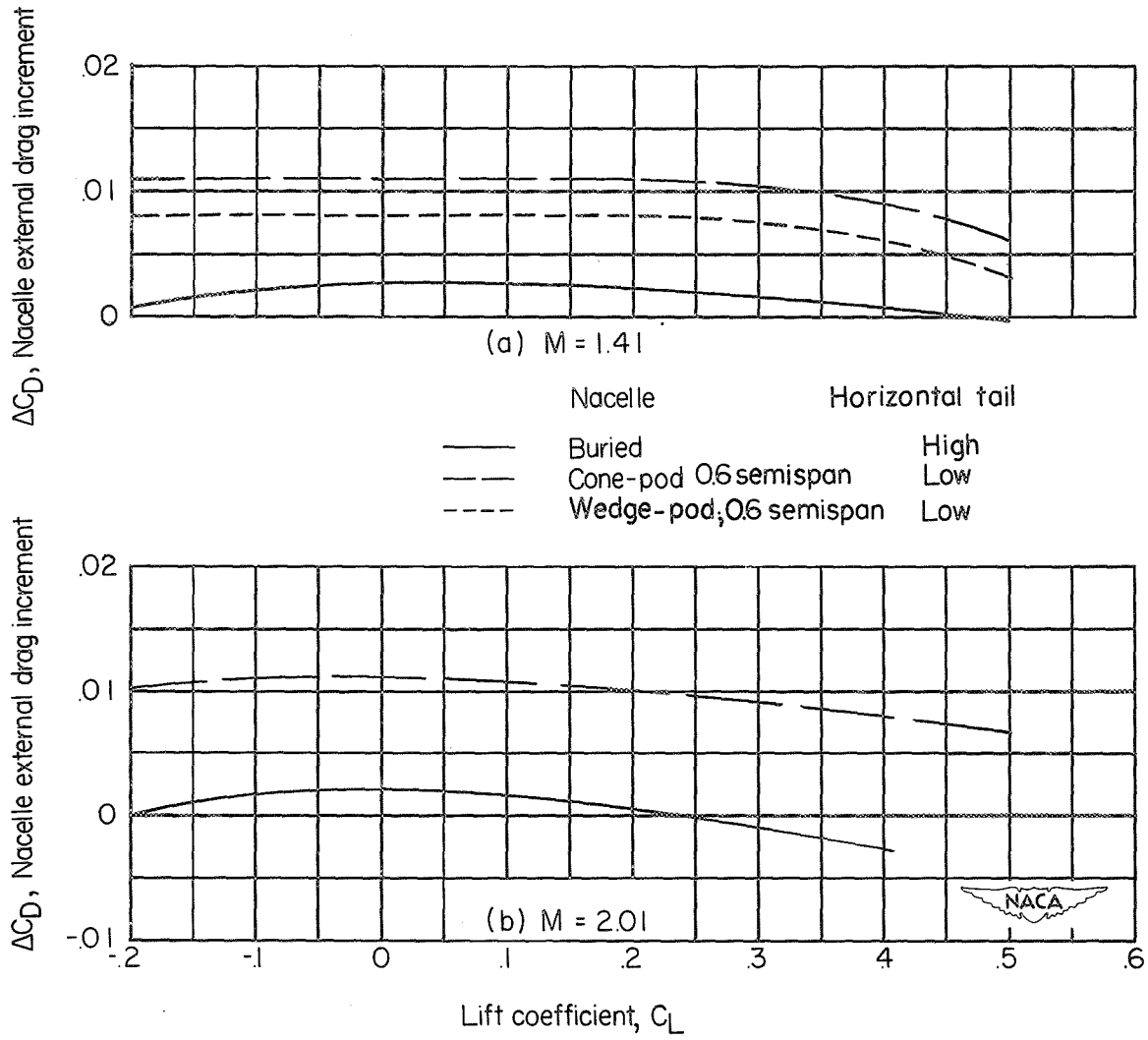

Figure 21.- External drag increment due to the addition of the buried or pod nacelles to the basic model.

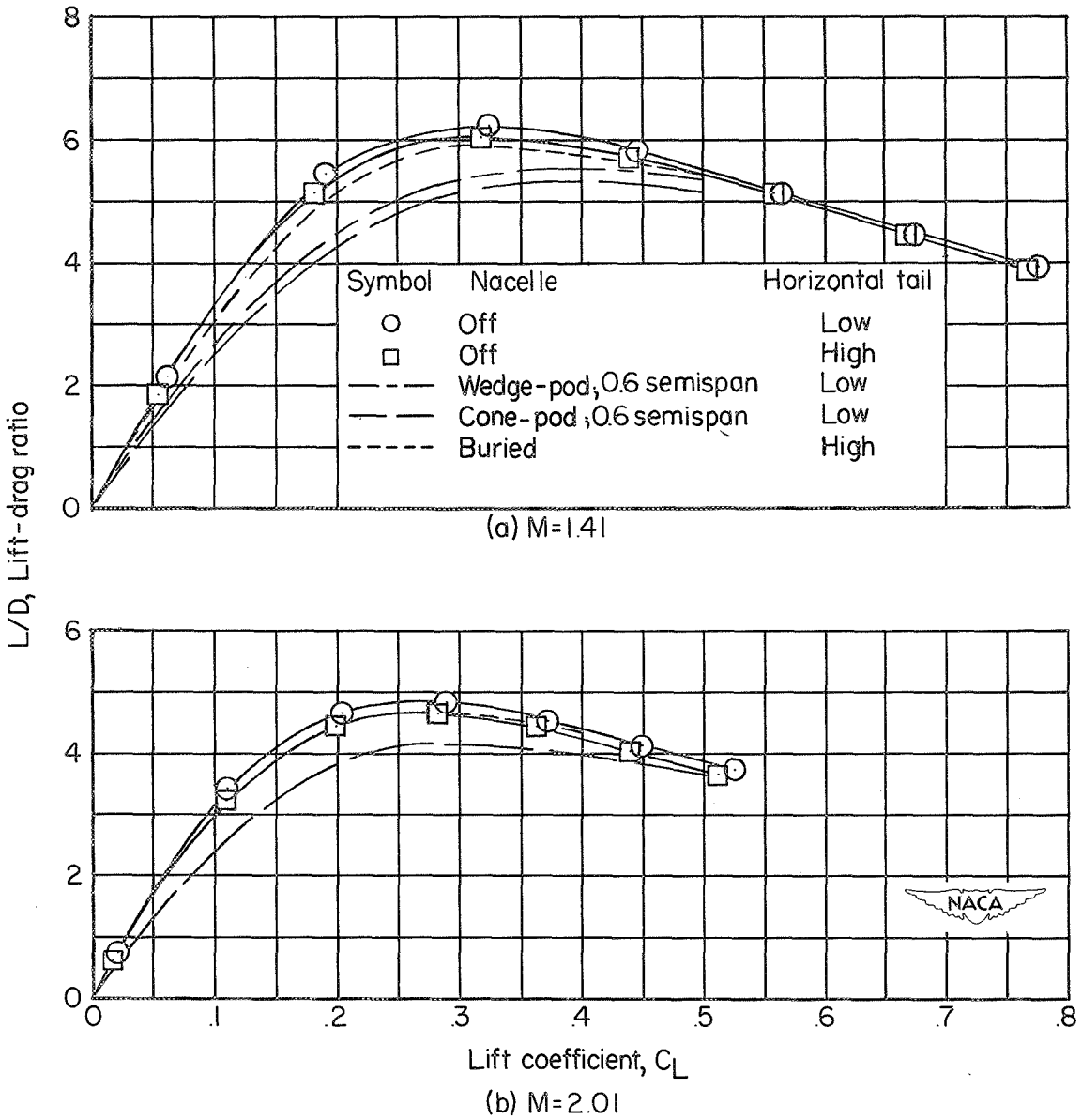

Figure 22.- Lift-drag ratios of the untrimmed basic model with and without the buried and pod nacelles.

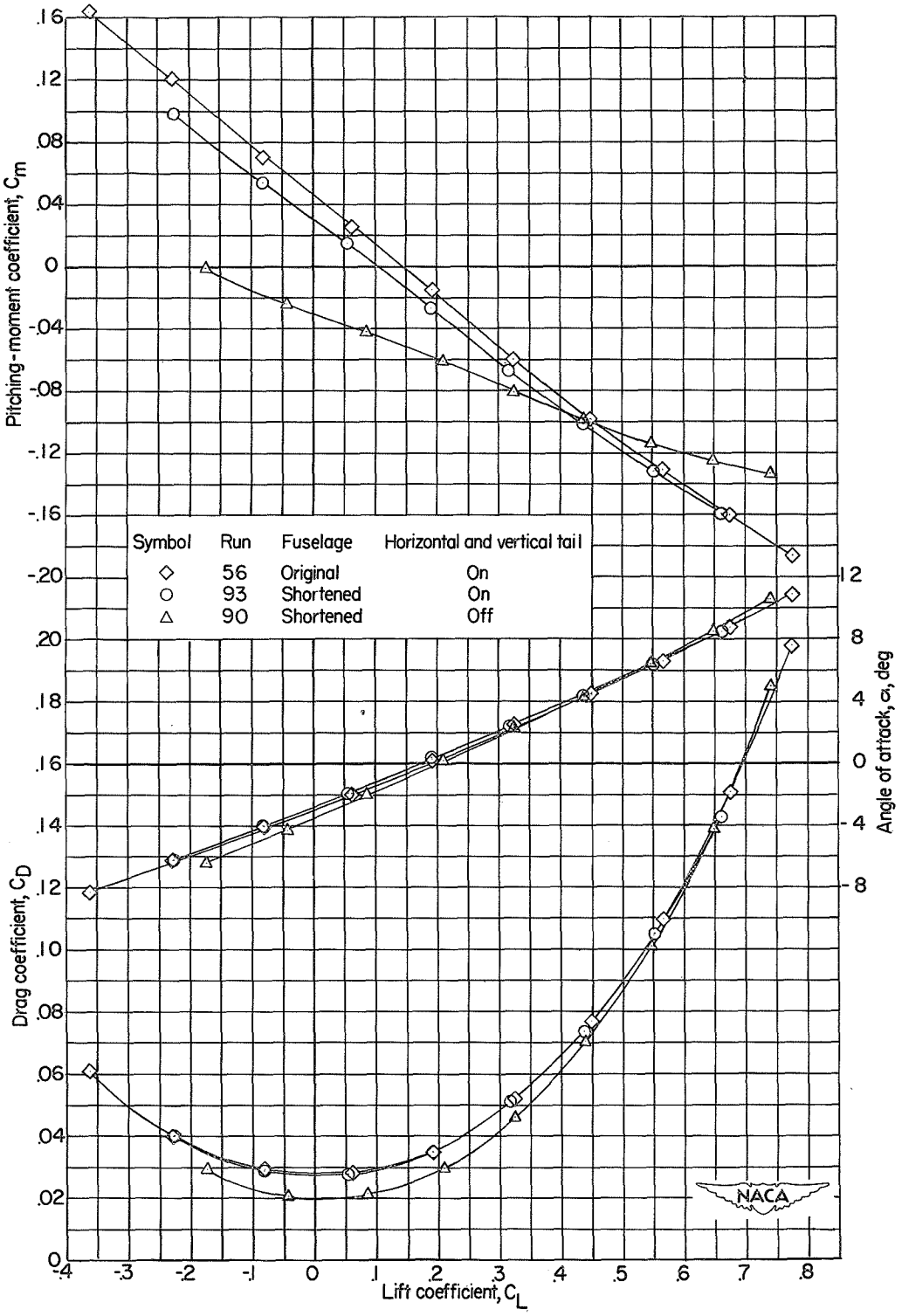

Figure 23.- Effect of fuselage length on the longitudinal stability characteristics of the fuselage plus wing and of the basic model with low horizontal tail. M = 1.41.

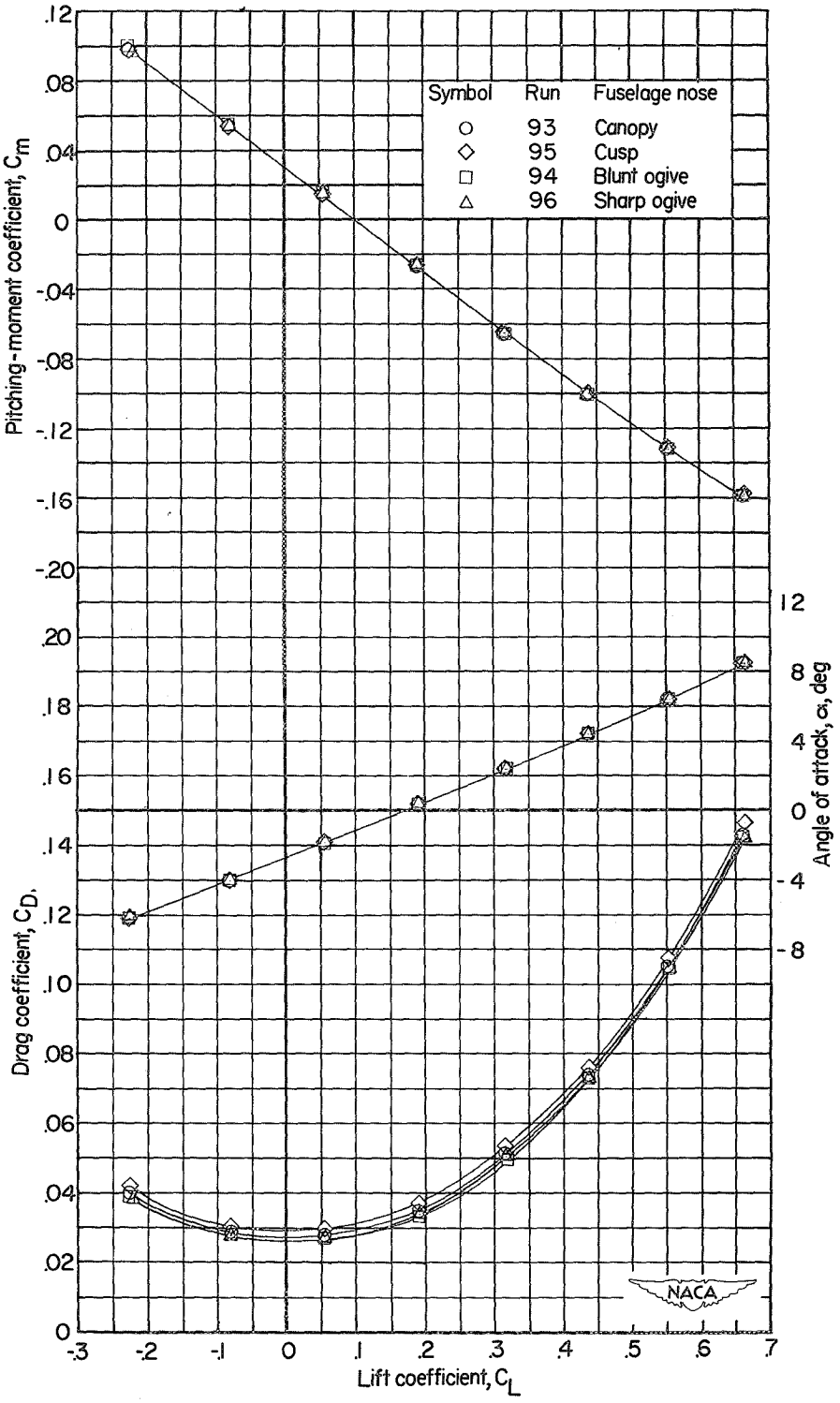

(a) M = 1.41; low horizontal tail; shortened fuselage.

Figure 24.- Effect of fuselage nose shape on the longitudinal stability characteristics of the basic model.

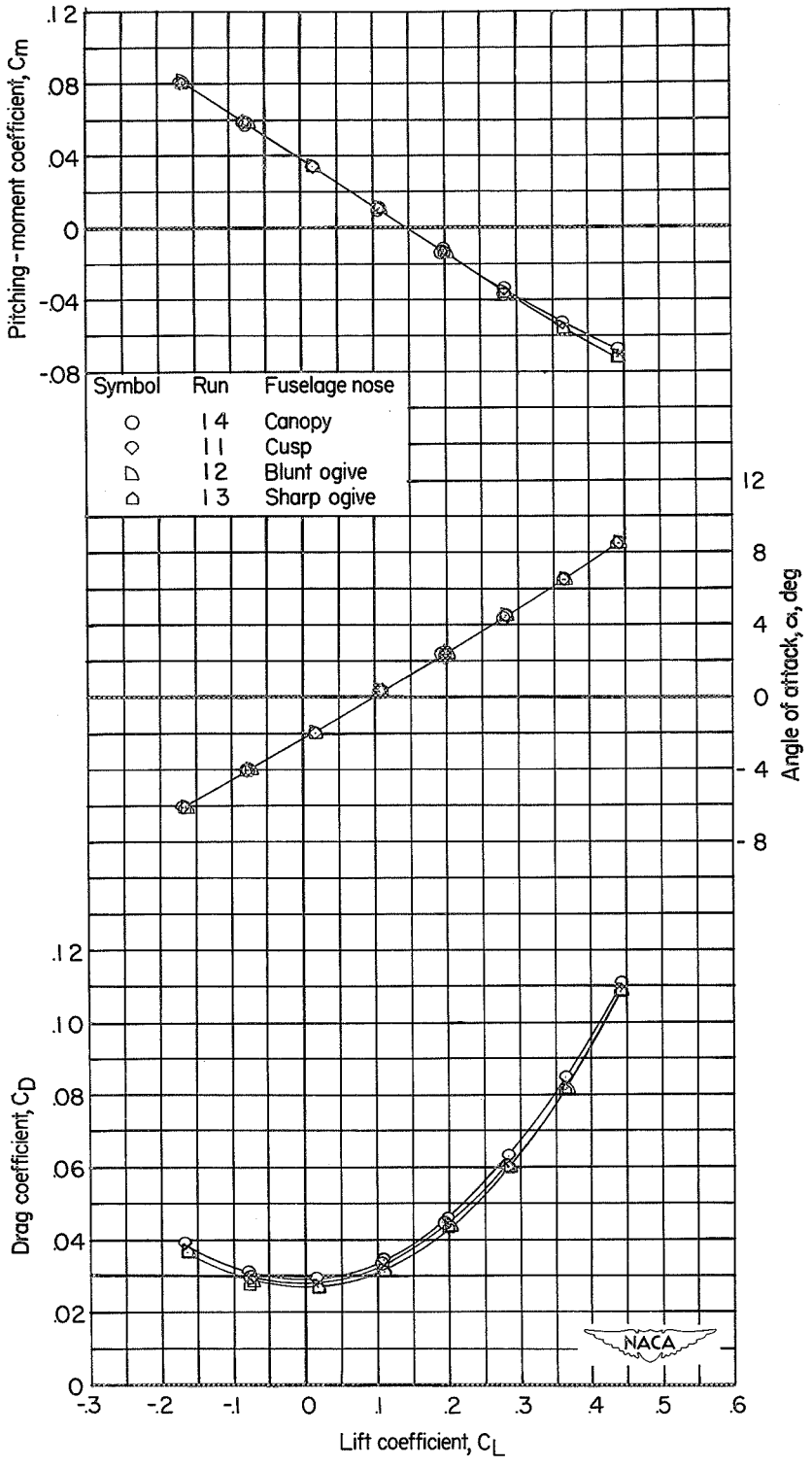

(b) M = 2.01; high horizontal tail; original fuselage.

Figure 24.- Concluded.

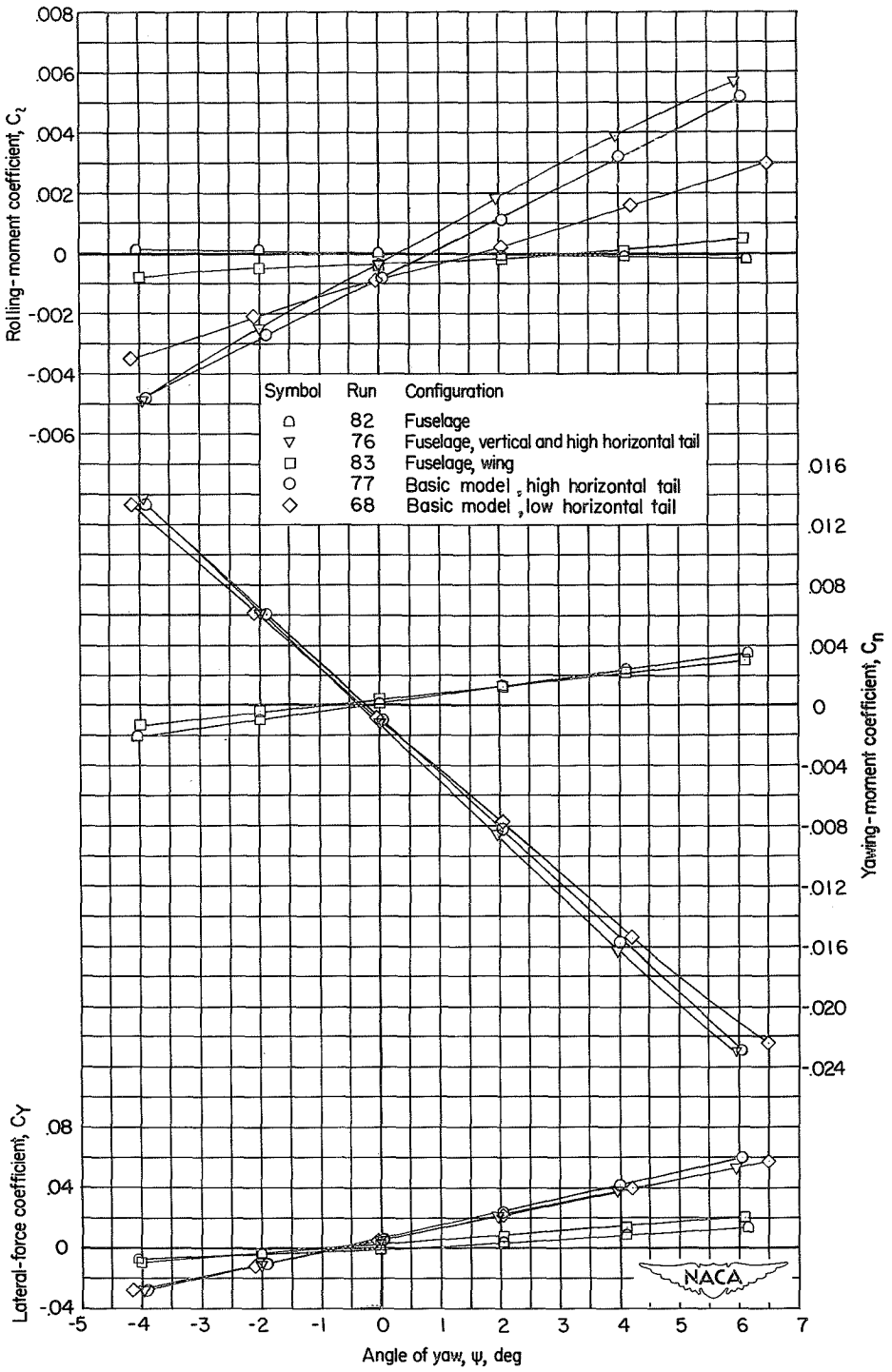

(a) M = 1.41.

Figure 25.- Lateral stability characteristics of various combinations of fuselage, wing, and tail.

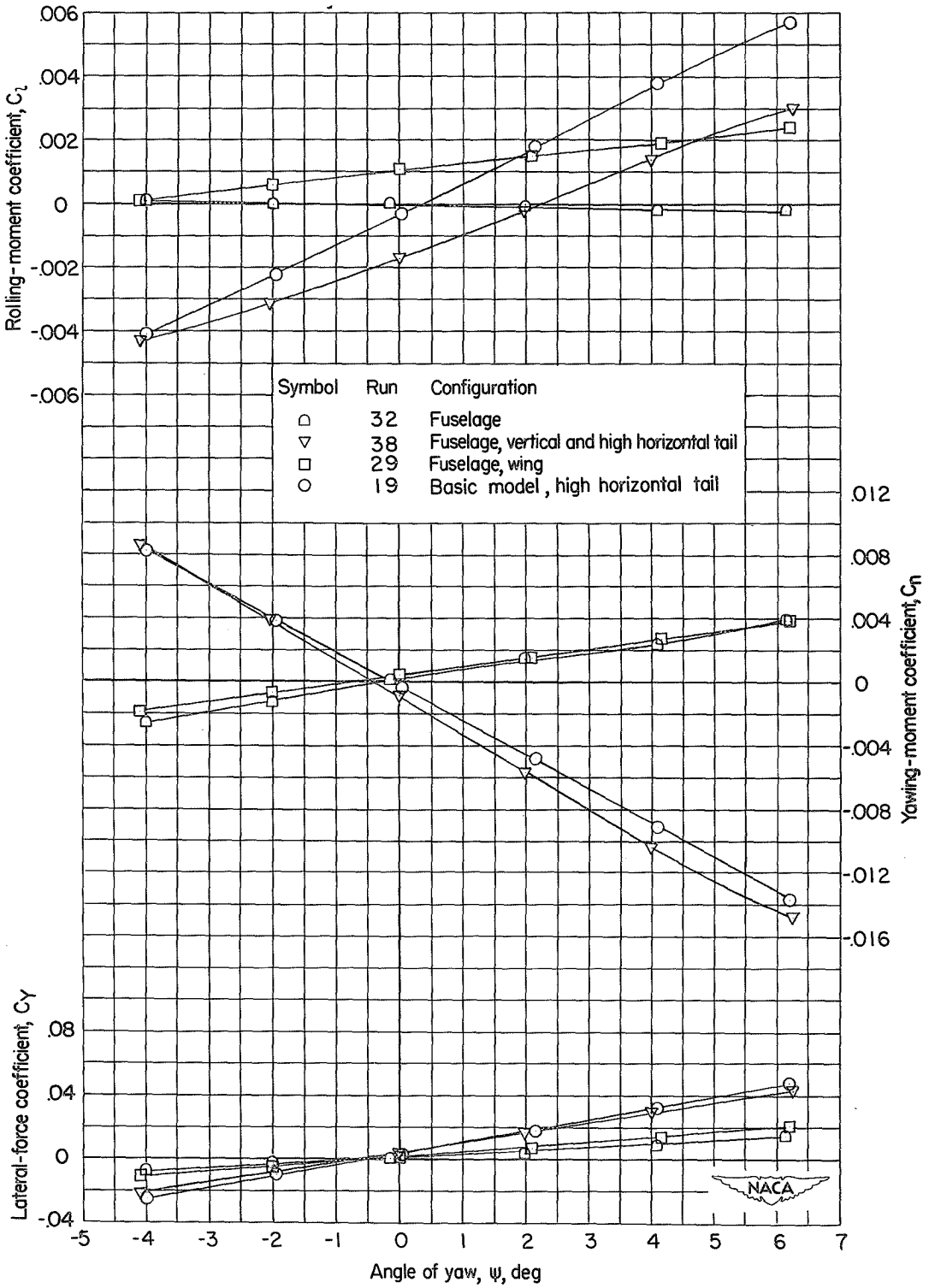

(b) M = 2.01.

Figure 25.- Concluded.

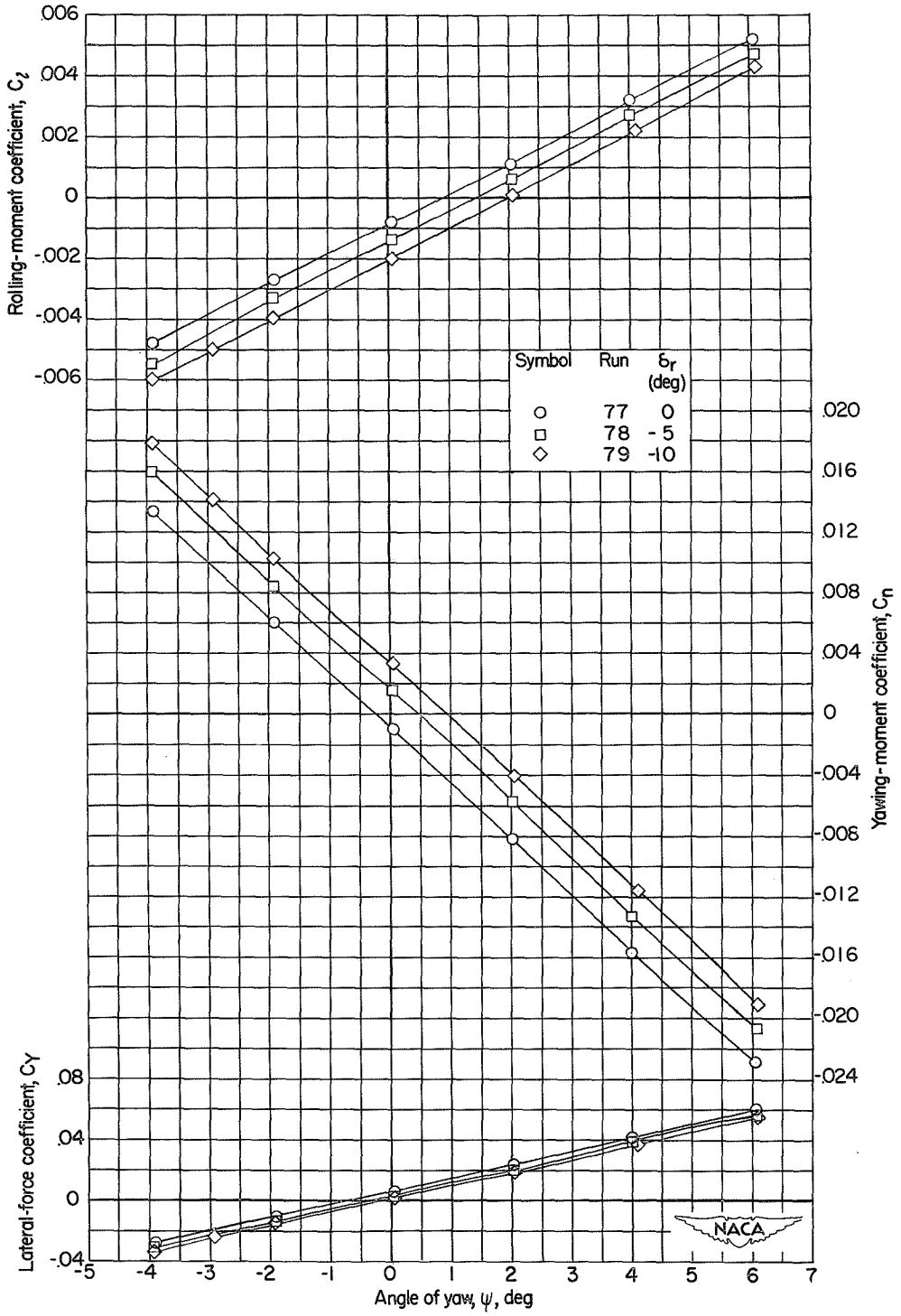

(a) M = 1.41.

Figure 26.- Lateral stability characteristics of the basic model with various rudder deflections. High horizontal tail.

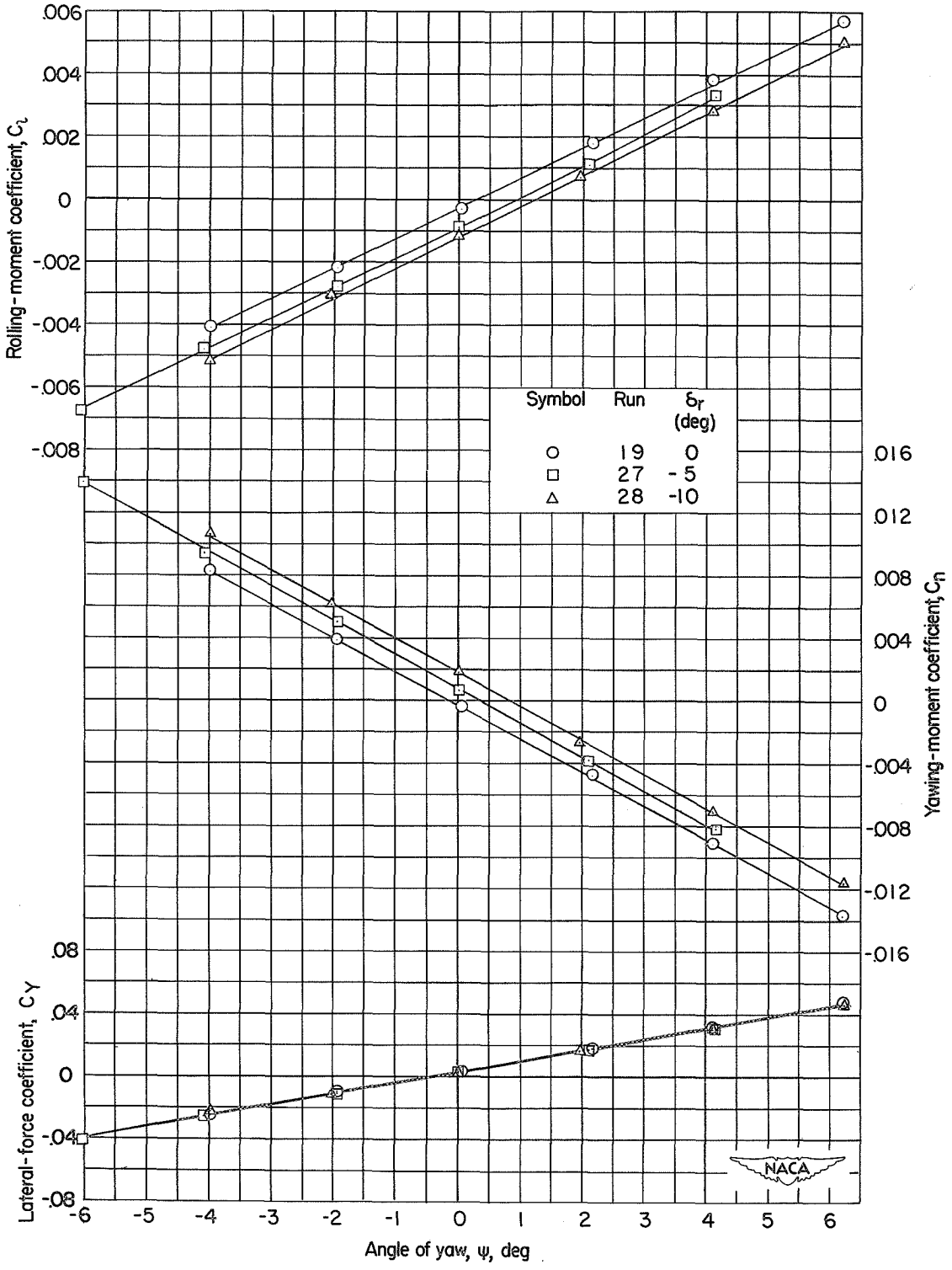

(b) M = 2.01.

Figure 26.- Concluded.

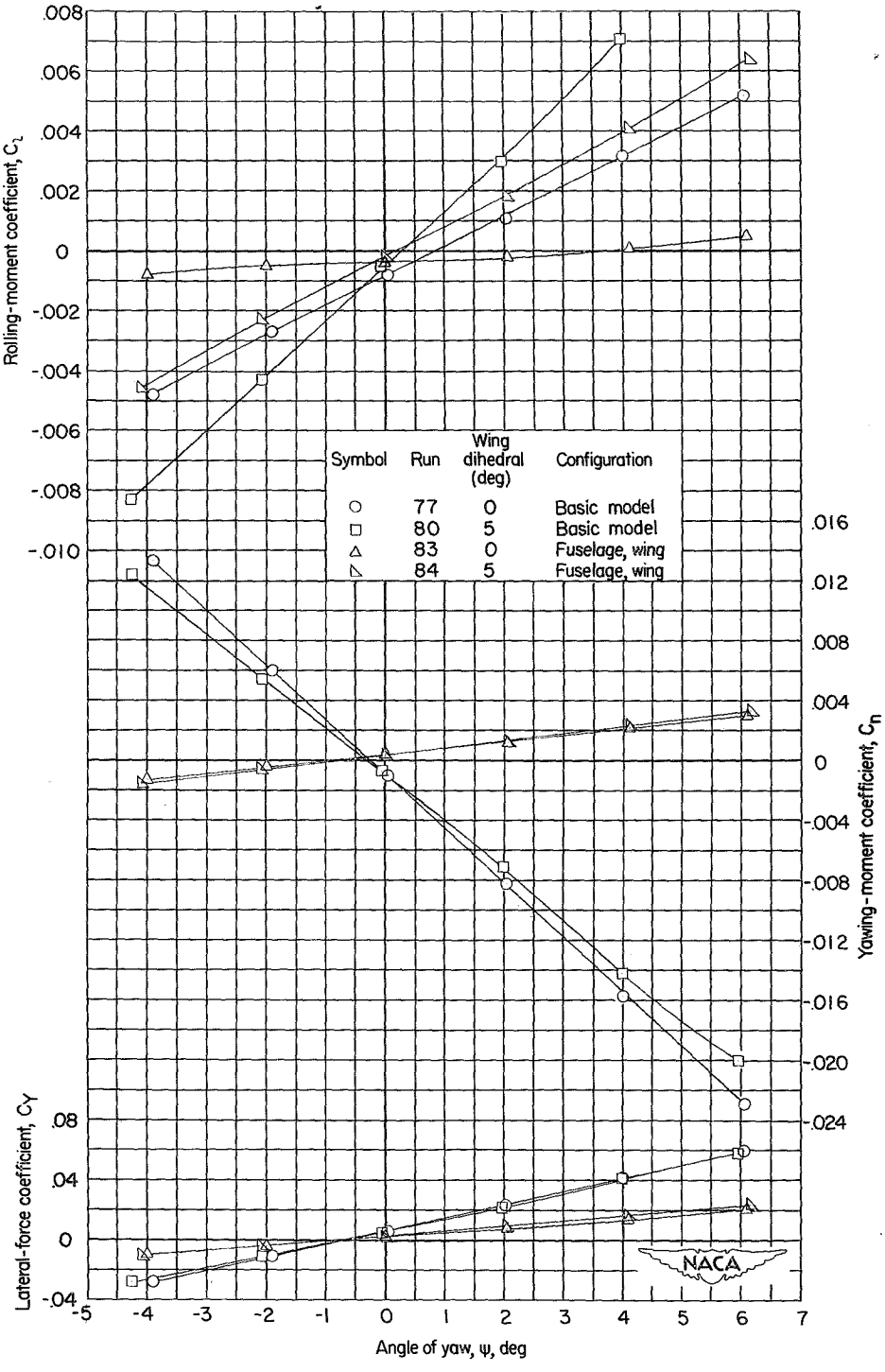

(a) M = 1.41.

Figure 27.- Effect of wing dihedral on lateral stability characteristics of fuselage plus wing and basic model with high horizontal tail.

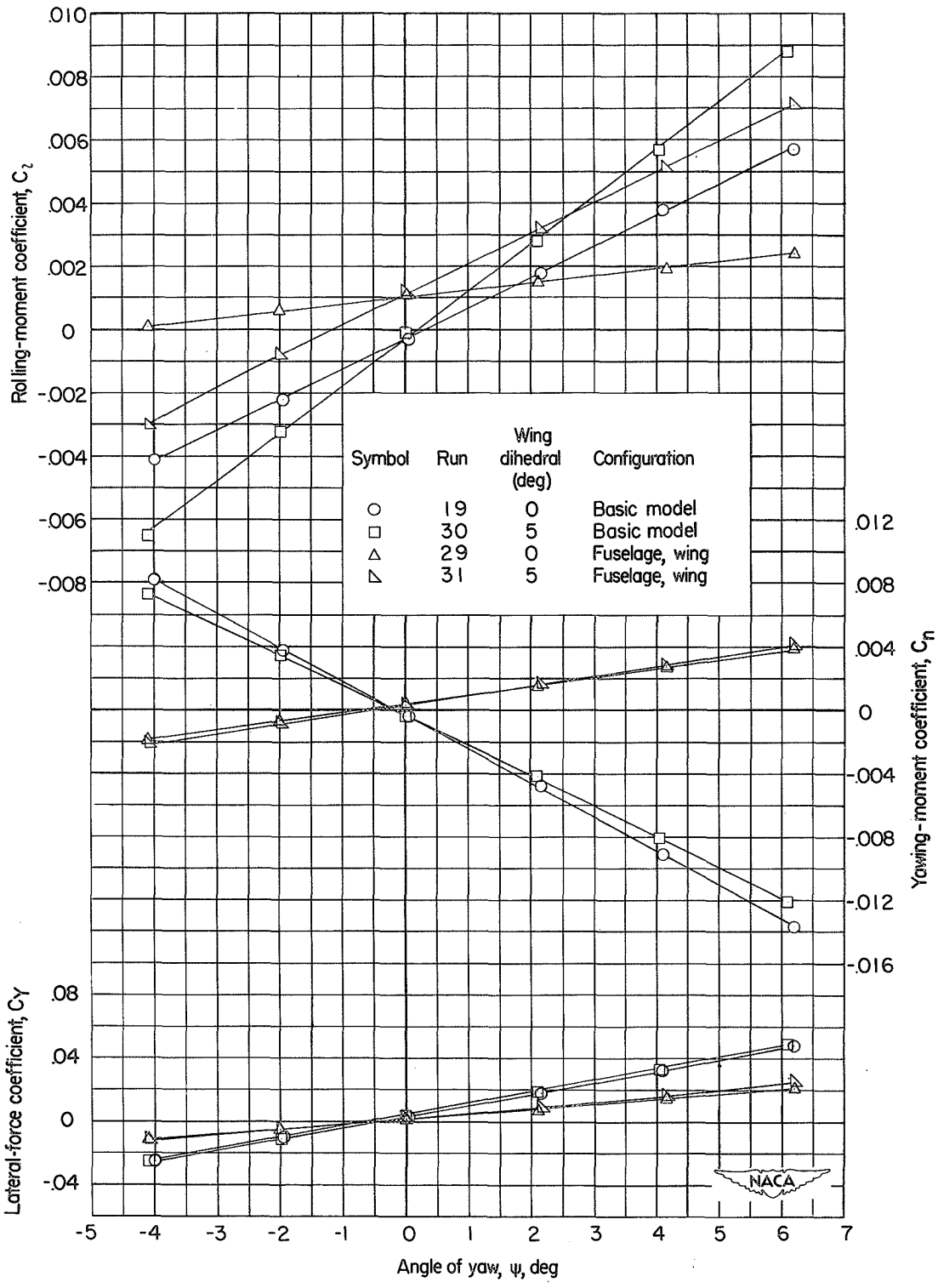

(b) M = 2.01.

Figure 27.- Concluded.

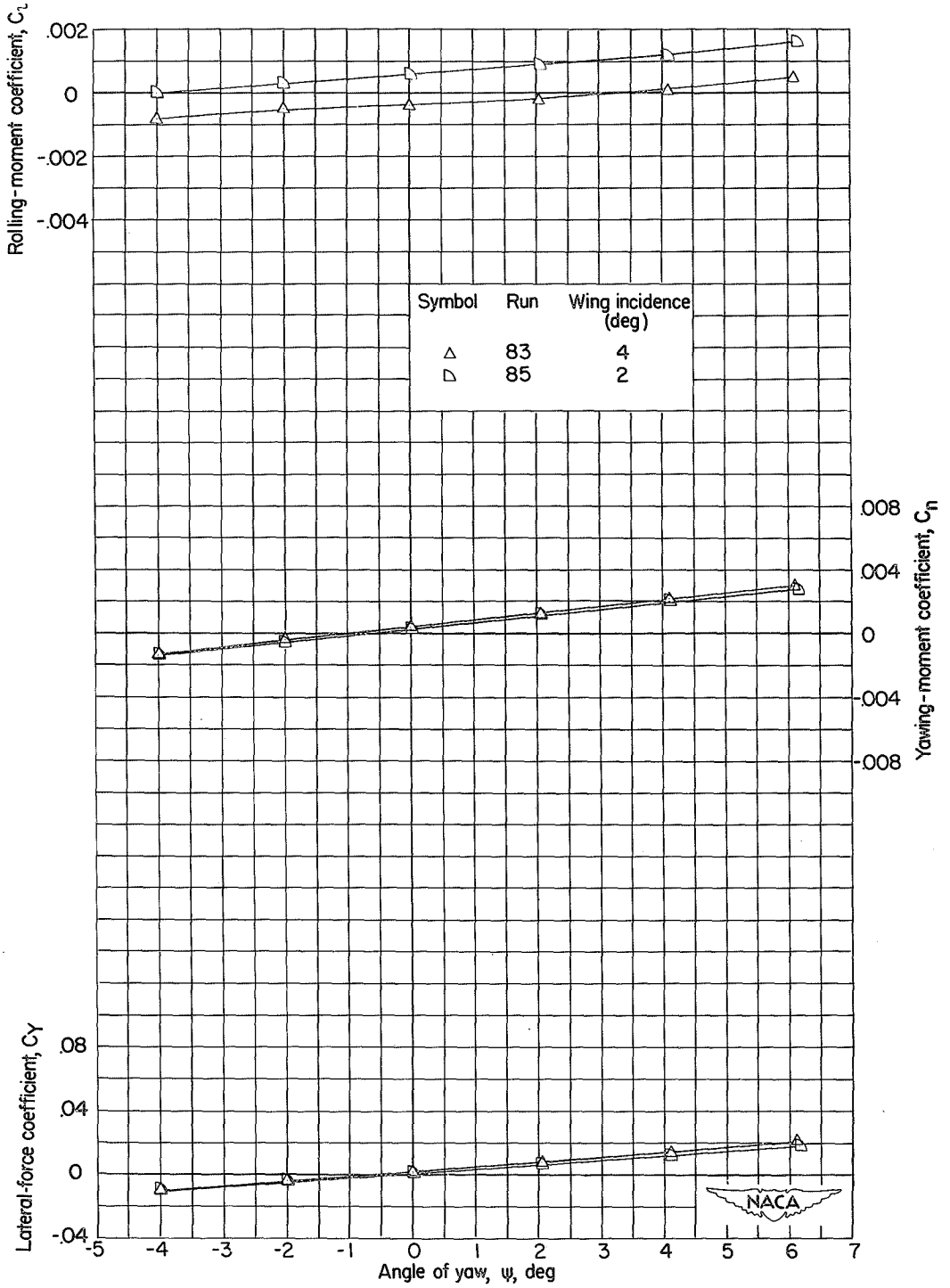

(a) M = 1.41.

Figure 28.- Effect of wing incidence on lateral stability characteristics of the fuselage plus wing.

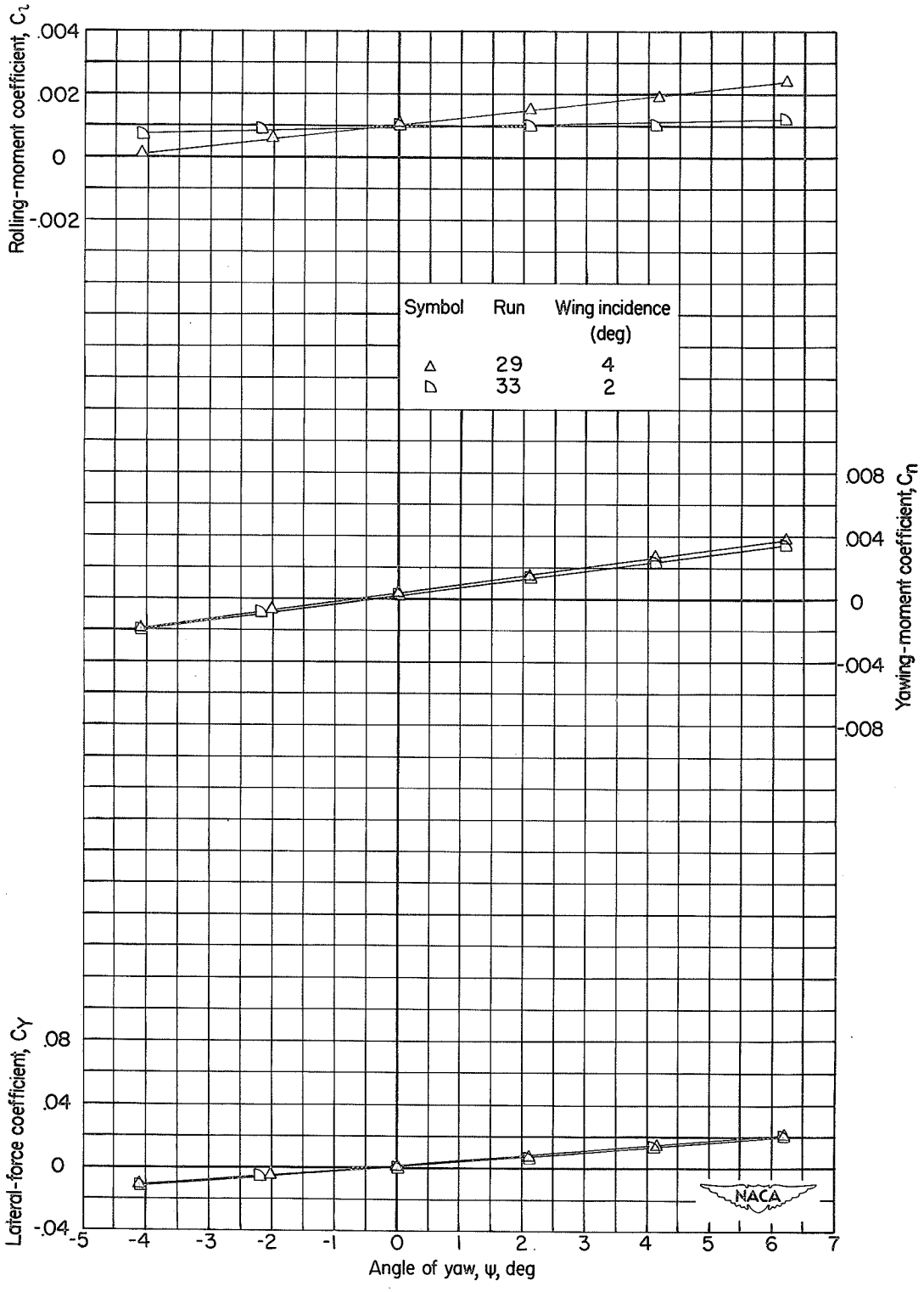

(b) M = 2.01.

Figure 28.- Concluded.

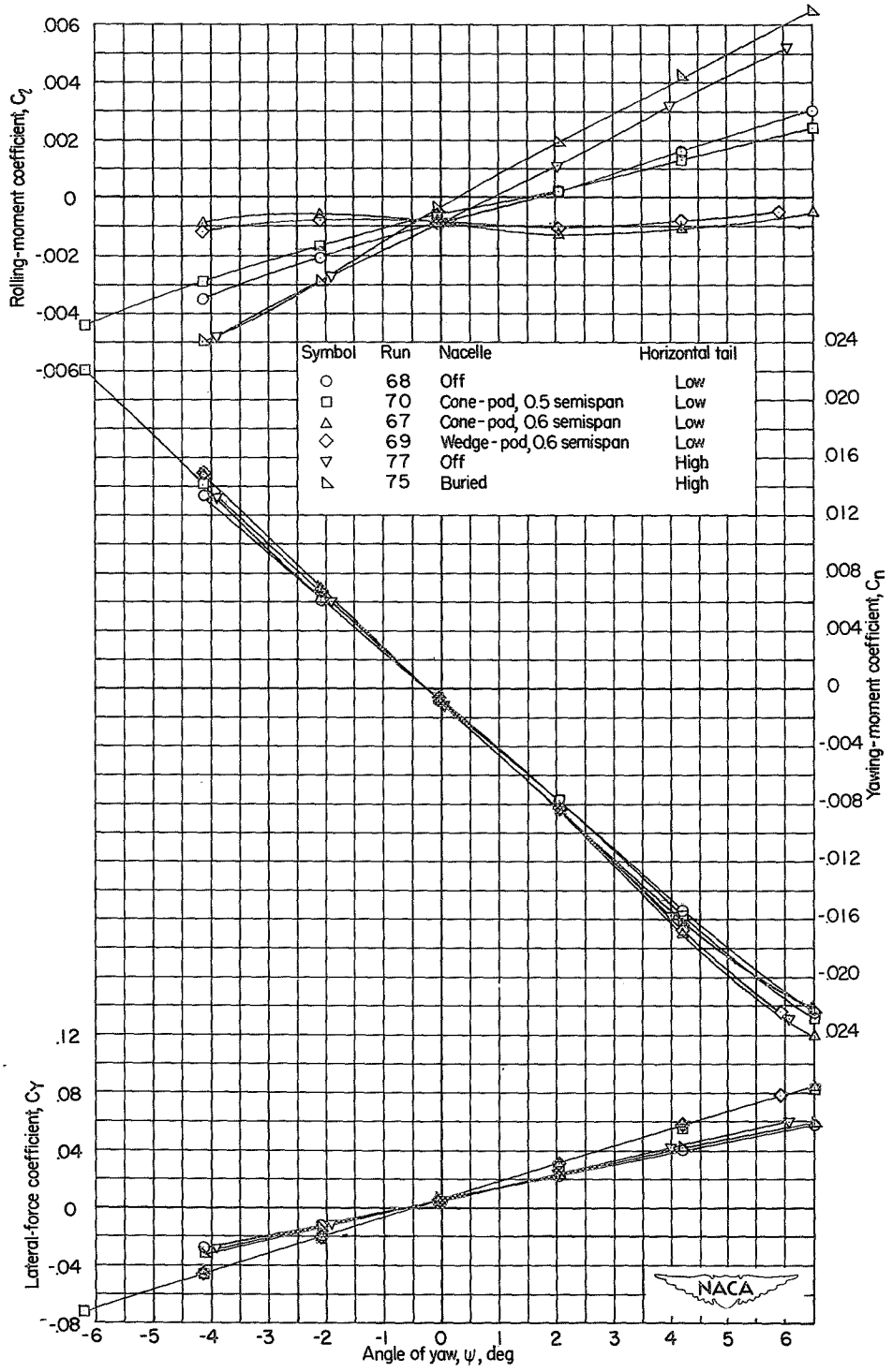

(a) M = 1.41.

Figure 29.- Effect of buried and pod nacelles on the lateral stability characteristics of the basic model.

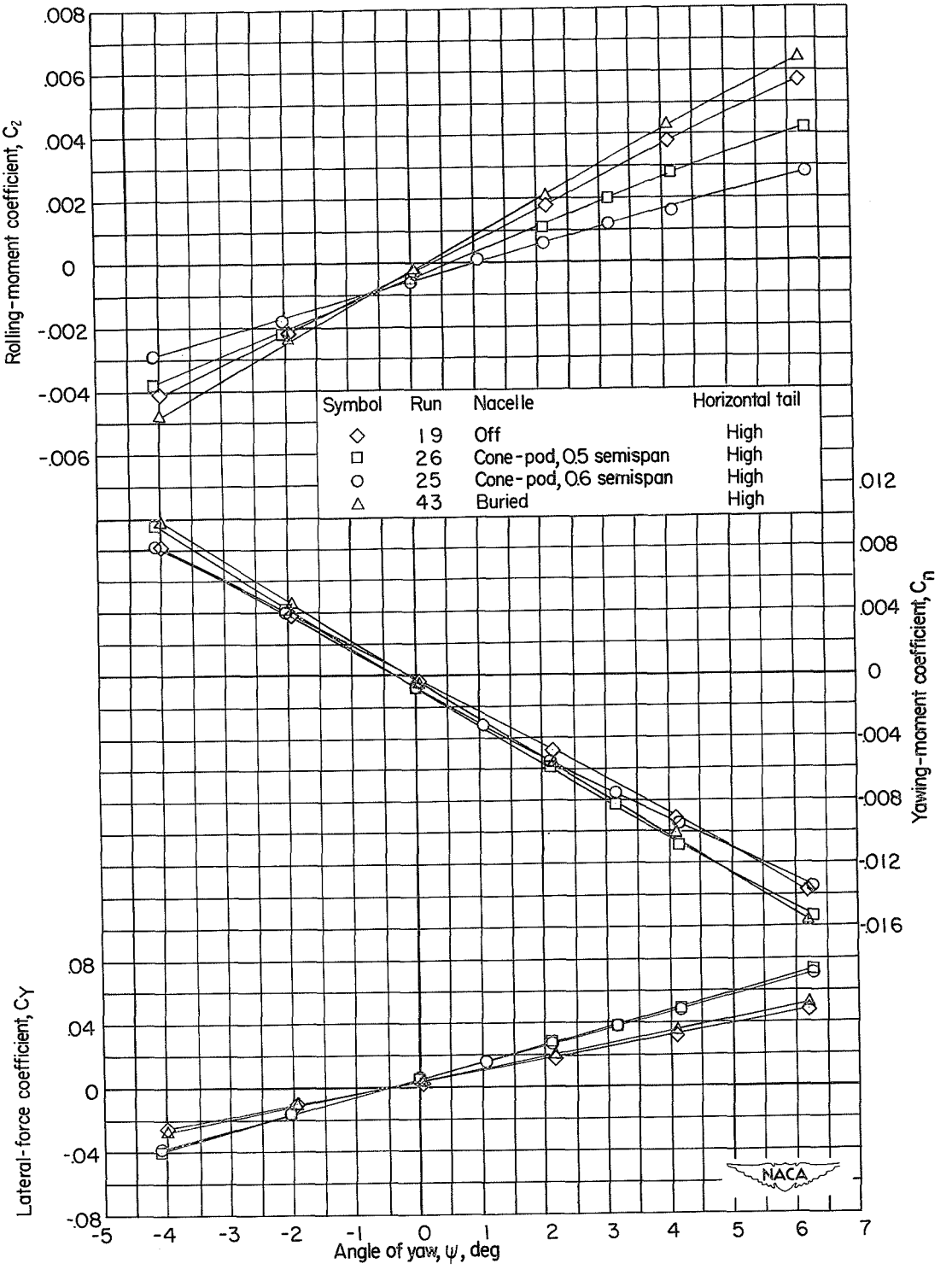

(b) M = 2.01.

Figure 29.- Concluded.

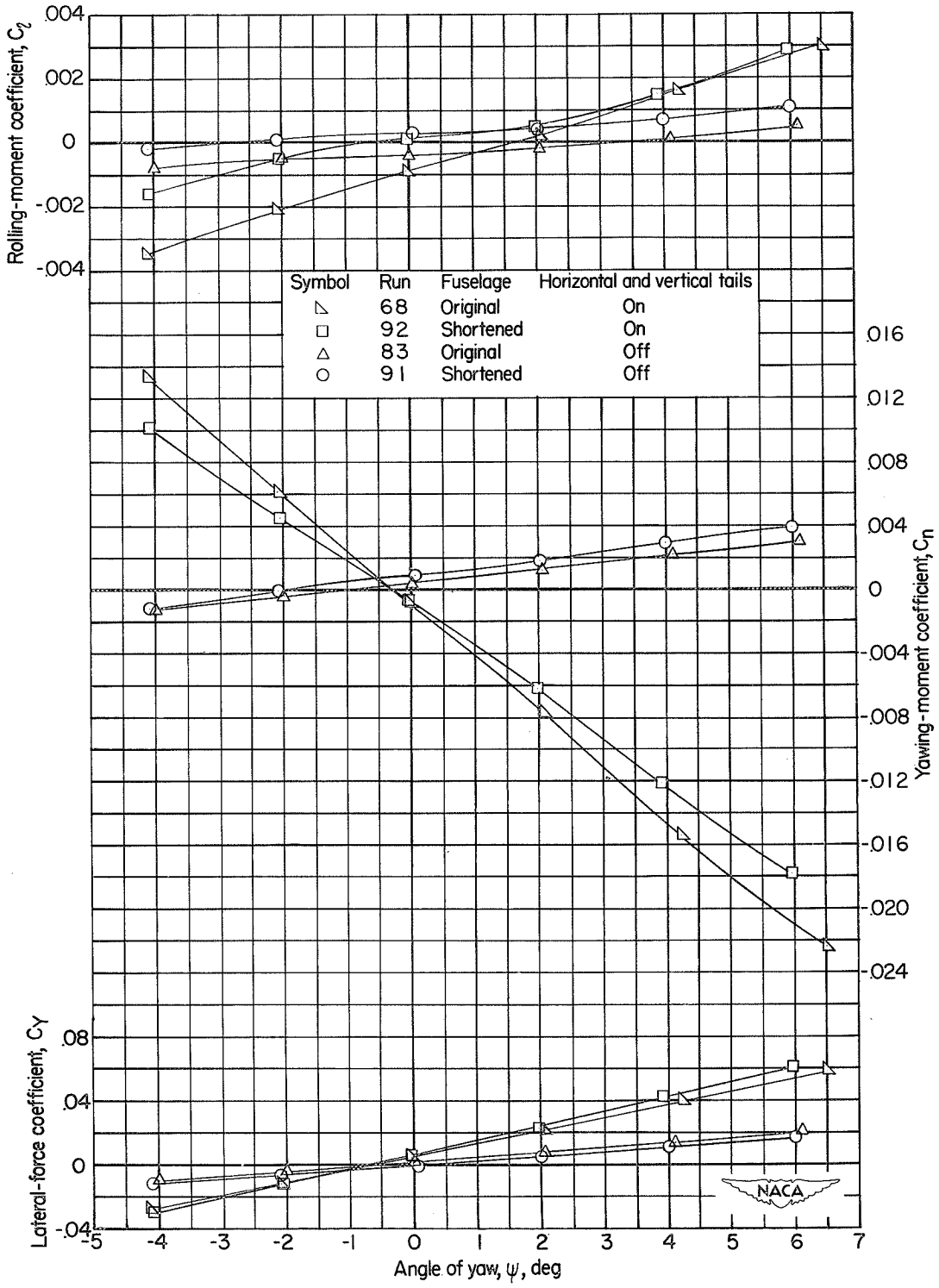

Figure 30.- Effect of fuselage length on lateral stability characteristics of fuselage plus wing and basic model with low horizontal tail. M = 1.41.

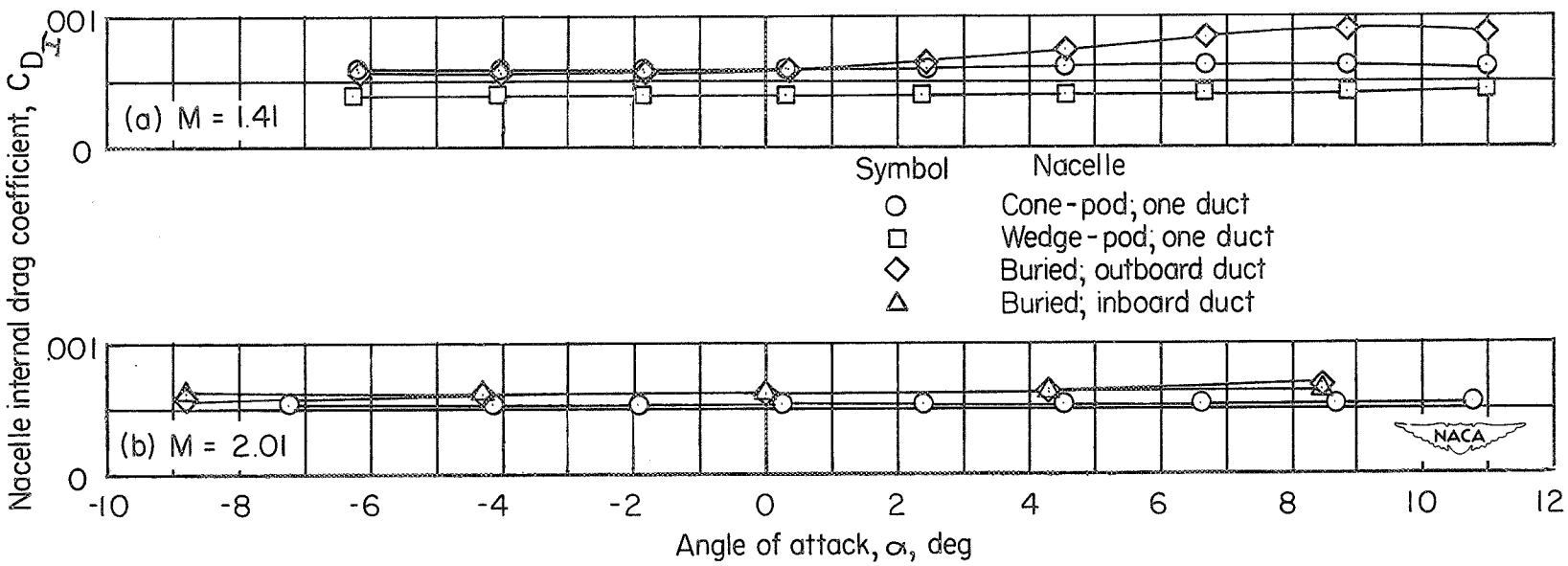

Figure 31.- Internal drag coefficients of individual ducts of the pod and buried nacelles.

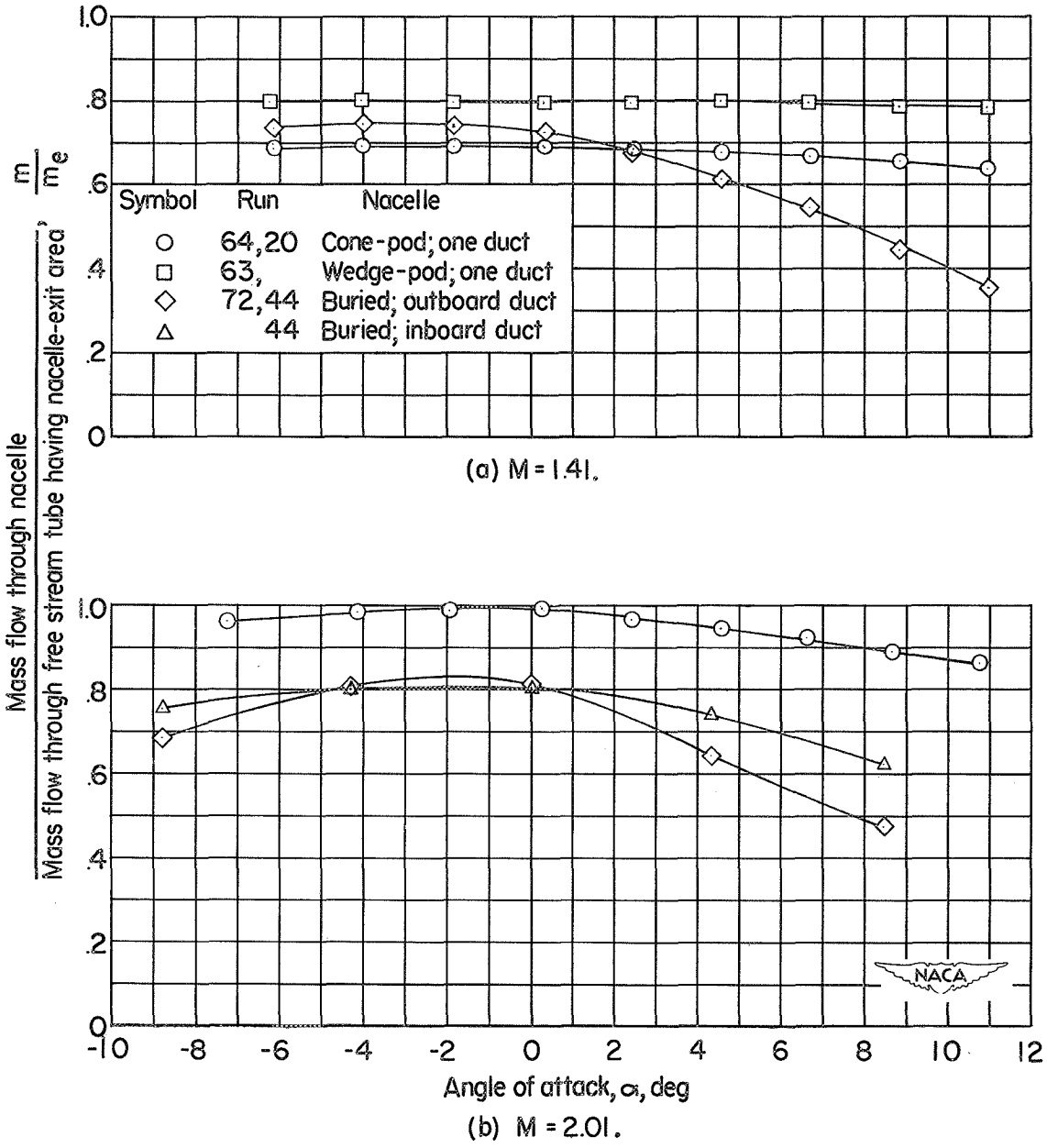

Figure 32.- Mass-flow coefficients of individual ducts of the pod and buried nacelles.

INDEX

ABSTRACT

An investigation of the aerodynamic characteristics of an 0.025-scale model of the MX-1712 configuration has been conducted in the Langley 4- by 4-foot supersonic pressure tunnel at Mach numbers of 1.41 and 2.01 and a Reynolds number of 2.6×10^6. The model incorporated a tapered wing having a thickness ratio of 5.5 percent, 47° sweep of the quarter-chord line, an aspect ratio of 3.5, and a taper ratio of 0.2.

The longitudinal and lateral force characteristics of the model and various combinations of its components were investigated along with the effects of a modified wing, two horizontal tail positions, and a shortened fuselage.